NPS67-82-009

NAVAL POSTGRADUATE SCHOOL
Monterey, California

DUAL PROBE DIGITAL SAMPLING (DPDS) TECHNIQUE FOR ROTOR FLOWS--REVIEW OF THE DEVELOPMENT AND AN ASSESSMENT BASED ON EARLY RESULTS

H.-J. Heinemann

April 1982

Final Report; October 1980-March 1982

Prepared for:
Naval Air Systems Command
Washington, DC 20361

NAVAL POSTGRADUATE SCHOOL
Monterey, California

Rear Admiral J. J. Ekelund
Superintendent

David A. Schrady
Acting Provost

The work reported herein was carried out during the period October 1980 to March 1982. The author was supported for twelve months by the DFVLR (German Aerospace Research Establishment) and by the project under Contract No. N62271-80-M-2214. The work was completed while the author was Naval Air Systems Command Visiting Research Professor in Aeronautics at the Naval Postgraduate School from October 1981 to March 1982; support for this period was under Work Request N00019-82-WR-21036 as part of Energy Utilization and Airbreathing Propulsion, AIRTASK (A3103100/186A)/1R024-03-001, under the cognizance of Dr. G. Heiche, AIR 310.

This report was prepared by:

WILLIAM M. TOLLES
Dean of Research

REPORT DOCUMENTATION PAGE

READ INSTRUCTIONS BEFORE COMPLETING FORM

1. REPORT NUMBER: NPS67-82-009	2. GOVT ACCESSION NO.
3. RECIPIENT'S CATALOG NUMBER	
4. TITLE (and Subtitle): Dual Probe Digital Sampling (DPDS) Technique for Rotor Flows--Review of the Development and an Assessment Based on Early Results	5. TYPE OF REPORT & PERIOD COVERED: Final Report October 1980 - March 1982
6. PERFORMING ORG. REPORT NUMBER	
7. AUTHOR(s): H.-J. Heinemann	8. CONTRACT OR GRANT NUMBER(s)
9. PERFORMING ORGANIZATION NAME AND ADDRESS: Naval Postgraduate School Monterey, California 93940	10. PROGRAM ELEMENT, PROJECT, TASK AREA & WORK UNIT NUMBERS: N0001982WR-21036
11. CONTROLLING OFFICE NAME AND ADDRESS: Naval Air Systems Command Washington, D.C. 20361	12. REPORT DATE: April 1982
	13. NUMBER OF PAGES: 153
14. MONITORING AGENCY NAME & ADDRESS (if different from Controlling Office): Naval Postgraduate School Monterey, California 93940	15. SECURITY CLASS. (of this report): Unclassified
	15a. DECLASSIFICATION/DOWNGRADING SCHEDULE

16. DISTRIBUTION STATEMENT (of this Report)

Approved for public release; distribution unlimited

17. DISTRIBUTION STATEMENT (of the abstract entered in Block 20, if different from Report)

18. SUPPLEMENTARY NOTES

19. KEY WORDS (Continue on reverse side if necessary and identify by block number)

Compressor Flow Fields

Compressor Measurements

Probe Techniques

20. ABSTRACT (Continue on reverse side if necessary and identify by block number)

The state of the art in the development of the DPDS technique at the Turbopropulsion Laboratory at the Naval Postgraduate School is reported. In principle, this method allows the determination of three dimensional flow fields behind rotors. A review of the instrumentation and hardware is given and two different data reduction procedures developed earlier are described. The results of reducing one set of rotor exit data

using the two methods are compared. In order to verify the experimental procedures at low cost a bench-top periodic flow generator was used first to provide signals similar in type and frequency to those from the Transonic Compressor in which the rotor exit flow was measured. The data measured in the compressor were analyzed, and problems encountered in the routine application of the reduction methods were identified.

The possible application of similar techniques in the Rotating Annular Cascade (RGG) at the DFVLR Göttingen is assessed and recommendations are made for the coordination of future experimental programs.

ABSTRACT

The state of the art in the development of the DPDS technique at the Turbopropulsion Laboratory at the Naval Postgraduate School is reported. In principle, this method allows the determination of three dimensional flow fields behind rotors. A review of the instrumentation and hardware is given and two different data reduction procedures developed earlier are described. The results of reducing one set of rotor exit data using the two methods are compared. In order to verify the experimental procedures at low cost a bench-top periodic flow generator was used first to provide signals similar in type and frequency to those from the Transonic Compressor in which the rotor exit flow was measured. The data measured in the compressor were analyzed, and problems encountered in the routine application of the reduction methods were identified.

The possible application of similar techniques in the Rotating Annular Cascade (RGG) at the DFVLR Göttingen is assessed and recommendations are made for the coordination of future experimental programs.

TABLE OF CONTENTS

LIST OF FIGURES

ACKNOWLEDGMENT

The work described in this report was carried out while the author was supported for twelve months by the DFVLR and by the NPS. The work was completed while the author was Naval Air Systems Command Visiting Research Professor in Aeronautics from October 1981 to March 1982. The author acknowledges the financial support of those different institutions.

Furthermore, the author would like to express his many thanks to the director of the TPL, Dr. Raymond P. Shreeve, for his help and all the time he invested in the technical discussions. In addition, the support from all members of the TPL is also appreciated very much. Personal friendship, human integrity and technical knowledge of the people involved in the project made the 1½ year period an unforgettable time for the author.

I. INTRODUCTION

It is one important goal in today's axial turbine design--for stationary steam and gas turbines in electricity generating plants as well as for jet engines--to develop machines which are as compact as possible. Therefore larger enthalpy differences per stage are used in today's designs than was the case in the past. This results in supercritical pressure ratios for the conditions occurring in some parts of the blade rows, and leads to flows which are partly subsonic and partly supersonic. This regime is usually termed transonic, and is well known to be difficult to investigate both theoretically and experimentally. This holds true for external flows--flow past single airfoils, for example, but it is particularly true for internal flows--flow within turbomachines being an extreme case.

For large power-generating steam turbine plants the shaft speed is fixed by the RPM of the generator. Therefore an increase in work output is only possible by increasing the mass flow rate. As a result, progressively larger diameters of these kinds of machines are being used. Near the tip sections in the last stages of low pressure steam turbines this also results in transonic relative velocities.

Presently, it is not possible to fully describe the passage of the flow through the different stages of a turbine

from either experimental or theoretical approaches. In reality, very complicated three dimensional unsteady flow conditions exist.

However, in order to simplify the picture for design purposes, two dimensional flow models are usually used. Experimentally, two dimensional cascades of axial blade row segments are generated either in an annular cascade of high hub-to-tip ratio or by developing the coaxial stream surface of interest into a plane surface as a rectilinear cascade. Because of the limited number of blades which must be used, the simulation of the required periodic flow field in a rectilinear cascade is usually imperfect, and this is particularly true for transonic flow conditions.

This disadvantage is avoided in the case of an annular cascade, and for some years such a facility for Rotating Annular Cascades (RGG) has been in operation in the DFVLR-AVA in Göttingen, West Germany. In developing this facility, it was necessary to develop a new method of evaluating the measurements such that the results were representative of the flow through a truly two dimensional cascade. The method was required to be simple but reliable. Such a method was developed and was verified by investigations on two cascades of very different types [1, 2].

The fundamental advantage of the method is that the experimental determination of only the total pressure and total temperature in the homogenous downstream flow field is

necessary. This requires the existence in the downstream flow field of a region where non-uniformities from wakes have disappeared and where the boundary layers from hub and tip of the annulus have not penetrated. Although the existence of such a region was shown it was considered desirable to measure peripheral and time-varying flow properties as well.

In order to measure the unsteady flow field behind a rotor one must either use high response probes or an optical technique of some kind. While laser velocimetry techniques have many advantages, they are normally able to measure only two components of the velocity. They do not provide measurements of the pressure field, and in highly unsteady flows the accuracy must be questioned.

At the Turbopropulsion Laboratory (TPL) of the Naval Postgraduate School (NPS), the dual-probe digital sampling (DPDS) technique is being developed. The technique is based on the use of two Kulite semi-conductor pressure probes of very simple design. The approach has the potential of evaluating all three components of the periodic velocity vector in a turbomachine or rotating cascade. Following early work with a single probe in a compressor flow field [21], effort at NPS was devoted to developing and verifying a method of calibrating and applying the dual-probe system in the steady flow of a free jet [3]. The application of the probe system in the compressor flow field was delayed until recently by drive turbine bearing failure.

Now, some first data from the compressor and early attempts to analyze the data are reported here. While there are some open questions left by the work done so far, it is recommended nevertheless that the method be applied in the RGG at the DFVLR. Because of the early stage of development and complexity involved in the process it is suggested that the efforts at the DFVLR and NPS be conducted in close association so that improvements are directly available to both institutions.

This account should be viewed as a documentation of the learning process that the author has undergone. It reviews the earlier work listed as references. Key passages from those references have been included without change on occasion when any contraction of the wording would have detracted from the descriptions originally given. The list of references is organized so as to group the materials logically, rather than in the order that they are mentioned in the text. The references are reviewed in the following section. In sections III and IV, descriptions of both the experimental and computer hardware are given. Section V describes the DPDS-method and in section VI some results are shown. Finally, in section VII ideas for a first application in the RGG are described.

II. REVIEW OF PUBLICATIONS DEALING WITH UNSTEADY FLOW MEASUREMENTS IN TURBOMACHINES

In [3] to [43] publications are listed which are a useful source of information in the field of unsteady flow measurements in turbomachines. The quoted references are those that the author has used; the list does not cover the available literature completely. It should be mentioned that in the following text, the references referred to most often are those which concern the research activities of the TPL.

The sequence of the reference list is such that Masters Theses of the NPS ([4] to [10]) are given first, followed by Technical Reports of the NPS ([12] to [17]) and finally, publications in the open literature ([18] to [21] and [3]), which generally summarize much of the useful material from the theses and reports. In [11] a U.S. patent is referred to. References from [22] to [43] deal mostly with different kinds of high response probes used in the flow field downstream of rotors. Some results from laser measurements are reported in [37] and the use of Schlieren pictures for interpreting the flow field in [40]. In [31], [39], [41] and [42] the use of high response pressure transducers to measure the dynamic flow behavior on rotor blades and stator blades are reported. Case wall measurements based on the same kind of instrumentation are reported in [36] and in [32] a FORTRAN

program is given for reducing case wall static pressure data to contour maps. In [24], a general description of different problems which can occur in investigating flow fields in transonic compressors, is given.

The ability to measure the true time-averaged static and impact pressures is of considerable importance and is needed to permit a full interpretation of semi-conductor probe measurements in non-steady flow fields. This is discussed in [26], [27], [33] and [34]. For application in transonic flow fields the oil-filled total pressure probe described in [33] and [34] may be the most useful tool available.

III. REVIEW OF THE EXPERIMENTAL EQUIPMENT

A. TRANSONIC COMPRESSOR (TX)

The transonic compressor is located in the second test cell of the High Speed Turbine and Compressor Laboratory. This laboratory in total consists of three test cells, a control and instrumentation room and a compressor room containing a single 12-stage axial air compressor that provides the power for all experiments. There is also a "spin pit" for the determination of stresses in rotors. Details of the laboratory are reported in [44].

Compressed air at up to 11 lbs. per sec. at three atmospheres pressure can be valved to each cell from an Allis-Chalmers multi-stage axial compressor. The 1250 HP compressor has a variable speed drive with an automatic control and a by-pass surge suppression device. The mass flow rate from the compressor is metered by a sharp edged orifice meter located downstream of an aftercooler in the outlet pipe.

A line drawing of the TX is shown in Fig. 1. The compressor is a single stage axial fan designed to operate at 30,460 RPM with a relative tip Mach number of 1.5. The rotor diameter is 27.94 cms (11 inches), and the hub-to-tip ratio at the rotor face is 0.5. At the design RPM and referred flow rate of 8.62 kg/sec (19 lb/sec), the relative flow angle at the rotor tip is 65° and the design pressure ratio is 1.6. The

compressor rig is open loop with an air filter, throttle and flow nozzle in the induction pipe and with the compressor exhaust going to atmosphere via a radial diffuser. The flow rate is controlled by an electro-hydraulic rotating throttle plate located in the inlet duct. The inlet of the transonic compressor is designed to contract and to rapidly accelerate the flow in order to generate near uniform conditions, with thin boundary layers, at the rotor face.

The compressor test rig has the advantage of providing redundancy in measurements. The operating power can be determined in three ways: either from the mass flow rate and temperature drop through the turbine, or from the mass flow rate and temperature increase through the compressor, or from the speed and the torque measured by strain gauges on flexures between the compressor stator (mounted on bearings) and the machine casing.

B. INSTRUMENTATION

1. Probes for Radial Surveys

Probe survey ports are provided at four axial planes and fixed Kiel and temperature probes are installed for overall stage performance measurements as shown in Fig. 1. The case of the compressor can be rotated manually about the axis while the machine is running in order to position probes and sensors mounted in the case wall so as to obtain surveys in the peripheral direction (with respect to the fixed stator blading).

The combination temperature-pneumatic probe which is used is shown in Fig. 2. One of those probes is used in front of the rotor and the other one is located between the rotor and the stator. In use, the probes must be rotated about their axis to balance the pressures at the side sensors, p_2 and p_3, and the yaw angle can be read from a vernier scale. The center sensor, p_1, measures an indicated impact pressure, the pressures p_2 and p_3 approach static pressure and the fourth sensor, p_4, provides a measurement of the pitch angle, when the probe has been suitably calibrated.

The probe was designed specifically to be used downstream of the transonic rotor [4]. The use of separate sensors (the "claw" arrangement rather than pressure taps on a shaped surface) was to minimize the "immersion" effect. It is also likely that the separate sensors would be less influenced by unsteady effects from the rotor. The separation of the sensors peripherally is of no consequence because sensors at the same radius would automatically average in the same passing flow field. The pitch angles in the compressor are expected to be small and severe velocity gradients in the radial direction are not expected away from the hub and tip regions. The necessary radial separation of the fourth sensor is therefore not considered to be critical. Four sensors are used rather than five, to allow the simple arrangement of tubes shown in Fig. 2. This arrangement minimized blockage in a strong, simple, leak-free construction and gave suitably short response times.

The pneumatic pressures are sensed by a conventional differential strain gauge transducer and Scanivalve referenced to atmosphere.

The separation of the thermocouple sensor from the impact pressure sensor in the radial direction, Fig. 2, is also not important since it could be properly accounted for in the data reduction from radial surveys.

Probe calibration procedure and results, data from radial surveys and stage performance measurements are reported in [17].

In [21] a method was described for using two semiconductor pressure probes together with the technique of synchronized sampling, to obtain the distribution of the velocity vector downstream of a rotor. The geometries of the two probes, designated Type A and Type B, and their installation in the compressor annulus are shown in Fig. 3. The two probes are positioned as shown at the same radial displacement, but separated peripherally around the machine annulus. The probes are mounted in such a way that they can be rotated about an axis through the probe tip. The details of the geometry of the two probes are shown in Fig. 4.

The particular shape of the B probe is chosen to enable measurements to be made close to the case wall, and therefore limitations occur in the measurements which can be made close to the hub.

It was argued that, in principle, by rotating the probes in yaw about their tips and controlling the sampling of the data from each probe to be at the same position in the rotor frame, the system of two separate probes could be used to acquire data at a single point in the periodic flow from the rotor, thus obtaining data corresponding to those obtained from the sensors of four- or five-hole pneumatic probes when measuring velocity in steady flows. The technique involved the use of probes having the simplest geometry and thus avoided the large size, expense and unreliability of multiple sensor probes which incorporate multiple semiconductor transducers. It would be far cheaper to replace a single probe of simple geometry in the event of a failure compared to repairing or replacing a multiple sensor probe. Because of the simple sensor tip geometry (that of a cylinder at incidence to the flow) the unsteady response was likely to be as good as could be expected of any single physical sensor.

All probes are yawed and moved to different radial positions, manually. Both yaw angle and radial position are recorded automatically using position potentiometer circuits.

2. Wall Pressure Measurement

Twelve Kulite CQL-080-25 pressure transducers with natural frequency about 125 kHz are mounted with their diaphragms flush with the inner case wall of the compressor. The transducers are located along four axial lines separated peripherally by 10 and 90 degree arcs as shown in Fig. 5.

The transducers are used in conjunction with Datel Model 201C instrumentation amplifiers which have a flat frequency response to 100 kHz. Each Kulite pressure transducer is matched by a pneumatic static pressure tap at the same axial location in the case wall, but displaced circumferentially. Other pneumatic static pressure taps are provided upstream and downstream. The reference tubes of the transducers are connected by separate plastic tubes to a manifold fed from a controlled pressure source or to the pneumatic line from the pressure tap at the same axial location. Clamps were used to valve the reference side of the transducer either to the regulated pressure or to the corresponding pneumatic pressure tap.

3. The Timing Disk

To enable synchronization of the sampling of the semiconductor pressure transducer outputs with the rotation of the rotor, a timing disk is fitted to the rotor shaft, Fig. 6. The disk has a circle of eighteen equally spaced holes (equal to the number of rotor blades) at one radius and a single hole at a smaller radius. Light emitting diodes and photo detectors aligned with the holes generate bell-shaped electrical pulses at one-per-revolution and one-per-blade frequencies. The system is described in detail in [6].

The blade passing frequency, f, can be computed by multiplying the wheel speed (revolutions per second) with the number of blades. The maximum rpm of the TX is about 500/sec and the rotor constsis of 18 blades. Therefore, the expected frequency range is up to 10 kHz.

C. DEVICES FOR DATA ACQUISITION

The primary hardware devices used for data acquisition are the HP-21MX computer with its 20 Megabyte magnetic disc, printer, plotter, and two terminals, the "Pacer" and the HP-5610A 16-channel A/D converter. The complete data acquisition system is shown in Fig. 7.

1. Hewlett Packard HP-21MX Computer

The HP-21MX is a (Micro-programmable) mini-computer having 128 machine instructions and 32K of logical in 240K of main frame memory. A 20 megabyte capacity disc and disc drive surmount the core memory limitation and provide multiple use under time sharing.

An important feature which is typical of computers of this size is the input-output structure. With a limited number of relatively slow I/O devices to be serviced, the computer can communicate with all devices through a single port known as the I/O bus. Each device requires its own I/O interface on the bus. The interface acts as a filter and ensures that output information is received only by the device designated to receive it and that input information is put on the bus from only one device at a time. The I/O software drivers control the I/O hardware interfaces by commands to either "turn-on" or "turn-off".

2. Pacer

This peripheral device which was designed and constructed to trigger data acquisition from a stationary sensor at any fixed point in the rotating rotor frame, independent

of the rotor speed, is shown schematically in Fig. 8. In its original form, a detailed description of the internal operation is given in [6].

The bell-shaped optical signals from the timing disk are first converted in the "wave shaper" section into square pulses suitable for TTL (Transisitor-Transistor-Logic) circuits.

The "Pacer" consists of two major sections, a "synchronized command pulse section" and a "RPM counting section".

The "synchronized command pulse" section is the heart of the "Pacer". The one-per-rev. signal is used as a master pulse in the timing process. The one-per-blade signal is halved in frequency through a counter and input into a PLL (Phase-Locked Loop) circuit. The PLL "locks-on" and outputs a similar wave form at 256 times the input frequency. A comparator compares the number of counts following the master reset (taken from the one-per-rev. signal) with the programmed number received from the computer. When they agree, the command signal from the computer to the A/D converter is allowed to pass and conversion occurs.

The device can be programmed to time the data conversion to occur at any point in the rotor frame, since the "lock-on" makes it independent of the rotor speed.

The pacer can also be programmed to allow conversion either at a single location in a particular blade passage, or at the corresponding positions in each blade passage.

The "RPM counting section" continuously counts the number of 250 kHz time base pulses (obtained from the computer's

1 MHz clock) that occur between the one-per-revolution pulses received from the test rig. This number of counts is available as an output from the "Pacer" on every revolution of the rotor.

The original "Pacer" was recently modified to overcome the following three limitations which were realized when using the original version:

(1) The timing pulses generated with the "Pacer" were not always spaced linearly in time between blade pair synchronizing pulses. This resulted in data which in some cases was subtly distorted, and in other cases appeared to have noise riding on it.

(2) The range over which the "Pacer" could follow rotor RPM changes and remain synchronized was limited to approximately ±15% of the initial RPM at which the "Pacer" was set to take the data. This required a careful manual adjustment of trimming capacitors and resistors to obtain "lock-on" in each range of RPM in order to acquire data at different speeds.

(3) The rate at which data could be taken was limited. Rather than being able to sample data on every revolution of the rotor, the system was only capable of taking data once every 8 to 10 revolutions, depending on RPM.

Changes to the "Pacer" are described in detail in [10] which fully overcame the above three limitations. They involved changes in both hardware and software over those reported in [6]. The present system is extremely easy to use and presents no obvious limitations.

3. Hewlett Packard HP-5610A A/D Converter

Up to sixteen channels of analog input voltages in the range of ±1.0 volt can be sampled and recorded by the A/D converter under the control of the 21MX computer. The acquisition process is governed by the built-in features of the A/D converter and by the programs which can be written for the 21MX.

The HP-5610A Analog-to-Digital Converter is designed to convert analog voltages into ten data BIT's at the maximum throughput rate of 100 kHz. The HP-5610A can operate in one of six modes. The two fundamental modes of operation are "sequential"--in which all 16 channels are scanned in numerical order, and "random access", in which a specific channel is sampled on receipt of a command word and an encode command pulse from the 21MX computer.

Variations within these two basic modes are also possible which allow for externally supplied sequencing pulses and for externally controlled timing of samples.

Another mode which is used only for non-paced data is the "Free Run, Random Access" mode. In this mode the command word is required as before, but no encode command is needed from the computer. The A/D converter simply converts data as fast as it can (100,000 samples per second) on the selected channel.

The command word tells the A/D converter which mode of operation to use and which channel number to sample. The encode command pulse triggers the data conversion to start 2 usec

later. The data conversion itself is finished in a total time of 10 μsec. Using computer-issued encodes, which is the mode required for paced data, the sample cycle time is 20 μsec. Hence data can be converted at rates of up to 50,000 samples per second, depending on how rapidly each successive command word is received. With an input conversion aperture of 50 nanoseconds, rapidly changing signals (100 kHz) can be converted accurately.

The A/D digitizes data using a method of successive approximations. That is, a known test voltage is compared with the sample voltage beginning with 1/2 full scale (0.5v in the present system) and a decision is made whether the test voltage is high or low. The comparisons continue, halving the range each time until the machine accuracy is reached. For a resolution of ±1.0 volt to 10 BIT's the accuracy of the A/D converter is 1/512 = 1.95 mV.

IV. DUAL-PROBE DIGITAL SAMPLING (DPDS) TECHNIQUE

Until the development of miniature semiconductor transducers having large bandwidth frequency response, real-time pressure measurements in high speed compressors were not practicable. Currently, using these pressure transducers, coupled with fast analog-to-digital conversion and computer controlled time delay circuits, a variety of new real-time measurement techniques are possible. The well-known temperature dependence of the transducers (see for example [39]), can be overcome by an on-line calibration (OLC) such as is explained in Section IV C.

The difficulties to be overcome in the design of a sampling method include achieving timing accuracy at high blade passing frequencies and accounting for the small variations in rotor speed that are always present.

The technique of DPDS applied in the transonic compressor is illustrated in Fig. 6 and Fig. 9. Referring to these figures, a transducer which is positioned downstream of the rotor and fixed to the machine frame outputs a time varying signal which is basically periodic at the blade-passing frequency. By successively triggering the sampling of the transducer with a fixed delay following a one-per-rev. trigger pulse, the condition at a fixed point in the rotor frame can be determined. By programming the delay time, in principle

any chosen location in the rotor frame can be examined. However, at design speed, the blade passing frequency is near 10 kHz, and conventional time delay techniques, in the presence of speed fluctuations, can not provide the required resolution. A computer peripheral device called "Pacer" was therefore designed and developed to provide the programmable delay ([6] and [10]).

If the stagnation temperature is known, four quantities are sufficient to determine the velocity vector: for example, static pressure, p_w, total pressure, p_t, yaw angle, α, and pitch angle, ϕ. Following calibration however, any four independent measurements of pressures can be used to evaluate these same unknowns (as is done typically with a multiple sensor probe in steady flow [17]). In principle, the required measurements can be obtained by rotating the probes about their tips to four different directions where pressure readings can be taken. In reality, one must pay attention to the characteristic behavior of the probes, i.e. the output of the probes as a function of yaw angle, pitch angle and Mach number (M) in the ranges of these parameters which are to be measured in the compressor flow field. Experience shows in fact that it is preferable to evaluate curves of transducer pressure (p) as a function of probe yaw angle setting (α_p) and to refer these to calibration curves. It is obvious that probe readings at only four different yaw positions can not provide a precisely defined curve and therefore a comparison which is sufficiently

accurate. Certainly, more than four different probe settings are necessary. Seven positions were suggested in [3]; nine and eleven, respectively, are used for data reported here.

In principle, there are many possible methods for reducing data acquired in the DPDS technique. To date three entirely different approaches have been attempted at the TPL. The first, Method I, uses a particular set of polynomial approximations for the characteristics of the two probes obtained by calibration [3]. The second, Method II, is described in [14], and requires the representation of the calibration as an array of pressure coefficients. The method is a further development of the work reported in [13] and overcomes some of the earlier limitations. The description and results of the third method, Method III, which makes use of work reported in [15] in an approach which parallels that used for steady-state velocity probes [17], is given in [45].

In this report, TX data are analyzed using Method I and Method II only. Some details of the procedures will be given.

A. METHOD I--ANALYTICAL DATA REDUCTION [3]

Using the probe pressure coefficient, (c_p), defined as

$$c_p = \frac{p - p_s}{p_t - p_s} \tag{1}$$

where p = pressure at the probe sensor, p_s = static pressure and p_t = total pressure, the characteristic behavior of the A-probe as a result of observation (first) and calibration

(second) can be analytically expressed by the following three fourth order polynomial equations:

$$\frac{c_{pA}}{c_{p0A}} = A_0 + A_1\left[\frac{\alpha_A}{\alpha_{sA}}\right] + A_2\left[\frac{\alpha_A}{\alpha_{sA}}\right]^2 + A_3\left[\frac{\alpha_A}{\alpha_{sA}}\right]^3 + A_4\left[\frac{\alpha_A}{\alpha_{sA}}\right]^4 \qquad (2)$$

$$c_{p0A} = C_0 + C_1\phi + C_2\phi^2 + C_3\phi^3 + C_4\phi^4 \qquad (3)$$

$$\alpha_{sA} = D_0 + D_1\phi + D_2\phi^2 + D_3\phi^3 + D_4\phi^4 \qquad (4)$$

where α_A is the flow yaw angle with respect to the axis of the probe, α_{sA} indicates the value of α_A where static pressure is measured and ϕ is the pitch angle. c_{p0A} defines the maximum c_p value.

For the B-probe, only the equivalent to equation (3) is useful because its inclination (see Fig. 4) is such that the angle at which static pressure is registered, α_{sB}, does not exist at most positive angles of pitch. The fourth expression is therefore

$$c_{p0B} = E_0 + E_1\phi + E_2\phi^2 + E_3\phi^3 + E_4\phi^4 \qquad (5)$$

A_i, C_i, D_i and E_i (i = 0 to 4) are polynomial coefficients which are established by calibration. In Section V some more details are given when the evaluation of these curves for two new A- and B-probes is described.

In the above equations for every probe yaw angle position which is set in the data acquisition procedure (up to 11

positions have been used) a single value for each of α, ϕ, p_s and p_t can be derived.

The flow yaw angle, α, is taken simply as the position of the maximum of the probe output when the probe pressure is plotted versus the probe yaw angle setting in the machine, $\alpha_{p_A}(m)$. Of course, this could be done for the output of both probes and, in the ideal case, the same value would be calculated. To apply the calibration equations the yaw angles must first be calculated relative to the axis of the probe; i.e. $\alpha_a(m) = \alpha_{p_A}(m) - \alpha$.

The pitch angle, ϕ, can then be calculated iteratively for every data point, m, from the following implicit equation for ϕ obtained using Eq. (1) and Eq. (2):

$$\frac{p_A(m) - p_{0A} + \psi(\phi)\cdot\left[p_{0B} - p_A(m)\right]}{\psi(\phi)\cdot\left[p_{0B} - p_{0A}\right]} = A_0 + A_1\left[\frac{\alpha_A(m)}{\alpha_{sA}(\phi)}\right] + A_2\left[\frac{\alpha_A(m)}{\alpha_{sA}(\phi)}\right]^2 + A_3\left[\frac{\alpha_A(m)}{\alpha_{sA}(\phi)}\right]^3 + A_4\left[\frac{\alpha_A(m)}{\alpha_{sA}(\phi)}\right]^4 \qquad (6)$$

In Eq. (6)

$$\psi(\phi) = \frac{c_{p_{0A}}(\phi)}{c_{p_{0B}}(\phi)} \qquad (7)$$

where $c_{p_{0A}}$ and $c_{p_{0B}}$ are given by Eq. (3) and Eq. (5) respectively, and α_{sA} is given by Eq. (4). p_{0A} and p_{0B} are the maximum values evaluated by fourth order curve fits through

the m data points, for the type A and type B probes respectively. It should be noted that only the maximum value of the B-probe is used in this procedure. The solution of Eq. (6) to obtain ϕ, can be carried out using Newtonian iteration.

The static pressure for every data point, $p_s(m)$, can be calculated using

$$p_s(m) = \frac{p_{0A} - p_{0B} \cdot \psi(\phi)}{1 - \psi(\phi)} . \tag{8}$$

By applying Eq. (1) to p_{0A} the total pressure for every data point, $p_t(m)$, can be obtained using

$$p_t(m) = p_s(m) + \left[\frac{p_{0A} - p_s(m)}{c_{p0A}}\right] . \tag{9}$$

It can be seen from Eq. (6) that for $p_A(m) = p_{0A}$ the left side of the equation becomes unity. In the ideal case (perfectly symmetric probe tip geometry) $\alpha_A(m)$ should be equal to 0 when $p_A(m) = p_{0A}$, $A_0 = 1$, and no solution for $\phi(m)$ is then possible.

B. METHOD II--NUMERICAL DATA REDUCTION [14]

Method II uses the values of c_p as defined by Eq. (1) and obtained from calibration data in the form of arrays corresponding to a particular grid of yaw and pitch angles. Since stem effects and manufacturing imperfections will lead to departures from the perfectly symmetric probe behavior in yaw, a method which does not require an analytical expression for

the probe characteristics has potential advantages. The authors of [14] developed a numerical solution which avoided any requirement for curve fitting and, in principle, allowed a determination of p_s, p_t, α and ϕ with only four measurements. In the current version, the pressure coefficients defined in Eq. (1) are assumed to be totally insensitive to Mach number and Reynolds number. Nevertheless, if any significant variations did occur an additional iteration scheme could be added to the computer solution.

From four different measurements--three from the A-probe and one from the B-probe are suggested--four c_p values can be calculated. It is assumed that each characteristic has only one maximum in the range of interest and therefore one combination of yaw and pitch angle (α, ϕ) exists where the four c_p values fit those in the calibration tables. The FORTRAN computer program given in [14] provides a systematic trial-and-error search process, essentially a convergence scheme on the two variables yaw angle and pitch angle. A linear, double-interpolation scheme is available as well as a second-order, double-interpolation scheme.

The computer program in [14] was entered into the HP-21MX computer together with the c_p data arrays, also given in [14], which are based on analytical functions. The c_p values so derived are automatically symmetric for positive and negative yaw angles, α.

First, the program was run for the examples given in [14]. The results agreed perfectly. Second, the method was applied using the actual (unsymmetric) c_p calibration data arrays. Incomprehensible and obviously incorrect results occurred. After changing row and column indices of the c_p arrays in the FORTRAN program (referring to [14], statements 3010 to 3040, page 31 and statements 4830 to 4900, page 44; in addition, IFLAG = 0 is omitted after statement 4990) results were evaluated, which were in the expected range. On rerunning the corrected program using the example data, only minor deviations from the first results were found. Hence the corrected program is thought to be working for non-symmetric probe characteristics. Additional checks using calibration data from two new probes are reported in Section V.

C. ON-LINE CALIBRATION (OLC)

The reduction procedures described in the previous two sections require the input of correct values of the probe pressures. Because of the temperature sensitivity of the transducers, which affects mainly the zero balance but to a lesser degree the output slope of the strain gauge, corrections have to be made to the transducer voltages to obtain reliable quantitative pressure measurements. The problem occurs even though a temperature compensation module is included in the transducer circuit. The problem of temperature dependence is widely discussed in the literature; for example,

[8], [23], [33], [39]. Two approaches are in common use; either the signals are used as a measure of the fluctuations only and the time-averaged pressure level is measured by a second device, or flow temperature is measured simultaneously and corrections are computed based on an earlier temperature calibration.

Progressive improvements have been made by the transducer manufacturers to reduce temperature sensitivity during the past decade. Also, in one case, automatic electronic compensation similar to linearization of hot wire circuits, is reported [46].

In the TX an on-line calibration procedure for all Kulite transducers (A- and B-probe and wall statics) is used to account for temperature dependent effects. For the A-probe the method is described in detail in [8] and, therefore, only a brief summary is given here.

To evaluate the slope (differential pressure vs. voltage output), x_1, of the transducers in situ, while ready to take data, the transducers are referenced to different pressures (6 at maximum) and a linear least squares routine is used to obtain x_1. Experience shows that almost without exception the slope is linear and reproducible to within the accuracy of measurement for the modest changes in temperature involved in the experiments (~10-20^{o}C).

Additionally, the above procedure establishes an intercept value, $\tilde{x}_0$, which can be monitored over longer times to

examine any temperature drift which may occur while test conditions are held constant. Experience shows that normally deviations equivalent to less than .5 in H_2O pressure occur while dynamic pressures are never less than 20 in H_2O. Larger deviations can be interpreted as poor temperature compensation, which was the case, on one occasion, for one of the case wall transducers which was subsequently replaced.

In order to interpret the intercept, x_0, the assumption is made that a pneumatic probe measures the correct time averaged pressure when positioned at the same radial location and set to the same yaw angle as the high response probe. This is to be regarded as a delicate problem because investigations are published, for example [33], [34], which clearly indicate that this can be a totally wrong assumption. To date, it has been of minor importance for the TX measurements due to low peak-to-peak pressure amplitudes which have been measured so far. An example is given in [17] and there it is indicated that the parameter "ratio of wave amplitude to mean value," on which the error depends, is 10 times less than the lowest value investigated in [34]. For future measurements at higher rotational speeds, care will be taken to reexamine the importance of averaging errors under the then prevailing machine conditions.

When the transducers are referenced to the time averaged pneumatic pressure their outputs are set to "0". In applying the calibration, samples of Kulite output voltage are reduced

to values of pressure, p_{probe}, using the calibration coeffcients x_0 and x_1 in the equation

$$p_{probe} = x_0 + x_1 \cdot e + p_{ref} \tag{10}$$

where x_0 is expected to be very close to zero. In acquiring data, the transducer reference tube is usually open to atmosphere and the reference pressure, p_{ref}, therefore equals atmospheric pressure.

The total pressure, p_t, read by the combination probe, Fig. 2, is used for the A-probe to evaluate the intercept, x_0. The intercept for the B-probe can not be found in this way because of its inclination, Fig. 4. Rather, the static pressure, p_s, and flow pitch angle, ϕ, from the combination probe are used in Eq. (5) to compute the maximum output of the B-probe, p_{0B}. This procedure is necessary to adjust the transducer of the B-probe to "0" on-line. It is noted that the process does not involve equating to a pressure which is measured directly in the TX. In principle a pneumatic equivalent to the B-probe geometry could be used, but it is feared that minor differences of the inclination angle or tip geometry could lead to totally unacceptable errors. The present procedure is one which ensures that the time-averaged results of the Type A and B probe system are the same as those given by the combination probe. Within this constraint, the Type A and B system can resolve the time-dependent behavior as a blade-to-blade distribution of flow properties.

V. SOME RESULTS FROM HIGH RESPONSE PRESSURE PROBES

A. PRELIMINARY INVESTIGATIONS

1. Results from Periodic Flow Generator (PFG)

A small periodic flow generator (PFG) was used by the author as a means of becoming acquainted with the high speed data acquisition system in the simplest way. The apparatus is described in detail in [5] and [7] and only the main features are given here.

Regulated air is delivered through a settling chamber to a small nozzle. A sprocket (or interrupter) wheel driven by a speed-regulated electric motor, is mounted directly above the jet such that the teeth of the sprocket pass through the jet. The spaces between the teeth simulate blade passages and "one per revolution" and "one per blade" signals are generated from a similar arrangement of holes, light emitters and detectors as is used on the TX. With 60 teeth on the wheel and 10,000 rpm from the motor, blade passing frequencies up to 10 kHz are obtained to simulate the conditions expected in the TX. The high response pressure transducer is mounted on the centerline of the jet behind the plane of the sprocket wheels, so that, ignoring transient flow deflections in the unsteady process, the jet impact pressure is measured. In the potential core of the free

jet, the transducer would be expected to register a pressure equal to the supply pressure.

In addition to tests conducted solely for the purpose of learning, several small experiments were carried out of some general interest. For example, results were obtained to document how well the "Pacer" works. In Figs. 10 and 11 two examples are shown which are results obtained to verify that the "Pacer" was performing correctly as a trigger device. On the interrupter wheel one "blade" pair was distinguished by fixing a wire across the gap between two teeth. By using the "Pacer" to obtain measurements behind the different "blade" pairs, the blade space containing the wire would be detected by the appearance of a "wake". From the two figures, which show the results for two different frequencies, it can be seen that the wake was present only for pair 2. All the other signals were quite similar, as also were those for pairs 5 to 9 which are not shown.

At this stage it was not possible to take samples every revolution and, therefore, the test time was much longer than expected. This problem has since been solved [10] and examples are given below when measurements from the TX are discussed.

In Fig. 12 results of taking paced (synchronized) samples of a sine-wave, produced by a signal generator, are given for four different numbers of repetitions. Again, the

"Pacer" was used as the trigger device. The number of repetitions simply indicates how often a sample at a particular location was taken. An average value was calculated and is shown plotted in Fig. 12. A trace of non-uniformity is seen only for the case of a single sample.

The PFG was also used to obtain comparisons of the response of different kinds of pneumatic and high response probes similar to those given in [7]. The goal was to get additional information to add to the work reported in [26], [33] and [34], for example, particularly to obtain results at higher frequencies. Unfortunately, the small dimensions of the jet and wheel did not allow controlled variations of frequency alone to be made and, again, the learning experience was the main benefit derived from the experiment. In Section VI suggestions are given on how more detailed investigations could possibly be carried out in the RGG at the DFVLR.

2. Calibration of New Type A and Type B Probes

In [3], the procedure for calibrating the Type A and Type B probes in a free jet is described. The old probes in [3] were the ones shown in Fig. 4. Two new probes were bought which were smaller in size in the sensing area. The diameter of the head was 1.63 mm (instead of 2.36 mm). Additionally, the inclination angle of the B probe was 35 degrees (instead of 55 degrees) as was used in [3]. The new probes were both derived from Kulite Type XB-062-25 transducers.

The probes were calibrated in the 107 mm diameter free jet exhausting into the room and supplied from the laboratory compressed air system. A sketch of the calibration apparatus is shown in Fig. 13. The probes were mounted in a probe holder which allowed adjustments to be made in yaw and pitch of the probes about the probe tips. The Mach number of the jet was controlled from approximately .2 to .7 in steps of .1. The Mach number was obtained from the stagnation pressure measured just upstream of the freejet nozzle, and atmospheric static pressure. The upstream stagnation pressure was determined to be equal to the stagnation pressure at the test probe station to within measurement accuracy. All pneumatic pressures were recorded using a single strain gauge transducer, signal conditioning and Scanivalve, with the Steady State Data Acquisition System shown in the upper half of Fig. 7. The reference sides of the Kulite transducers were vented to atmosphere or supplied with controlled air pressure (also recorded through the Scanivalve system). The yaw angle of the probes was recorded by the data system from rotational-position potentiometers to an uncertainty of about 0.05°. The pitch angles of the probes were set manually and read against a vernier scale to an uncertainty of 0.5°.

The calibration was carried out for pitch angles $-15^{\circ} \leq \phi \leq 25^{\circ}$ in steps of 5° and yaw angles $-80^{\circ} \leq \alpha \leq 80^{\circ}$. 150 measurements were taken while rotating the probe from $\alpha = 80^{\circ}$ to

$\alpha = -80^{\circ}$. During this procedure the probes were yawed continuously but slowly enough to acquire data with verified accuracy.

a. Results for the Type A Probe. For an arbitrarily chosen flow condition the output of the probe, p_A, is shown as a function of yaw angle, α, in Fig. 14. In Fig. 15 results for different Mach numbers are given. In this case data are plotted only for values $p_A \geq 0$ in. H_2O. In [3] it was reported that for a constant pitch angle, ϕ, the probe reads static pressure (indicated by $p_A = 0$) at approximately the same yaw angle position independent of the Mach number. This can be seen in Fig. 15 where the static pressure is registered at a yaw angle of $\alpha \simeq \pm 64^{\circ}$ for each Mach number. This is shown in more detail for an arbitrarily chosen flow condition in Fig. 16, in which a larger ordinate scale has been used. At positive yaw angle, all curves cross the abscissa at the same location. This is almost but not exactly the situation for the negative yaw angle.

An exception to the preceding statement occurred for the lowest Mach number, $M \simeq .2$, and for the complete range of pitch angles investigated. Reynolds number effects were suspected, but unfortunately this parameter could not be changed independently in the calibration set-up over a sufficiently wide range.

The data reduction procedure for the calibration followed, initially, the method described in [3]. For

convenience, a FORTRAN computer program was written to carry it out. The quantities which must be evaluated are described in Section IV. Here is described only how the coefficients are determined.

First, the non-dimensional pressure coefficient, c_p, defined in equation (1), is computed. (Data which are obviously incorrect are ignored.) The probe yaw angles, α_s, where static (atmospheric) pressure is indicated are evaluated by applying a least squares linear curve fit through nine measured values which are close to the expected value of α_s. In addition to the smallest positive c_p value the adjacent 4 positive and 4 negative values are taken.

A small difference in magnitude was found in the positive and negative values of α_s (up to 2 degrees) which indicates the presence of a small error in setting the probe to zero in the holder when aligned with the flow. Therefore, the average magnitude from positive and negative values of α_s is taken.

The computation of the maximum c_p value, $c_{p_{0A}}$, is done by using a least squares curve fit of fourth order through the measurement points which are within the range $-30^\circ \leq \alpha \leq +30^\circ$. When the same method is applied for the complete range of α it leads to deviations from the data which are largest in the area of the maximum. Simply asking for the highest actual value of c_p can result in a value which is too large because of the experimental scatter.

(Only obviously wrong values are ignored.) Of course the maximum should be expected to occur at $\alpha_s = 0$. But, again because of scatter this is not assumed. Although deviations of the value of α corresponding to the calculated value of $c_{p_{0A}}$ and the value of α which results from selecting the mid-point between positive and negative values of α_s can be up to 10 degrees, only negligible differences in the value c_{p_0} itself occur because of the flatness of the probe characteristic near its area of maximum output.

As an additional example in Fig. 17 plots for $c_p/c_{p_{0A}} = f(\alpha)$ are shown for M = .6 and $25^o \geq \alpha \geq -10^o$. After non-dimensionalizing α with α_s, 54 different curves for $c_p/c_{p_{0A}} = f(\alpha/\alpha_s)$ are obtained and a fourth order polynomial curve is fitted by the least squares method to each of the 54 data sets.

For $-1.1 \leq \alpha/\alpha_s \leq +1,1$ in steps of .1 23 values of $c_p/c_{p_{0A}}$ are calculated for each of the 54 polynomials. 1242 values are then used to calculate 5 coefficients for a single fourth order representative curve, Fig. 18. Because of the fact that the probe behaves somewhat differently at M = .2 additionally, coefficients are provided which exclude the test at this Mach number. For comparison the result for the old A probe is also plotted.

The deviation of the results for M = .2 is even more distinct when $c_{p_{0A}}$ is plotted versus pitch angle, ϕ, Figs. 19 and 20, and α_s versus ϕ, Figs. 21 and 22. These

are additional curves which are used in the reduction of data from TX measurements. The data in Figs. 19 and 21 are shown connected for each Mach number by straight lines. For each of the curves a fourth order curve fit is computed, and with the aid of the coefficients 25 values are calculated in the range of interest. With the resulting 150 numbers two curves as described in the last paragraph are evaluated, Figs. 20 and 22.

b. Results for the Type B Probe. For the Type B probe only c_{p0B} as a function of ϕ is required [3]. The procedure used for acquiring calibration data is the same as was described for the A probe. Because of the 35^{o} inclination the B probe shows a totally different characteristic in comparison to the A probe. This can be seen from results shown in Figs. 23 and 24, which are representative examples of the acquired data. The final result is given in Fig. 25 together with the coefficients. The straight lines reqresent the experimental data and the dotted ones are the results after the curves are fitted. It is to be seen that a distinct Mach number dependence occurs. That was not the case for the old B probe and, therefore, only one curve is plotted in Fig. 25.

From a first attempt to calibrate the probe a severely unsymmetric characteristic was measured which was subsequently found to be due to some very small dust particles in some holes of the screen [45]. When the screen was cleaned (which had to be done extremely carefully) a nearly perfect

behavior resulted. This experience is mentioned because dust particles cannot be avoided completely in any research facility like the TX. It is suggested that, when data are suspect and instrumentation has been checked, this occurrence of fouling should be taken into account as a possible cause of incorrect measurements. The question can be resolved by a visual inspection of the probe tips under a microscope.

3. Application of Reduction Programs to Calibration Data

The programs which were written to evaluate the velocity vecotrs from probe measurements were applied first to the calibration data. The idea was to provide results which would indicate the degree of accuracy in applying the approximations. In [3] a similar test is described. There, both probes were physically remounted in the calibration rig at corresponding yaw and pitch angles and verification of different flow conditions were calculated using the reduction program.

In the case of the new probes, remounting and retesting the probes was not necessary since calibration data were taken at entirely similar flow conditions for the two probes. The reduction procedure was simply applied to the data taken during calibrations and the results compared with the known conditions set in the test apparatus.

a. Results for Analytical Data Reduction. Figs. 26 to 28 show some of the results of several that were obtained using the method described in Section IV. Diagrams

in Figs. 26 and 27 are results from the old probes and those in Fig. 28 are from the new pair of probes. Using Eq. (6), for data at fixed Mach number and pitch angle the values for p_{0A} and p_{0B} are constant and $p_A(m)$ and $\alpha_A(m)$ are the probe pressure and yaw angle. Mach number, M, and pitch angle, ϕ, can be evaluated for each value of $p_A(m)$ and $\alpha_A(m)$ and these are shown in Figs. 26 to 28. The fixed test condition is indicated as a reference value. It is to be seen that the method gives unacceptably large errors in the area of aobut $-40^\circ < \alpha < +40^\circ$, where dotted lines are used to connect corresponding results. This is to be expected. But even in remaining regions the results are not accurate, especially the Mach number which depends (in an iterative process) on the evaluation of the static pressure. (The values for total pressure are quite acceptable.) In the pitch angle there seems to be a better consistency because deviations from the test condiitons are reasonably constant in the area where good results are expected.

Those general remarks are true for both pairs of probes. For the new probes, much more calibration data are available and, therefore, the evaluated coefficients and corresponding results were initially expected to be better than those for the old probes. But of this there is no indication in the plots. The reason which is suggested at the moment is that the procedure is sensitive to the accuracy of the fourth order curve fit. The calibration (vs yaw) is

represented quite well for the B probe and for the A probe away from the neighborhood of $\alpha = 0$, but it may be that it is not good enough for the A probe near to $\alpha = 0$. In [8] a sine function was used to represent the calibration data for an A probe. The function provided a good fit to the "flattened" type of characteristic. It is possible that the use of a similar function for the (smaller) new probes would improve the results obtained with the analytical method of reduction.

In Fig. 28 results are shown for reductions carried out using coefficients evaluated for different Mach number ranges. Results for symbols x and + are evaluated using coefficients given in Figs. 18, 20, 22 and 25. It is to be seen that the curves always show similar trends and are without significant differences in quality with respect to accurately reproducing the known test conditions. What is somewhat surprising is that even the data reduced using the coefficients evaluated for the very same flow Mach number and pitch angle condition set in the calibration rig ($M = .5$ and $\phi = 0^{o}$), which are shown plotted with symbol o, show a very similar behavior. Therefore, it is likely that the problem lies in the particular choice of analytical function and the high sensitivity in an analytical approach of this kind.

b. Results for Numerical Data Reduction. The numerical reduction method of [14]--Method II, was used to reduce the calibration data for the old A and B probes. The available results from the TX were obtained with this set of

probes and therefore a test of the procedure for these probes was desirable.

In Figs. 29 and 30 the results for pitch angle, ϕ, yaw angle, α, and Mach number, M are shown plotted versus $\pm\alpha$. Using the abscissa in this way should indicate that two (of the four required) pressures are taken from the left and right branches of the calibration curve for the same absolute value of α. The other two pressures are the maximum outputs of each of the A and B probes. It should be mentioned that every other combination of pressures (which, in principle, it is possible to use) gave poorer results in comparison to the aforementioned choice. For example, it is possible to use three values from the B probe and only one from the A probe, and even four values from only one probe will lead to a successful solution of the iteration. It is stated however in [14], and now confirmed by experience, that using both maximum values of the probes and two others which correspond to symmetric yaw angle positions will give the best results. Indeed, the yaw position which is recommended in [14] is $\pm 25^{\circ}$, but for real values of calibration data yaw angles in the range of about 50° to 65° must be used. This is quite clearly indicated in the diagrams of Figs. 29 and 30. It is to be seen that in this range of α the required flow quantities show an asymptotic behavior (for simplification the results are connected by straight lines) and the results are in quite reasonable agreement with the test conditions. In

areas near maximum probe outputs ($\pm\alpha < 25^{\circ}$) incomprehensible results occur as was the case of the analytical method ($-40^{\circ} < \alpha < +40^{\circ}$).

The scatter of the results is less in comparison to that found using the analytical method (Figs. 26 to 28, where the same scales are used). Therefore, for the moment the numerical method is recommended as the more successful one.

If $\pm\alpha$ values are used which are lower than those from the recommended range, yaw angle deviations from the test conditions increase very rapidly. The behavior of the yaw angle calculated using data at large yaw angles is not as obviously asymptotic as are the Mach number and pitch angle. This can be interpreted as an indication of the sensitivity of the reduction procedure. In view of the magnitude of the possible error in α it might be better to derive the yaw angle as described for the analytical method in an earlier section from the position of the maximum of the probe output. It is suggested that these different results for yaw angles be compared. This topic will be discussed in connection with the results from the TX.

B. RESULTS FROM THE TX

Results from high response pressure transducers are obtained with the A and B probe system in the measurement plane between rotor and stator, and with twelve different

flush-mounted transducers at locations in the outer casing wall. For identification the wall static transducers are labeled K6 to K13 a number (see Fig. 5). The number indicates the axial location, where 9 is at the rotor entrance plane and smaller numbers indicate planes upstream from there.

An example of the data obtained from the Type A and B probes using the acquisition procedure described in Section III are given in Fig. 31. Some general remarks can be made. Outputs for both probes are shown plotted for one blade pair for two different numbers of repetitions (compare Fig. 12). [Note that all results for the A and B probes presented in this report are taken at the mid-span position (50% of blade height).] The number of counts in the circumferential direction is indicated by n; one passage is divided into 128 counts. The noise reduction in fluctuations which accompanies increasing the number of repetitions is clearly seen. Of course, this would improve if even higher numbers of repetitions were used. With the software improvements described in [10], and with the number of repetitions equal to ten, the data acquisition time has been reduced to about 10 secs from the 45 seconds which were needed with the old software in [6]. Additionally, it should be mentioned that the averaged value indicated in the diagrams by a broken line is nearly independent of the number of repetitions used. The wakes of the blades are clearly indicated and it

is to be seen that they occur almost exactly 128 counts apart, which is another indication of the precision of the high speed data acquisition.

In Fig. 32 pictures taken from an oscilloscope are presented to demonstrate transducer outputs for the A and B probe and for the wall statics, in this particular case K9.5 and K10. It is clear from the 1/30th sec. exposure that much more noise occurs for the probes inserted into the flow than for the measurements made at the wall even if the different scales are taken into account. However, results in Fig. 31 also indicate that increasing numbers of repetitions will result in well-defined average signals. This would not at first be expected from watching the probe outputs on the oscilloscope.

Results for A and B probes can now be discussed in more detail.

1. Results for A and B Probes

In Figs. 33 and 34, results for different numbers of repetitions are shown (in this case for the B probe only). In these diagrams, following the DPDS procedure described in Section IV, signals are shown from the B probe when set at specific yaw angles, α (for definition see Fig. 3). It is noted that the averaged values for corresponding curves with different numbers of repetitions would differ slightly, because data were taken on different days. It is to be seen that with increasing values for α the basic behavior of the

signals within the wakes changes. For example, in the case of $\alpha = -43^{\circ}$ within the wakes extrema are indicated as minima and in the case of $\alpha = +103^{\circ}$, maxima occur. The difference between peak to peak output values decreases for α-values which are between these extremes.

With the aid of Fig. 35 a qualitative explanation of this behavior can be given. Here velocity vectors, probe positions and curves of "probe output, p, versus angle, α," are sketched. (It is of no importance for the following qualitative description but it should be mentioned to avoid misunderstanding that these curves are actually different for different positions of the probe across the blade passage.) If the rotor blade wake is a simple wake, the relative velocity in the wake, w_{2D}, is smaller than that outside the wake, w_2, but the relative flow angle is almost constant. This can be seen to increase the absolute flow angles seen by the probe (α_2 = outside the wake; α_{2D} = inside the wake). This results in probe outputs p_{c2} and p_{c2D} for $\alpha = -43^{\circ}$ as sketched on the right hand side of Fig. 35. Here, $p_{c2} > p_{c2D}$, but both have negative values (that means below atmospheric pressure), compare the result for $\alpha = -43^{\circ}$ in Fig. 34. If the probe angle, α, is increased both values p_{c2} and p_{c2D} are "traveling" on curves $p = f(\alpha)$ in the positive α direction. For example, in the case of $\alpha = +52^{\circ}$ both values are quite the same, and therefore distinct peak-to-peak differences do not occur. For $\alpha = 103^{\circ}$ $p_{c2D} > p_{c2}$ which explains the "inverted" signal behavior.

It is recommended in [3] that measurements for seven different yaw angle positions should be obtained to enable an adequate reduction of data from the DPDS technique. The first data were obtained (examples are shown in Figs. 33 and 34) following this suggestion. However, it was subsequently found that more angle settings were required to improve the data reduction procedure. Both acquisition program [16] and reduction program allow measurements at eleven different probe settings, and this feature was used in subsequent tests.

Two sets of data from the TX using the old A and B probes are shown in Figs. 36 to 39. They can serve to illustrate some general statements with respect to the DPDS technique. (Following the failure of the A probe as a result of handling, further measurements were not possible with this system.)

Each section of Figs. 36 to 39 shows results for both A and B probes for different blade-to-blade positions and each represents a discrete value of the probe angle setting. For the first data set in Fig. 36 and Fig. 37 the number of repetitions was 10 and for the second set in Fig. 38 and Fig. 39, 40 repetitions were used.

Comparing the corresponding signals from the two data sets, it can be seen that for the first set an apparent "phase" shift occurs between the A and B probe results which is not the case for the second data set. In fact a change

was made in the data acquisition software following the first data set. It was found that one probe was placed at a different circumferential location (135° instead of 90°, Fig. 5) after a bearing failure of the drive turbine was repaired and the instrumentation was replaced. Therefore, the number of counts separating the two probes which was programmed in the acquisition software (to provide measurements with the two probes from the same blade pair) did not match the hardware any more. After correcting the number of counts in the program, the signals became aligned correctly, as seen in Figs. 38 and 39.

There is, indeed, no obvious check which would ensure that measurements are obtained from the same blade pairs, but the test with the PFG described in Section V.A.1 indicated clearly that the trigger system worked correctly, when correctly programmed.

The phase-shift of the first set of data could be corrected partially by providing an offset of a fixed number of counts in the reduction program. 28 counts were needed, but the disadvantage remains that signals were taken behind different blade pairs. Furthermore, a complete reduction over two passages was not possible, unless the results which were offset to negative counts were patched to the data at the other end to complete the two passages (a procedure which may be doubtful).

The corrected software in [10] needed test times of about 25 minutes for one complete set of data from 2 probes at a fixed radial location, taken at eleven probe settings with 40 repetitions. A third of this time was required to manually adjust the probe yaw angles. Although the ratio of "test time to quality of signal" is acceptable, it may be worthwhile to provide remotely actuated probes in the future, firstly to decrease the test time and secondly for the convenience and safety of the operator.

Applying the data reduction (with on-line calibration) to the signals obtained from the A and B probes results in 2 x 256 different curves of $p = f(\alpha)$ as shown for the first data set in Figs. 40 to 45. The curves shown are the result of plotting probe pressure, p, for different circumferential locations, n (counts) for the 11 yaw angles, α. Measured data points are connected with straight lines for clarity. In Figs. 40 to 45 the curves are drawn to a scale which is shown once at the bottom for the lowest curve and the other curves each offset in sequence by about 3.4 inches of water. In Figs. 42 and 45 the results in the area of the wake of the first blade is shown in more detail, with each curve offset by almost seven inches of water.

A second set of data were obtained at a highly throttled flow condition where a higher degree of flow separation can be expected to occur in the rotor blading. The same yaw angle settings were used. Plots of $p = f(\alpha)$ for these data

indicate that especially within the wakes (particularly for the A probe) yaw angles greater than 103^{o} were needed in order to fuuly describe the right side of the characteristic curve. An example is shown in Fig. 46. This is a difficulty because the reduction procedure requires adequate data on both left and right branches.

In wake flow areas the probe signal seems to be relatively more unsteady when the probes are set to flow angles which are close to the mean flow direction. This can be seen in the A probe signals shown in Figs. 46a and b. For a probe angle which is close to the aligned flow direction ($\alpha = 52^{o}$, Fig. 46a) it is seen that within the wake the noise is relatively more pronounced than it is outside the wake. For the same numbers of repetitions, at large values of probe yaw angles ($\alpha = 103^{o}$, Fig. 46b), the noise inside the wake flow appears to be very similar to that outside the wake flow and quite similar to that outside the wake flow at the probe angle of 52^{o}.

In view of this there are two possible ways to increase the quality of the signals without extending the data acquisition time. First, the number of repetitions can be increased for probe angles which are close to flow-aligned conditions and can be decreased for the rest of the angles; or second, for all probe angle settings the number of repetitions can be increased when data are acquired in wake flow areas and can be decreased outside those areas. The

identification of wake flow areas can be made from a display of the transducer output on the screen of the oscilloscope.

At first glance, a comparison of the curves shown in Figs. 40 to 46 with those from the calibration, Fig 17 for example, will lead to the conclusion that the test data result in pressure characteristic curves similar to those obtained in calibration tests. And it may be considered surprising that signals like those shown for example in Figs. 36 and 37 result in quite well-shaped curves, especially outside the wakes; moreso, in view of the unsteadiness evident in the oscilloscope traces (Fig. 32). Nevertheless, going further into the details it turns out that the initial statement does not hold true everywhere, especially on the ends of the left and right branches and particularly within the wake flow areas. It is known from applying the reduction methods to the calibration data that pressures must be used which are obtained at probe yaw angles which are approximately $\pm 60^{\circ}$ away from the angle for maximum probe output. Techniques are discussed below which may help to overcome this very important problem.

While being aware of the aforementioned problem in practice a data reduction procedure is described next which is based on the assumption of having a perfect pressure characteristic curve. This is done to gain a better understanding and illustrate the initial problems of the DPDS technique.

From the first data set, the results at n = 31 (or n = 3, if the added offset of 28 counts is not included) are shown plotted in more detail in Fig. 47. It is noted that it was carefully verified that applying the offset did not change the shape of the probe characteristic.

Using a fourth order curve-fit to the data points shown plotted with the symbol • (through which a curve has been hand-faired) and calculating corresponding points using the fourth order polynomial results in pressure values indicated by the x symbols. It is seen that in this case the polynomial curve fit was a good representation of experimental results. Next, a line is drawn parallel to the abscissa and moved with respect to the abscissa to find iteratively the pressure p_s, where the length of the line between the sides of the curve is equal to 128°. This procedure is used because calibration data showed that static pressure is sensed by the A probe at about 64° (or $\pm 64^{\circ}$) independently of Mach number and pitch angle (Figs. 16 and 22). In Fig. 47 values are indicated for p_s and α_L, α_R and the corresponding midpoint, α_A, which is regarded as the flow yaw angle.

In addition, it is assumed that the A probe indicates total pressure, p_t, in its maximum output value, which is very reasonable as long as pitch angles, ϕ, are roughly in the range $|\phi| < 12^{\circ}$. In the ideal case, the maximum pressure, p_{max}, which is evaluated from the fitted curve,

should be located at α_A, but a lack of symmetry in the characteristics is known to be present from the calibration tests. The difference between α_A and the angle for maximum output is about 7 degrees in the example shown. Because of the flat behavior in the neighborhood of the curve's maximum, $p(\alpha_A)$ is used as total pressure, p_t, instead of p_{max}. The ratio p_s/p_t then allows the calculation of the local Mach number, M.

The assumption that the A probe is not indicating static pressure, p_s, at $\alpha_R - \alpha_L = 128^o$ but $\pm 1^o$ from this value will lead to deviations in Mach number of about ±2% from the previously calculated value. The general trends of the calculated Mach number distribution for a set of data would not change but the average value would change. The same situation will occur if the yaw angle is evaluated at p_{max} and p_{max} is taken to be the stagnation pressure.

For both Mach number, M, and yaw angle, α results of the aforementioned procedure for all n = 256 counts are shown in Fig. 48 for the first set of data. The results follow a credible trend, but the precision will be questioned in the following discussion.

In principle, the same procedure can be applied also to the second data set (at reduced flow, throttled compressor conditions). Some mathematical tricks are needed to overcome the problem of missing data in wake areas. This has been done; however the results are not presented because the accuracy is seriously questioned. In comparison to the first

results a smoother Mach number distribution, higher yaw angles and larger wake widths are calculated, all of which could be interpreted as the result of a more severe flow separation due to the highly throttled test conditions.

The yaw angle distribution can also be evaluated using results from the B-probe. The characteristic of this probe is slightly unsymmetric as is the case for the A probe and therefore results for α_B will again depend on the pressure level at which the calculation is made. Because of its extreme inclination to the flow even at zero pitch angle static pressure is not well defined at a particular α-value and must be based on the results from the A probe. It was found that a difference of about 10 degrees (dependent on which level of pressure was chosen at which to evaluate it) occurred in the values of α calculated using the A or the B probes. This was true for both sets of data. If all uncertainties in the various methods of evaluating α were considered, the difference (which was consistently there) of 10 degrees could not be explained. However, a misalignment between one or both probes and the angle scale on the probeholders is a probable explanation since no verification of the angle zero had been made after several months of operation. Unfortunately a failure occurred in the A probe as a zero check was being prepared. Since the old A and B probe set would not be used further, reasons for the deviations in yaw angles were not resolved.

Results calculated here for the flow quantities are not considered to be satisfactory using either the analytical or the numerical data reduction methods, particularly for the pitch angle, ϕ. It was first thought that the discrepancies in the data-sets described earlier (the presence of an offset between A and B probe data, and incomplete data for the right side of the pressure characteristic) might be responsible. Therefore, parts of another data-set obtained by F. Neuhoff (and reduced using a third data reduction procedure [45]) was used to check the general behavior of the characteristic pressure curves derived from the probe outputs. This particular set of data was entirely free of the disadvantages mentioned earlier: data were taken behind the same blade pair, 40 repetitions were used and the yaw angles covered the required range, even in wake areas. It was found that the curves of $p = f(\alpha)$ for the third data set were quite similar with respect to their basic shape to those shown in Fig. 40. Consequently, applying either reduction method to this set of data will lead to similarly doubtful results.

In can be stated therefore that the basic problem in the data reduction so far is that the shape of both left and right branches of the characteristic pressure curves obtained from test data do not fully agree with the behavior obtained during the calibration of the probes. Since only the maximum pressure value is taken from the B probe the problem lies only with the A probe.

Because of varying pressure levels accompanying the varying Mach numbers and pitch angles which are to be determined, a comparison of the calibration curves with the application curves on the basis of raw pressure is not useful. For a more reliable check the non-dimensional pressure coefficient, c_{p_A}, given by Eq. (1), is examined as a function of α. For the calibration data, the plots of $c_{p_A}/c_{p_{0A}} = f(\alpha)$ are shown in Fig. 17. Although the curves are quite independent of the different flow conditions, and the value of $c_{p_{0A}}$ depends only on pitch angle, ϕ, and is very close to unity for $0^\circ < \phi < 15^\circ$, it is not possible to generate a direct comparison with the test data unless some assumption is made concerning the value of p_s or of Mach number.

The total pressure, p_t, can be evaluated reliably using the procedure described in Fig. 47 but the static pressure, p_s, in Eq. (1) is not known. Therefore the expected Mach number range was used as a parameter and corresponding p_s values were used in the computation of c_{p_A}. This procedure was applied to the data from about 70 counts of the third data set [45], which were taken at 9 different yaw angles, α.

In Fig. 49 one example is given for data obtained outside the wake flow. This flow condition could correspond, for example, to n = 1 in Fig. 40. The calibration curve $c_{p_A} = f(\alpha)$, plotted on transparent paper, can be used to search "by hand" for the particular curve to which it

best fits. For the example shown this is the curve for M = .42. The flow angle, α, can then be "corrected" in areas where the two curves do not fit. The resulting values are given in the diagram. It can be seen in Fig. 49 that the two smallest and the largest values of α_A have to be "corrected" and that the "correction" for the smallest value is the largest. The curve containing the new values of α_A is shown, and it is seen that it agrees very well with the calibration curve.

In Fig. 50, as a second example, results are shown for data obtained within the wake flow area (for example at n = 43 in Fig. 40). It is clear that there is agreement between the test data and the calibration curves at a higher Mach number, M = .48, and to "correct" α_A on the left branch requires corrections which are about twice as large as were required in the first example. For the right branch approximately the same magnitude of correction is required.

This behavior can be explained with reference, again, to Fig. 35. The value of the absolute velocity in the wake may increase due to the fact that the relative velocity, w_{2D}, is reduced. (Note that if $w_{2D} \to 0$, $c_{2D} \to u$.) Moreover, the sketches indicate that for the left branch (for example, $\alpha = -43^{\circ}$) the flow direction to the sensor of the probe for c_{2D} will be at a more extreme yaw angle than for c_2 which may explain the necessity for the large corrections. For the right branch the flow yaw angle is more extreme for c_2

than for c_{2D}, but possibly not as extreme as for c_{2D} at $\alpha = -43^{\circ}$, which can explain the use of about the same correction.

It should be mentioned again that the general behavior demonstrated for these examples is typical of the passage positions from which they were taken. A similar behavior was found for both data sets shown in Figs. 36 to 39. The implication is that the data reduction could be carried out with data from fewer repetitions (10 and 40, respectively, have been used) if an explanation (and a proper correction) for the yaw angle problem can be found. Also an "incorrect" behavior of probe pressure with yaw angle was observed for the B probe measurements. However, a "correction" procedure for the B probe requires an additional step, since c_{p_B} depends on ϕ, as can be seen from Fig. 24.

There are many possible reasons for the observed behavior. What can be said at the moment however is speculative because detailed investigations have not been carried out. For example, the exact position of the probe tip in the flow during rotation must be questioned. It is difficult to ensure precise mechanical rotation about the center of the sensor tip when the probe is yawed in its eccentric mount. If the probe tip is slightly long, there is an error in position which increases with increasing probe yaw angle (in both positive and negative directions). Different probe mounts are used for calibration compared to compressor

applications and while the probes are rigid in construction, small differences in bending could occur in the two situations. It is recalled that there was no opportunity to recalibrate the first set of probes. Although the dimensions of the old probes were as small as possible and yet accommodate the transducer, they were possibly too large for their intended application. In Fig. 48 the relative size (tip diameter) of the old probes is indicated at an arbitrarily chosen circumferential location. The further application of the smaller probes will give some information concerning this problem.

Errors in tip position on rotation would result in an apparent phase shift of the signals obtained at different yaw angles. A wake decay due to probe movement to different axial distances is demonstrated, for example in [31]. An apparent decay is to be seen, for example, in Fig. 38 where the positions for minimum output are slightly displaced for the A and B probe results for yaw angles of $\alpha \leq -15^{\circ}$. Moreover, a comparison of the position of minimum output for $\alpha = -42^{\circ}$ and $\alpha = -15^{\circ}$ for the A probe shows a shift of about 10 counts. However, it must be remembered that in the wake <u>all</u> parameters of the flow are changing and the apparent shift in minima may be qualitatively correct.

It is not possible at the moment to give a full explanation for the behavior of the probes in the compressor flow field. If the potential explanations speculated above

are eliminated, then the general question of how high response pressure probes behave for different yaw positions in unsteady wake flows must be examined. So far, other investigations on this topic are not known to the author.

It should be mentioned that this question is also particularly relevant when multiple sensor probes are used. In such probes, the transducers are placed in various surfaces away from the probe's face. The different transducers are differently oriented with respect to the flow direction at all times, so that any difference in response which depends on orientation will be difficult to account for. From Figs. 49 and 50 it is evident here that at about $|\alpha| > 40^{\circ}$ departure from the calibration behavior begins. Since multiple sensor probes are larger in size in comparison to the probes described here it is suggested that their unsteady response will depart from their steady behavior.

The numerical data reduction has been applied to the results modified as in Fig. 49, since it was shown in Section V that this method was more reliable in comparison to the analytical one (Figs. 26 to 30). The results are indicated with a x symbol in Fig. 51. Comparing the curves with those evaluated for calibration data (for example Fig. 29), it can be seen that approximately the same tendency occurs for the flow quantities ϕ, α and M. The results given for yaw angle, α, are here to be interpreted as deviations from the angle, α_A, evaluated with the procedure demonstrated in

Fig. 47. As before, the best results are obtained in the range of about $50^{\circ} \leq |\alpha| \leq 65^{\circ}$. At this point, the data reduction has been carried out as usual except that the values of α at the right and left branches were corrected. Thus the values of c_p can be calculated from p_t and p_s for every data point and those results can be compared with the calibration curve $c_{p_A} = f(\alpha)$. When this is done, it is found, as might be expected, that deviations occur for about $|\alpha| < 50^{\circ}$. Since the calibration table covers only the range of $-70^{\circ} \leq \alpha \leq +70^{\circ}$ deviations from asymptotic values in areas $|\alpha| > 65^{\circ}$ might also be expected.

When the method described in [45] is applied to these data nearly precisely the same results are found.

The value obtained for pitch angle, ϕ, was about -2.5°. In [17] it is reported that the time averaged value calculated from measurements with the combination probe was about $\phi = +4.5^{\circ}$ and, therefore, results for ϕ within the wake must increase considerably to establish an average value of about the measured magnitude. The reduction of the example given in Fig. 50 showed increases in the pitch angle in the wake, but of insufficient magnitude to produce an average of $\phi = +4.5^{\circ}$.

This, in turn, raises the question of how reliable are the pneumatic measurements, in particular for measuring pitch angles. This topic was discussed to some degree in Section IV. A distinct problem in the DPDS technique is the

way the OLC must be applied to the B probe. In order to find out what would happen if the reference pressures of the B probe, $p_{ref\ B}$ (or equivalently the intercept) were wrong, the results were re-evaluated for differences of +2 and -2 inches H_2O respectively. From Fig. 51 it can be seen that this is a relatively minor influence on both M and α but it causes a change in ϕ of about $\pm 1.5^{o}$. In addition, data were reduced for p_A values which were increased by +2 inches H_2O when the original value of p_B was used. Results were equivalent to the case of -2 inches H_2O on the B probe and the original value of p_A (+ symbols are used for both cases).

The minor influence of these changes on α and M can be explained with reference to Fig. 47 although a different reduction process is used. A different reference pressure on the probes will change only the level of the curve and the evaluated yaw angle, α_A, would not change. With respect to Mach number, an impossibly large change in pressure level of say +20 inches H_2O (p_t = 462.4 in H_2O and p_s = 427.4 in H_2O) would change M by about 2% only. Such a change of total pressure would however result in extremely large changes in loss coefficients.

2. Results for Wall Static Pressure Transducers

Very briefly some results are reported which were obtained with 12 Kulite pressure transducers mounted flush at the outer casing wall. Their peripheral and axial locations are indicated in Figs. 1 and 5. Similar measurements

from the TX are reported in [5], [12] and [21] where 8 transducers were used. The programs to reduce data to contour maps used in [12] and [21], respectively, were written in BASIC language. A FORTRAN program to include the 12 different signals now available is in preparation. Such a program for about 40 transducers is reported in [32].

In Fig. 52 a series of signals is shown. The data acquisition time was about 10 minutes including measurements of all pneumatic pressures and two OLCs. The increase in the magnitude of the pressure fluctuations in going from upstream towards the rotor in the axial direction is clear, as is the rapid decrease at the rotor outlet. Outside the rotor exit plane the signal becomes flat and that there are two blades is no longer obvious. Signals for K9.5 and K10 can be compared with pictures taken from the oscilloscope, Fig. 32, on which the time-base can be adjusted to provide a record of more than one blade pair. Some differences in signals from different passages are evident which are probably due to small geometric differences in the hardware. In particular, this is certainly the case for the rotor leading edge plane at K9 as can be seen from Fig. 53. The signals from four different blade pairs are plotted, and differences in the maximum and minimum values are clearly evident. This is due to slight differences in the tip gap and in the chords of the blades. It is noted that the tips of the blades pass approximately across the center of transducer K9, on the average.

The largest amplitudes occur for the transducer K9.5, Fig. 52. Consequently this location was chosen to locate a pneumatic static pressure probe of special shape which was to be used in conjunction with the iterative data reduction procedure described in [34]. The geometric shape of the probe follows exactly the suggestions given in [34]. The probe was manufactured so that it could be substituted at any wall transducer location.

A comparison of the measurements obtained with the standard pneumatic static pressure tap, the diameter of which was 1 mm, with those obtained with the special design showed that there was no detectable difference. However, it is suggested that for higher rotor speeds with the attendent increase in fluctuation amplitudes the comparison should be repeated.

Additionally, signals from one of the transducers were acquired with different numbers of repetitions and a least squares curve fit method of up to the order of 10 was used to approximate each set of results. This was done in an attempt to overcome the problem of long acquisition times when the initial software [6] was in use. In principle, of course, the same procedure could be applied to A and B probe signals. In Fig. 54 results are shown for 5 different numbers of repetitions with a curve fit of ninth order. The original signal, which is plotted for Rep = 1 only, appears as noise about the fitted curve. It is quite remarkable

that results for different numbers of repetitions are almost the same. The procedure which is a form of data smoothing or averaging could be improved either by dividing the results for the 256 counts into more than 2 sections or by using a more sophisticated mathematical method (which might result in capacity problems for the 21-MX computer). Although the software improvements [10] have reduced test time remarkably, it may be worthwhile to keep this procedure in mind for future measurements if a speed-up of the data acquisition is required.

VI. PROPOSAL FOR A FIRST APPLICATION IN THE RGG

The test facility for Rotating Annular Cascades (RGG) of the DFVLR was first used for investigation on cylindrical (conical flow angle $\sigma = 0^{\circ}$) shaped test-wheels [1 and 2]. In this configuration the test-section, basically, consisted of two cylindrical rings forming an annulus. Following this program, since 1980 experiments have been underway dealing with conical cascade flows. Such flow conditions occur, for example, in the last stages of steam turbines, particularly in the tip regions. The goal was to obtain information on the flow behavior for those rotor areas where it is obvious that flow particles can not travel on streamlines which are nearly parallel to the machine axis (which is the commonly used simplification in flow models).

Three new test sections have been built for three different conical flow conditions: $\sigma = 30^{\circ}$ (hub and tip), $\sigma = 45^{\circ}$ (hub and tip) and $\sigma = 40^{\circ}$ (hub) and $\sigma = 45^{\circ}$ (tip). A sketch of the test section for the second case ($\sigma = 45^{\circ}$) is given in Fig. 55. It is noted that measurement planes and probe settings are chosen in the manner indicated so as to be able to make full use of available hardware. Details of the complex program which is carried out in cooperation with Forschungsvereinigung Verbrennungskraftmaschinen, e. V. (FVV), Frankfurt, West Germany are given (for example) in [47].

Basically, the measurement and evaluation method used for conical flows is the same one that was developed for cylindrical flows. Of course, somewhat different assumptions are involved in the data reduction procedures for each case. In the downstream flow field only those quantities which are easiest to measure need be evaluated; namely, absolute total pressure and absolute total temperature. Assuming that there exists a core-flow area in the axial or conical direction of the annulus where only minor changes in flow properties occur, two dimensional cascade data can be obtained. Results which were necessary to prove this assumption for the cylindrical flow conditions are given in [1] and [2]. In [48] it is demonstrated that for conical flow conditions ($\sigma = 30^{o}$) such a core-flow also exists. Nevertheless, it would be highly desirable to have information of the local time-dependent flow quantities also.

Among several motivations the most important is, of course, that it would be of more than only academic interest to verify that the core-flow areas are fundamentally two dimensional in character, and to use an independent, second measurement method to do it. Although in [1] and [2] the limits of this core-flow were defined with respect to blade shapes, cascade geometries and downstream Mach numbers, it is suggested that for different cascades (= test wheels) a check of those regions should be done. Of course, it is not necessary to measure point by point throughout the different

flow fields of interest, but some limited investigations should be carried out. It is expected that these areas can be evaluated both more accurately and more quickly (with respect to test time) with high response pressure probes. Therefore, it is suggested that they should be used in parallel with the existing probes and techniques in the future.

In addition, conditions can occur where the region of nearly two-dimensional flow is quite small. This has happened so far for extreme flow conditions (high supersonic relative downstream Mach numbers, in particular) in the cylindrical case as well as in the conical one. Results carried out up to now indicate that the quality of two-dimensional flow decreases with increasing conical flow angle, σ. The investigations for $\sigma = 45^{\circ}$ are now being prepared, and it can be expected that the flow behavior will continue this trend. This provides a further reason why preparations should be made to make available a second measurement method which has the potential of getting more detailed information on the flow.

Finally, it may also be possible to carry out measurements of general interest concerning the problem of how to measure time-averaged pneumatic pressures. The systematic investigations which are available so far are limited to fluctuation frequencies of about 4 kHz. This is due to the relatively small devices which have been used to produce a periodically interrupted flow field. The magnitude of the

tangential velocities is limiting and the need to have the wave length equal to several times the probe dimension has placed a practical limit on the available frequency. It would be worthwhile to extend this region to ranges of about 10 kHz, which are typical characteristic blade passing frequencies in many machines. For this purpose wheels in the test section of the RGG could serve as nonsteady flow generators, only. By using different kinds of probes, with a calibrated high response probe as a reference device, the comparison of results for the same axial and radial locations (of course, in different circumferential positions) can be expected to give quantitative results of interest. Another advantage of the test-section is that in the downstream flow field, measurements can be made in measurement planes which cover a wide range in the axial direction. This can not be done in the TX without removing the stator and could not be done in many other similar research facilities. Doing similar measurements at different axial distances could lead to additional information concerning the problem of time averaging fluctuating pressures.

In these investigations it is suggested that an oil-filled measurement device such as is described in [33] and [34] be included. The reported probe is well understood and proven by its originators who have agreed to demonstrate its application in the RGG.

In the previous section, estimates were made with the aid of examples of how an incorrectly evaluated time-averaged total pressure can influence results obtained using the DPDS technique. Open questions are evident, and so far no other experience exists concerning the behavior of the A and B probes in areas of high subsonic and supersonic nonsteady flows.

The following remarks concern the application of the DPDS technique in the RGG: The first goal should be to provide additional qualitative information of the complex conical flow field, if possible for the current tests and if this can not be done in the time available, for future experiments.

The blade passing frequencies in the RGG are of the same order of magnitude as those in the TX. The maximum wheel speed is only half (250 revs/sec), but the number of blades can be 2.5 times larger. This can occur for a tip-section cascade with a pitch-to-chord ratio of 1., low stagger angle (about 20°) and low incidence angle (of the same range). This would result in a frequency of f = 12.5 kHz, which can be regarded as the highest frequency to be investigated. Assuming f = 10 kHz and 50 blades the maximum speed will be 200 revs/sec (12000 RPM) which may be a more realistic value.

For hub section cascades, where lower pitch-to-chord ratios are used (about .5) the number of blades is about 100 and, again, assuming f = 10 kHz will lead to speeds of 100

revs/sec (6000 RPM), which is about double what has been found to be necessary from past experience.

First of all it is necessary to provide a trigger system for the data acquisition. In principal, a variety of solutions are possible. A sketch in Fig. 56 demonstrates the one which is suggested for the RGG. The test-wheels themselves act as timing disks and two photo-electrical sensors (NANO-SCAN, Skan-A-Matic Corp., Elbridge, NY) are used to provide pulses at one-per-blade and one-per-revolution frequencies. The installation of the sensors within the inner casing (position Ⓐ, Fig. 56) is expected to be easy, mainly because the sensors have a flexible "snout" which in addition can provide an adjustment of the distance between the sensors and the wheel. For initial tests, which will be carried out without a device similar or equal to the "Pacer," only the "one-per-revolution" signal is needed.

On the back side of the test-wheels (see Fig. 56) radial straight lines are required to be coincident with the centers of the blades. This must be done accurately to provide a stable input to the pacer and permit data acquisition behind blade pairs of interest independent of minor wheel speed variations. Both one-per-blade and one-per-rev. time-mark-radii should be chosen to be as large as possible, to provide the most distinct electrical pulses.

The complete arrangement can be checked out using a disk which represents the wheel and speeding it up to test

conditions (up to 12,000/min) outside the test section. Such tests would provide answers concerning the optimum distance between sensor and wheel (a first estimate can be taken from data given in Skan-A-Matic's handbook) and will also determine what width of the marks in circumferential direction is necessary. If the width is small in comparison to the distance between two adjacent blades a "wave shaper" section in a pacer device (see Section III) may not be necessary. Consequently, the marks should first of all be made by simply laying it out with a metal scribe. It is possible that reasonable results could be obtained using a small groove filled with some kind of reflecting material.

It may be possible to use the blades themselves to provide the time-marks. In this case the second sensor would be installed in position (B), Fig. 56 and from position (A) only the "one per revolution" pulse would be needed. This procedure should be used if it is more complicated than expected to provide well defined time-marks for the case (A) as described. Complications for case (B) may result from the abrasive material used in the outer casing groove to guarantee optimum tip clearance. Perhaps particles of this material would disable the sensor. In any event, a "wave-shaper" would be necessary because the geometry of the blades would produce some kind of a bell-shaped signal.

The necessary investment is approximately 4000.-DM which includes two units and a third one for replacement purposes.

In Fig. 57 a sketch of a total pressure probe which can be used as an equivalent to the A probe is shown. Although it is desirable (or may be necessary) that the flow should act directly on the head of the sensor and even small volumes should be avoided because of resonance problems, geometric restrictions of the hardware do not allow such a design at the moment. In particular, the diameter of the holes in the casing where the probes can be inserted into the flow field is 6mm and, of course, the maximum value of the axial extension of a probe must be slightly less than this value. A rearrangement is not possible at the present time. Therefore, the proposed modified A probe is a compromise between what is possible and what is needed, however it is expected that it can serve adequately for familiarization with the new technique.

As shown in Fig. 57, the probe will rotate about an axis through the probe tip. Because of the design, manufacturing problems might occur, particularly since the transducers must be handled extremely carefully. In the knee-area (Fig. 57) a hole (for the transducer) and a slot (for the reference tube) are necessary to adjust the sensor in the indicated position. An adhesive secures the transducer in that location and is used for closing the hole and the slot. It may be worthwhile to use dummy transducers initially to find out whether the installation will work in the suggested way.

In Fig. 58 a second probe for the RGG is sketched which can serve for measurements of the static pressure (see for example Fig. 32). First of all this device should be used to obtain wall-static pressures in the different measurement planes where probes can be inserted. In addition, radial probe traverses in the annulus are possible using the probe because the dimensions are chosen to fit the traverse mechanisms. This may be most worthwhile in the upstream regions where the pitch angle, ϕ, is expected to be small but, nevertheless, it may also be of interest to try it downstream.

In comparison to a transducer which is flush-mounted in the usual way at the casing wall the probe in Fig. 58 takes more time to build and the additional expense is justified only because of its more varied use. It is, however, easier to build than the total pressure probe shown in Fig. 57 and does have the advantage that the flow acts directly on the sensor.

In addition, a pneumatic equivalent to the static pressure probe of Fig. 58 should be manufactured. This will allow an on-line calibration as discussed in Section IV, and comparisons can be made with a static pressure probe which is already available. In the annulus downstream, a five-hole cone probe (giving time averaged total pressure, yaw angle and pitch angle) would provide a better understanding of the time averaged flow field.

The RGG can also be used for the calibration of probes. In [1], [2], respectively the calibration of a temperature probe was carried out. In this case, the test-wheel was replaced by calibration rings which produced a contour over the inner cylindrical wall. The calibration rings were calculated as two-dimensional half-nozzles. Each ring was instrumented along the contoured surface with tappings to obtain surface pressure measurements to compare with the design distributions. Calibrations in the subsonic regime were carried out using a single ring producing a simple contraction. Different Mach numbers were produced by adjusting the flow rate generated by the radial supply compressor. For two different supersonic Mach numbers, 1.2 and 1.4, two different rings were constructed to designs which were produced by the method of characteristics.

In the case of conical test-sections, calibration rings are not necessary. The test-wheel is to be replaced by a disk which serves to complete the inner contour. With different compressor speeds and different bypass ratios the Mach number can be varied because the annulus is acting as a nozzle. In the measurement planes Ⓗ and Ⓘ, Fig. 55, even supersonic speeds can be set as can be seen from static pressure measurements along the inner and outer contours [47].

The Reynolds number can be controlled independently of the Macy number. This is effected by controlling independently

the total pressures and total temperatures in the closed cycle. The total pressure is regulated by either sucking with a rotary compressor of sliding vane type or by supplying air through the bypass-duct. The temperature is controlled by the cooler following the radial supply compressor [1 and 2].

With the devices and test procedures described in the previous paragraphs it should be possible to obtain information on the wake-flow behavior and boundary layer effects in the inner and outer casing wall areas. Information could be obtained initially simply by recording signals photographically from the screen of an oscilloscope, as demonstrated in Fig. 32.

So far, no provisions are discussed for the evaluation of pitch angles, ϕ. In [48] calculations based on a 3-dimensional time marching method are reported which indicate a remarkable streamline shift even when the blade height is relatively small. In the example given the flow was deflected from $\sigma_1 = 45^\circ$ at the inlet plane to $\sigma_2 \approx 30^\circ$ downstream. These numbers may be used to estimate the σ-ranges which may possibly occur in the experimental conditions. However, it is recommended that the techniques described above be applied first, and a device to enable pitch angle measurements should be designed later when a background of experience in the RGG has been established.

VII. CONCLUSION

The Dual Probe Digital Sampling (DPDS) Technique for measuring three dimensional flow fields in turbomachines has been described and its development at the Turbopropulsion Laboratory in recent years has been reviewed. Analysis of the first results in the transonic compressor at the Naval Postgraduate School was reported.

Two different data reduction procedures--an approximate analytical and a numerical one--were examined. When tested on data obtained in free jet experiments, the numerical method, which used calibration data arrays rather than analytical approximations of calibration data, was found to give the better results. This was explained as being the result of the inability of fourth order polynomial functions used in the analytical procedure to adequately represent the data over the required range of yaw angles. Nevertheless, the application of the numerical method of reduction to data from the compressor did not allow the velocity vector distribution to be determined with acceptable certainty.

In the analysis of the initial results, which is reported here, the behavior of high response probes as a function of yaw angle in a steady flow free jet and in the unsteady flow behind the rotor were shown to be different. The differences were greatest for data acquired within the clearly unsteady

region of the rotor blade wakes. Differences were least for data acquired within the nearly periodic region outside the blade wakes. Consequently it was concluded that measurements obtained in the compressor can not be reduced at the present time by a straightforward application of the reported methods to the acquired data using the calibration carried out in steady flow; to do so will lead to incorrect results with an unknown uncertainty. This result is thought to have important implications concerning the interpretation of unsteady data from more complex multiple-sensor probe geometries.

Speculative reasons for the differences in behavior were offered; however, time was not available to the author to investigate further. The full understanding must be left as the goal of the future program. It is suggested that close collaboration between and coordination of the programs at the Naval Postgraduate School and at the DFVLR-AVA Göttingen Fluid Dynamics Branch, where similar measurements are to be made in rotating cascades, will lead most efficiently to the required understanding and to further development of the DPDS and other high response probing techniques.

LIST OF REFERENCES

1. Heinemann, H.-J., "Ein neues Mess-u. Auswerteverfahren für Untersuchungen an rotierenden Runggittern," VDI-Forschungsheft 594 (1979), VDI-Verlag, Düsseldorf, West Germany.

2. Heinemann, H.-J., "The Test Facility for Rotating Annular Cascades of the DFVLR and Its Measurement and Evaluation Method," IEEE International Congress on Instrumentation in Aerospace Simulation Facilities, Monterey, California, September 24-26, 1979. Published in ICIASF '79 Record, IEEE Cat. No. 79CH1500-8AES.

3. Shreeve, R. P., McGuire, A. G., and Hammer, J. A., "Calibration of a Two-Probe Synchronized Sampling Technique for Measuring Flows Behind Rotors," IEEE International Congress on Instrumentation in Aerospace Simulation Facilities, Monterey, California, September 24-26, 1979. Published in ICIASF '79 Record, IEEE Cat. No. 79CH1500-8AES.

4. Dodge, F. J., "Development of a Temperature-Pneumatic Probe and Application at the Rotor Exit in a Transonic Compressor," M.S. Thesis, Naval Postgraduate School, Monterey, California, June 1976.

5. Paige, G. C., "Measurement of Case Wall Pressure Signatures in a Transonic Compressor Using Real-Time Digital Instrumentation," M.S. Thesis, Naval Postgraduate School, Monterey, California, June 1976.

6. West, J. C. Jr., "Digital Programmable Timing Device for Fast Response Instrumentation in Rotating Machines," M.S. Thesis, Naval Postgraduate School, Monterey, California, December 1976.

7. Larson, V. J., "Unsteady Effects on the Measurement of Total Pressure in Rotating Machines," M.S. Thesis, Naval Postgraduate School, Monterey, California, September 1977.

8. Winters, K. A., "Development of a Method for Measuring Velocity at the Exit of a Compressor Rotor Using Kulite Probes with Synchronized Sampling," M.S. Thesis, Naval Postgraduate School, Monterey, California, March 1978.

9. Harrison, J. A., "The Application of a Laser Doppler Velocimetry System to Flow Velocity Measurements in a Transonic Compressor," M.S. Thesis, Naval Postgraduate School, Monterey, California, December 1978.

10. McCarville, P. A., "Hardware and Software Improvements to a Paced Data Acquisition System for Turbomachines," M.S. Thesis, Naval Postgraduate School, Monterey, California, June 1981.

11. U.S. Patent No. 4,181,962, January 1980, "Digital Programmable Timing Device," inventors James C. West, Jr. and Raymond P. Shreeve.

12. Simmons, J. M., and Shreeve, R. P., "Data Acquisition and Analysis Techniques for Measurement of Unsteady Wall Pressures in a Transonic Compressor," Naval Postgraduate School Technical Report NPS-67Sf77071, Monterey, California, July 1977.

13. Adler, D., and Shreeve, R. P., "A General Procedure for Obtaining Velocity Vector from a System of High Response Impact Pressure Probes," Naval Postgraduate School Technical Report NPS67-79-007, Monterey, California, July 1979.

14. Adler, D., and Taylor, P. M., "A Procedure for Obtaining Velocity Vector from Two High Response Impact Pressure Probes," Naval Postgraduate School Technical Report NPS67-80-007, Monterey, California, August 1980.

15. Zebner, H., "Procedure and Computer Program for the Approximation of Data (with Application to Multiple Sensor Probes)," Naval Postgraduate School Contractor Report NPS67-80-001CR, Monterey, California, August 1980.

16. Zebner, H., "Transonic Compressor: Program TXCO for Data Acquisition and On-Line Reduction," Naval Postgraduate School Contractor Report NPS67-80-02CR, Monterey, California, October 1980.

17. Neuhoff, F., "Calibration and Application of a Combination Temperature-Pneumatic Probe for Velocity and Rotor Loss Distribution Measurements in a Compressor," Naval Postgraduate School Contractor Report NPS67-81-03CR, Monterey, California, December 1981.

18. Shreeve, R. P., "Real Time Measurements in a Transonic Compressor," in Transonic Flow Problems in Turbomachinery, editors: T. C. Adamson and M. F. Platzer, Hemisphere Publishing Corporation, Washington/London, 1977.

19. Shreeve, R. P., Anderson, D. J., and Olson, J. A., "Velocity Vector Determination from Multi-Sensor Pneumatic Probe Measurements," AIAA Journal, Vol. 15, No. 11, November 1977, pp. 1539-1540.

20. Shreeve, R. P., Dodge, F. J., Hawkins, W. R., and Larson, V. J., "Probe Measurements of Velocity and Losses from a Small Axial Transonic Rotor," paper presented at AIAA 11th Fluid and Plasma Dynamics Conference, July 10-12, 1978, Seattle, Washington. AIAA Paper No. 78-1198.

21. Shreeve, R. P., Simmons, J. M., Winters, K. A., and West, J. C. Jr., "Determination of Transonic Compressor Flow Field by Synchronised Sampling of Stationary Fast Response Transducers," in Nonsteady Fluid Dynamics, ASME 1978 Winter Annual Meeting, San Francisco, California, December 15-16, 1978.

22. Thompkins, W. T. Jr., and Kerrebrock, J. L., "Exit Flow from a Transonic Compressor Rotor," AGARD-CP 177, 1976.

23. Kerrebrock, J. L, Epstein, A. H., and Thompkins, W. T. Jr., "A Miniature High Frequency Sphere Probe," in Measurement Methods in Rotating Components of Turbomachinery, Joint Fluids Engineering Gas Turbine Conference of ASME, New Orleans, Louisiana, March 10-13, 1980, editors: B. Lakshminarayana and P. Rundstadler, Jr.

24. Kerrebrock, J. L., "Flow in Transonic Compressors, AIAA Journal, Vol. 19, No. 1, January 1981.

25. Junkhan, G. H., "Analysis of Simulated Axial-Flow Turbomachine Wakes for Estimation of Frequency-Response Requirements for Fast-Response Pressure Probes," Engineering Research Institute, Iowa State University, Ames, Iowa, ERI-73170, Preprint, Project 636(101), August 1973. [This paper was prepared for submission for review for possible presentation at the 1974 ASME Gas Turbine Conference.]

26. Krause, L. N., Dudzinski, T. J., and Johnson, R. C. "Total Pressure Averaging in Pulsating Flows," Progress in Astronautics and Aeronautics, Volume 34: Instrumentation for Airbreathing Propulsion, editors: A. E. Fuhs and M. Kingery, The MIT Press, Cambridge, Massachusetts, U.S.A. and London, U.K., 1977.

27. Grande, E., and Oates, G. C., "Response of Miniature Pressure Transducers to Fluctuations in Supersonic Flow," in: Transonic Flow Problems in Turbomachinery, editors: T. C. Adamson and M. F. Platzer, Hemisphere Publishing Corporation, Washington/London, 1977.

28. Bennett, J. C., "Measurements of Periodic Flows in Rotating Machinery," AIAA 10th Fluid and Plasma Dynamics Conference, Albuquerque, New Mexico, June 27-29, 1977.

29. Spivak, J. A., "Development of a Fast-Response Total Pressure Probe for Use in an Axial Flow Fan," Applied Research Laboratory, Post Office Box 30, State College, Pennsylvania, 16801, Report Number 79-182, October 1979.

30. Matsunaga, S., Ishibashi, H., and Nishi, M., "Accurate Measurement of Nonsteady Three-Dimensional Incompressible Flow by Means of a Combined Five-Hole Probe," in Nonsteady Fluid Dynamics, the Winter Annual Meeting of ASME, San Francisco, California, U.S.A., December 10-15, 1978.

31. Fleeter, S., Jay, R. L., and Bennett, W. A., "Wake Induced Time-Variant Aerodynamics Including Rotor-Stator Axial Spacing Effects," in Nonsteady Fluid Dynamics, the Winter Annual Meeting of ASME, San Francisco, California, U.S.A., December 10-15, 1978.

32. Prince, T. C., "Transducer Pressure Data Reduction Program," General Electric, Flight Propulsion Division, Report No. R67FPD170 (1967), Cincinnati, Ohio.

33. Weyer, H. B., and Schodl, R., "Development and Testing of Techniques for Oscillating Pressure Measurements Especially Suitable for Experimental Work in Turbomachinery," Transactions of the ASME, Journal of Basic Engineering, Vol. 93, December 1971, pp. 603-609.

34. Weyer, H. B., "Bestimmung der zeitlichen Druckmittelwerte in stark fluktuierender Strömung, insbesondere in Turbomaschinen." DLR-FB 74-34, 1974.

35. Weyer, H. B., and Schodl, R., "Unsteady Flow Measurements in Turbomachinery," AGARD-AG-207, 1975.

36. Weyer, H. B., and Hungenberg, H. G., "Analysis of Unsteady Flow in a Transonic Compressor by Means of High Response Measuring Techniques," AGARD-CP 177, 1976.

37. Schodl, R., and Weyer, H. B., "Nonintrusive Measurements of the Flow Vectors within the Blade Passages of a Transonic Compressor Rotor," in Transonic Flow Problems in Turbomachinery, editors: T. C. Adamson and M. F. Platzer, Hemisphere Publishing Corporation, Washington/London, 1977.

38. Eckardt, D., "Untersuchung der instationären Strömung in hochbelasteten Turboverdichtern mit Hilfe neu entwickelter Messverfahren," VDI-Berichte Nr. 193, 1973, VDI Verlag, Düsseldorf, West Germany.

39. Gallus, H. E., "Results of Measurements of the Unsteady Flow in Axial Subsonic and Supersonic Compressor Stages," AGARD-CP 177, 1976.

40. Gallus, H. E., Bohn, D., and Broichhausen, K.-D., "Unsteady Upstream Effects in Axial-Flow Supersonic Compressor Stages," ASME Paper 79-GT-55, ASME Conference, San Diego, California, March 1979.

41. Wallmann, Th., "Experimentelle Untersuchungen zur Wechselwirkung zwischen stehenden und umlaufenden Schaufelreihen einer Unterschall-Axialverdichterstufe," dissertation RWTH Aachen, West Germany, 1980.

42. Lambertz, F., "Instationäre Schaufelkräfte Axialer Turbomaschinen und ihre Auswirkungen auf dynamische Belastung und Lärmentwicklung," dissertation RWTH Aachen, West Germany, 1980.

43. Bammert, K., and Rautenberg, M., "Messung zeitlich veränderlicher Strömungsvorgänge im Radialverdichter, VDI-Berichte Nr. 193, 1973, VDI Verlag, Düsseldorf, West Germany.

44. Vavra, M. H., and Shreeve, R. P., "A Description of the Turbopropulsion Laboratory in the Aeronautics Department at the Naval Postgraduate School," Naval Postgraduate School Technical Report NPS-57Va72091A, Monterey, California, September 1972.

45. Neuhoff, F., "Further Development of a Dual-Probe Digital Sampling (DPDS) Technique for Measuring Flow Fields in Rotating Machines," Naval Postgraduate School Contractor Report NPS67-82-01CR, Monterey, California, November 1982.

46. Welsh, B. L., and Pyne, C. R., "A Method to Improve the Temperature Stability of Semiconductor Strain Gauge Pressure Transducers," Royal Aircraft Establishment (RAE) Technical Report 77155, Farnborough, U.K., October 1977.

47. Lehthaus, F., and Heinemann, H.-J., "Experimentelle und theoretische Untersuchungen über den Einfluss der Konizität auf die Strömung durch Turbinengitter im transsonischen Geschwindigkeitsbereich (2. Arbeitsfortschrittsbericht)," DFVLR-Report 251 80 C 05 (1980).

48. Braunling, W., and Lehthaus, F., "Experimentelle und theoretische Untersuchungen über den Einfluss der Konizität auf die Strömung durch Turbinengitter im transsonischen Geschwindigkeitsbereich," DFVLR-Report IB 222 82 A 01 (1982).

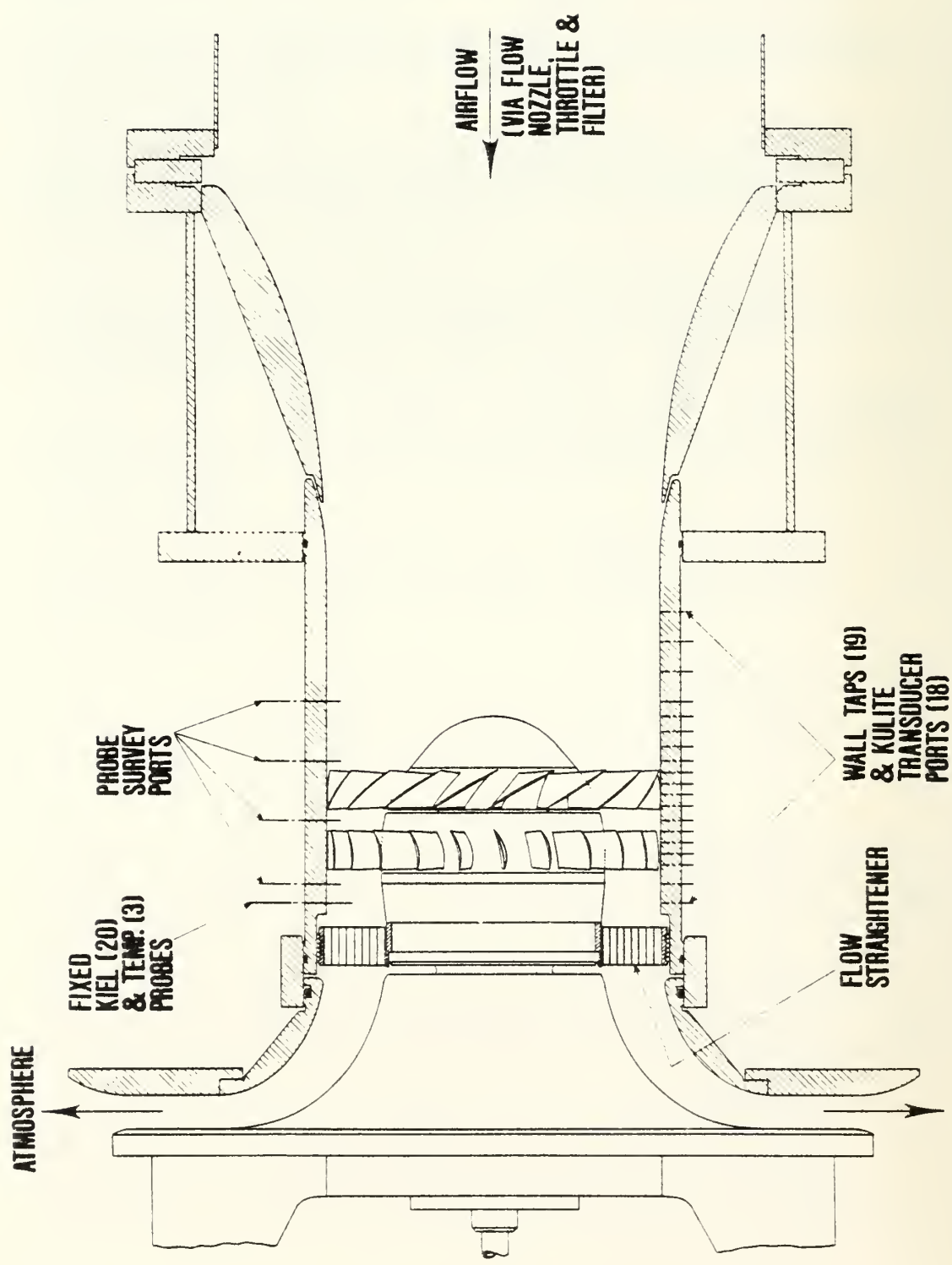

Figure 1: Transonic Compressor (TX)

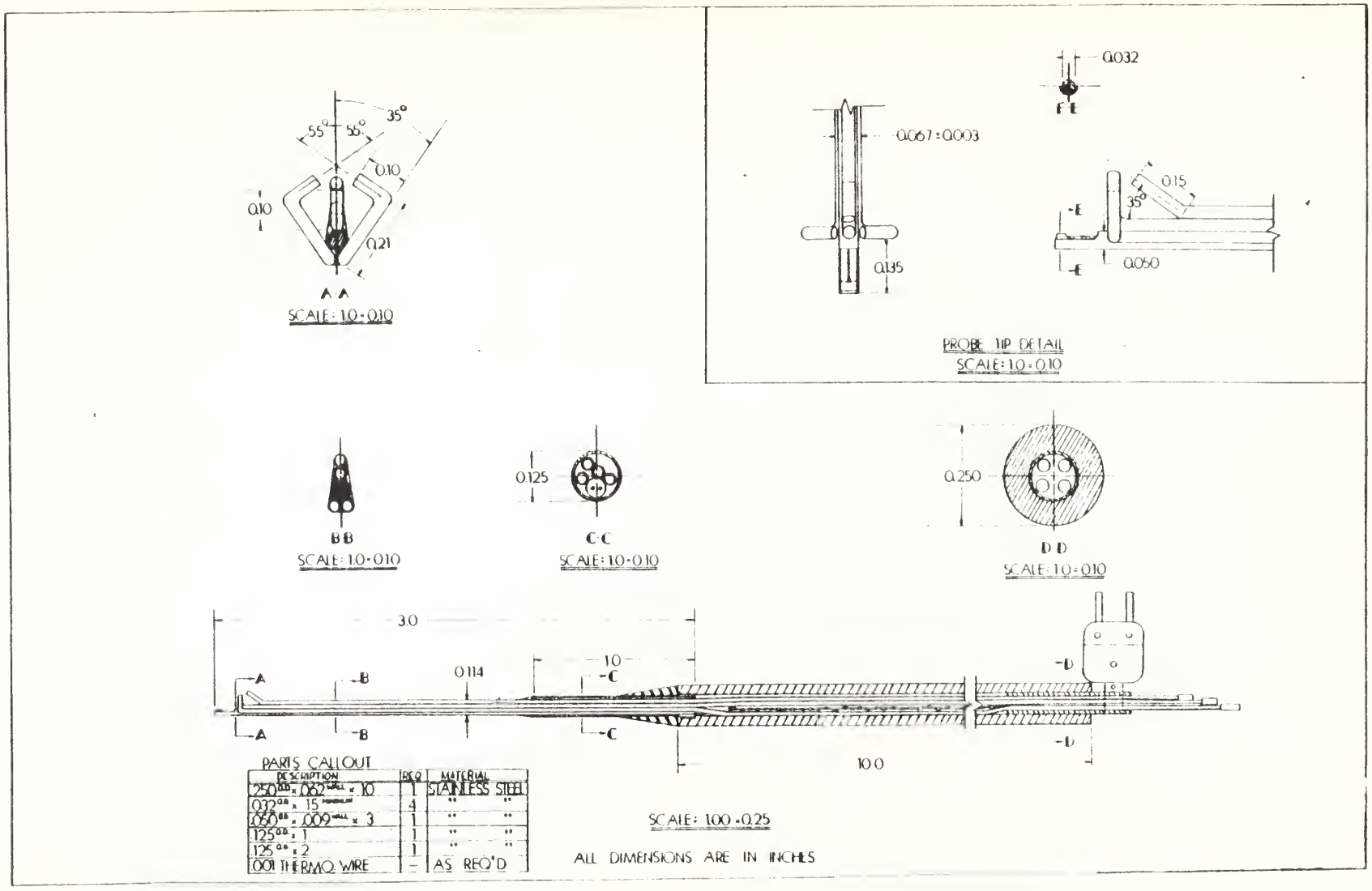

Figure 2: Geometry of the Combination Probe

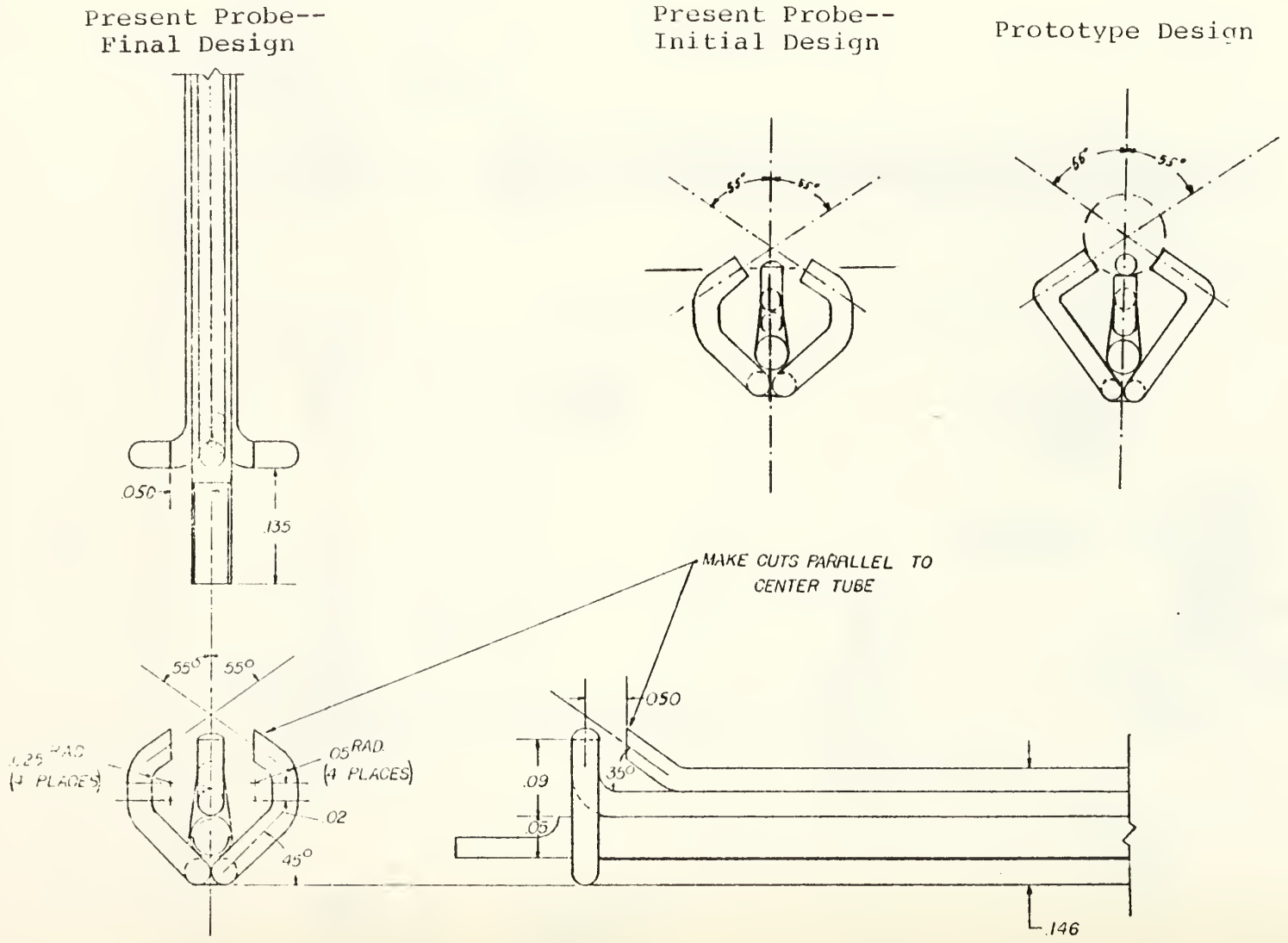

Figure 2 (Continued)

Figure 3: Arrangement of probes in the TX

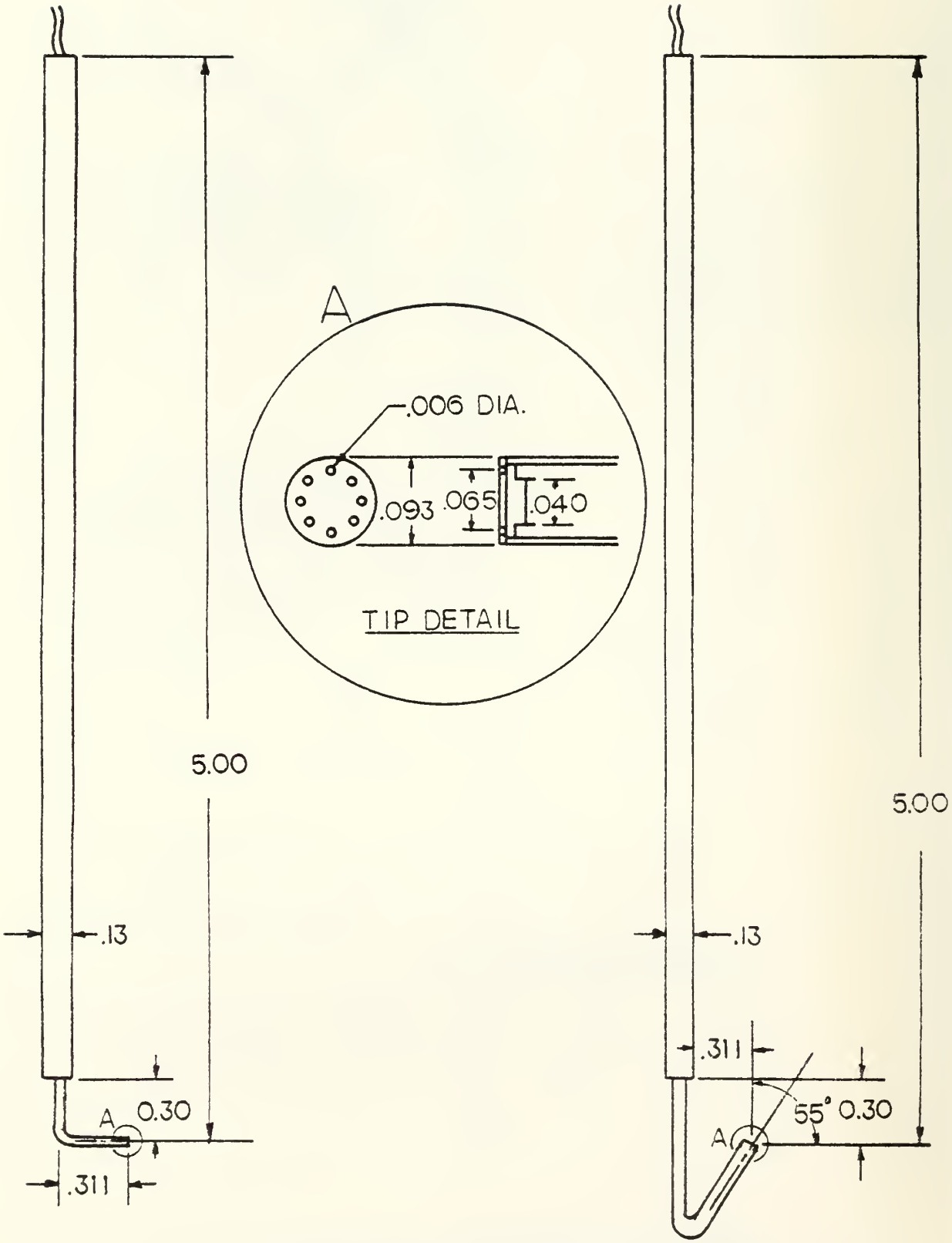

Figure 4: Probe Geometries

as viewed from drive-end (with 0° case angle):

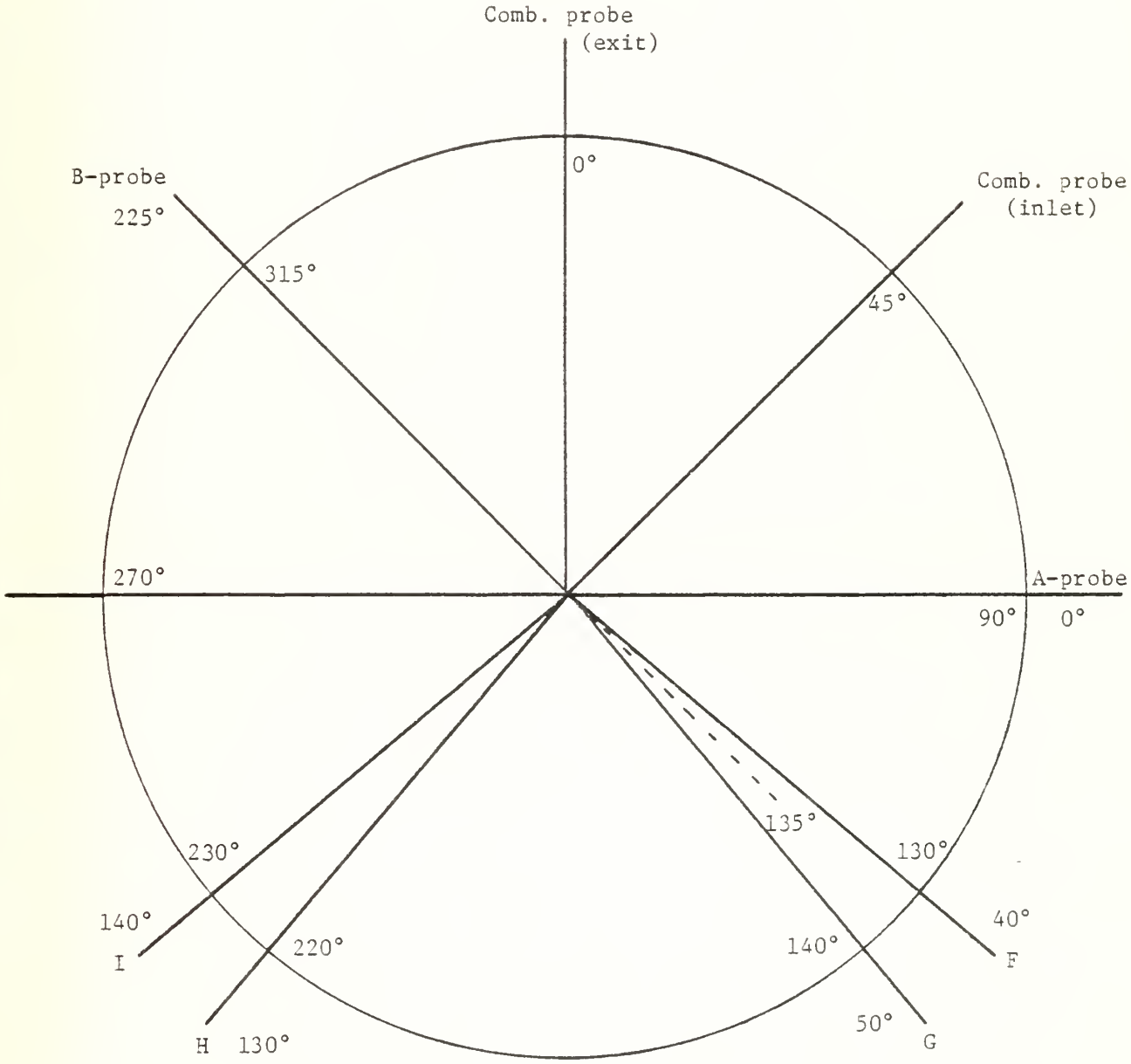

A/D Channel	0	1	2	3	4	5	6	7	8	9	10	11	12	13
Kulite K	A	B	6	7	7.5	8	8.5	9	9.5	10	10.5	11	12	13
Counts	0	1440	256	320	832	256	896	320	832	256	896	320	256	320
Axial Location [mm]			34	21	13	8	3	0	-6	-11	-15	-21	-29	-43

Figure 5: Configuration of probes and locations of case-wall transducers

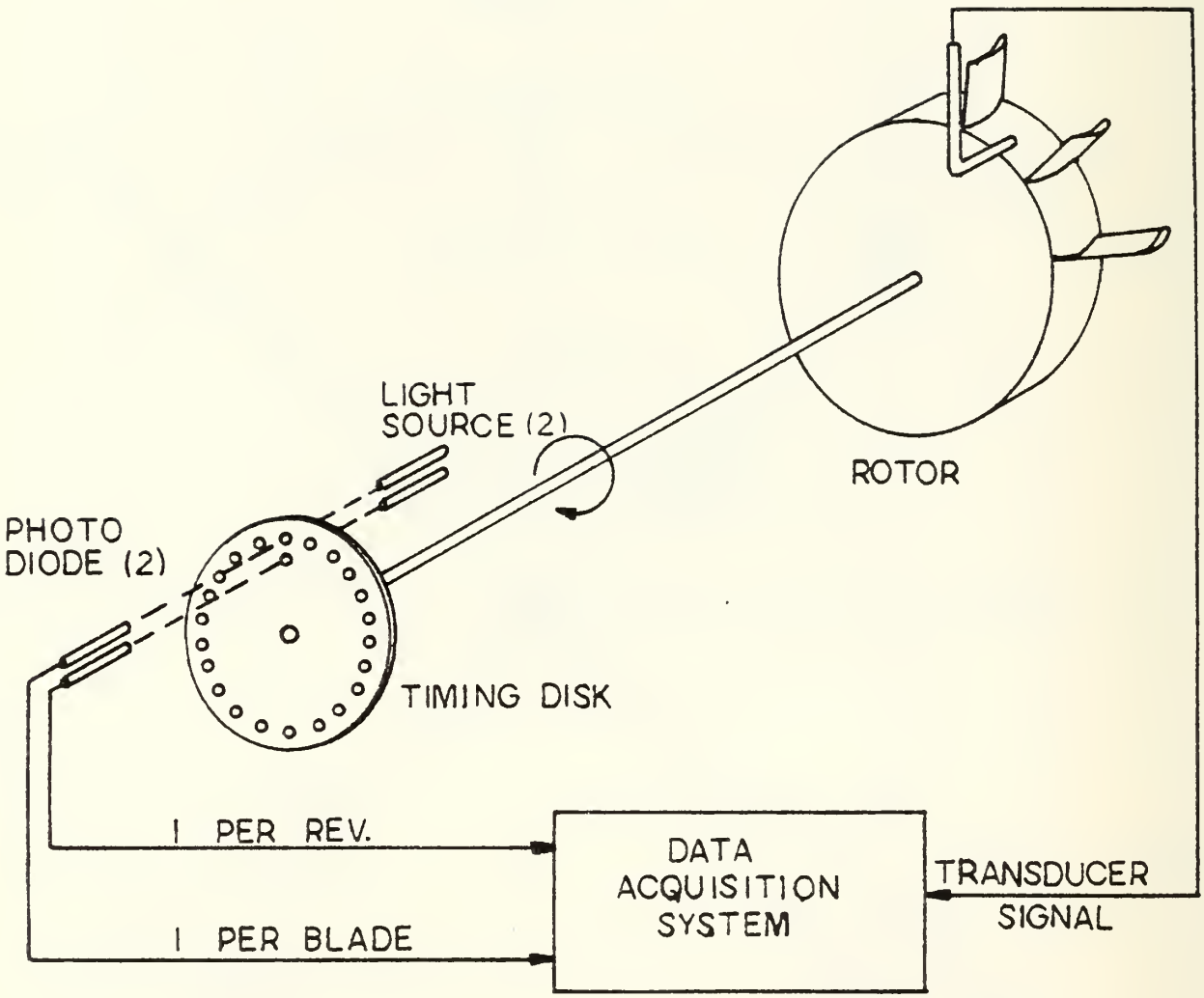

Figure 6: DPDS Technique

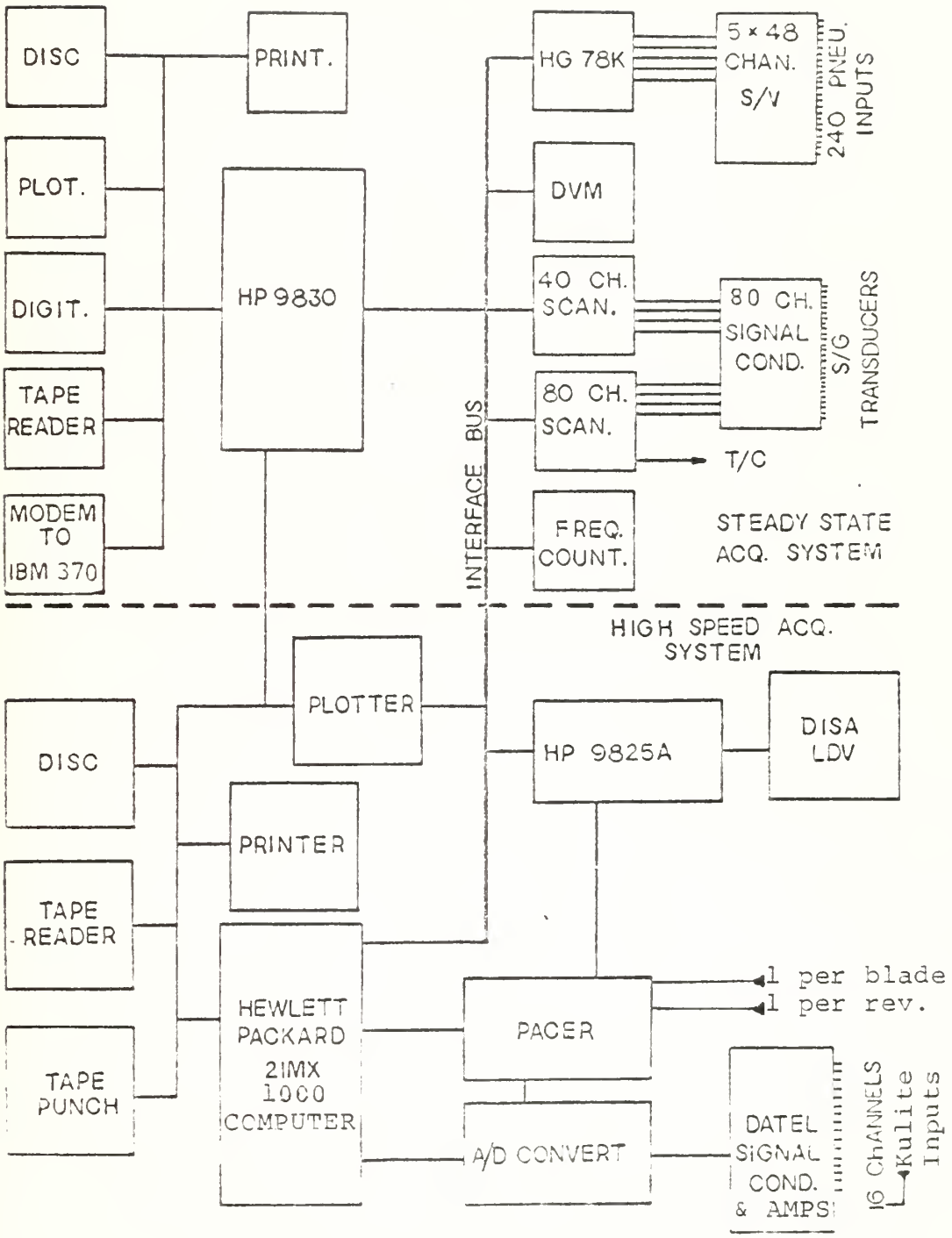

Figure 7: Data Acquisition System

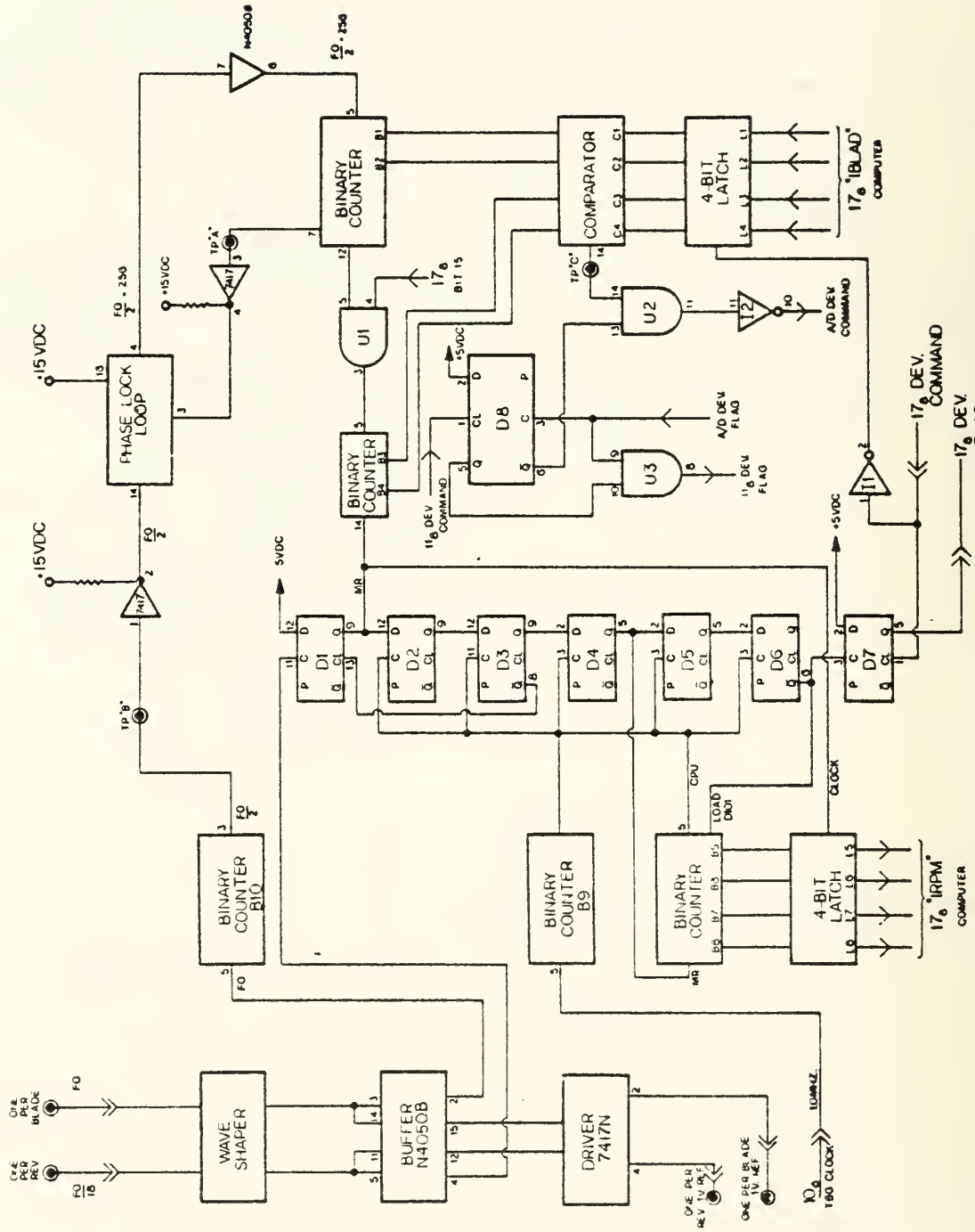

Figure 8: Schematic of "Pacer"

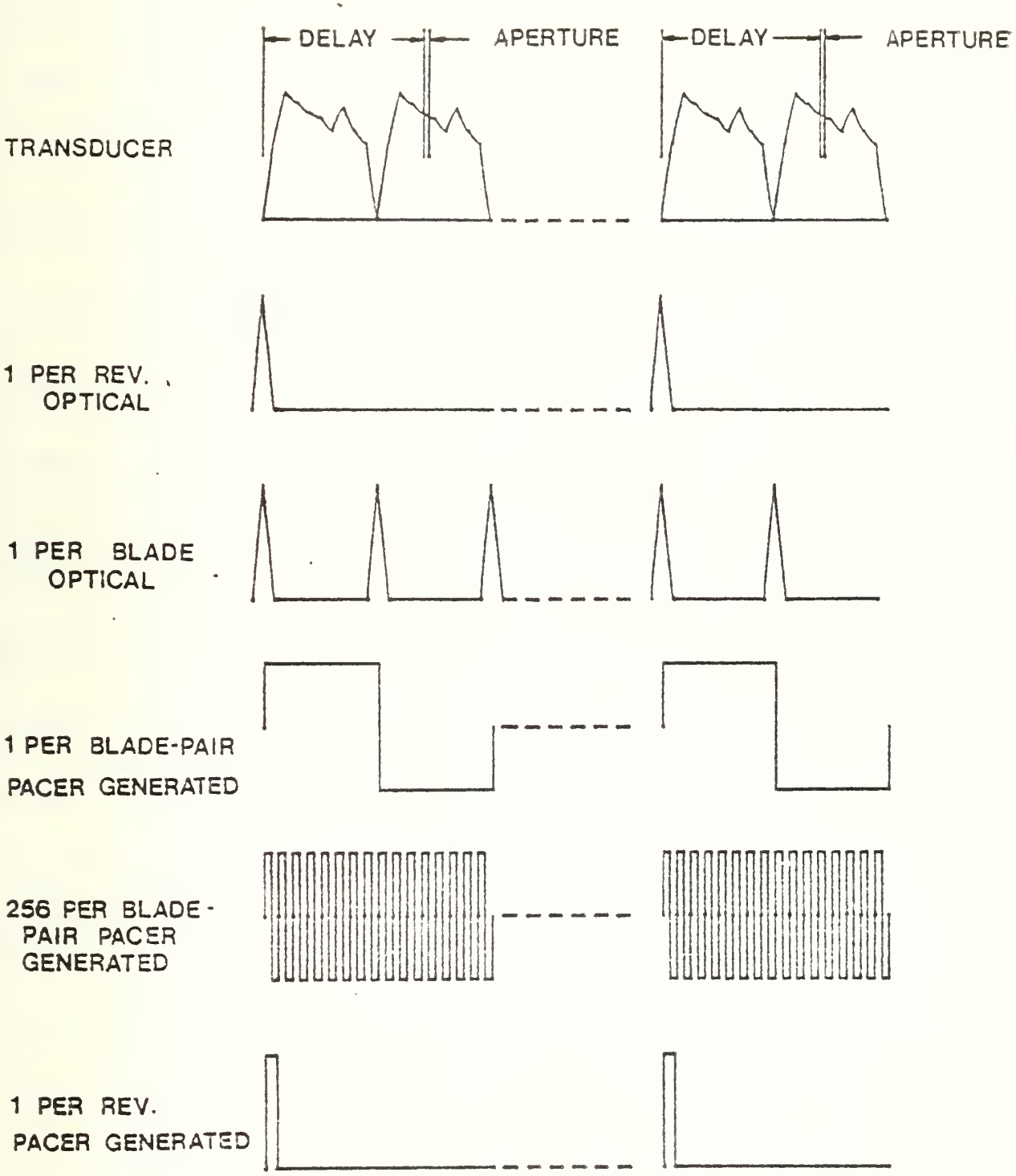

Figure 9: Synchronized sampling signals

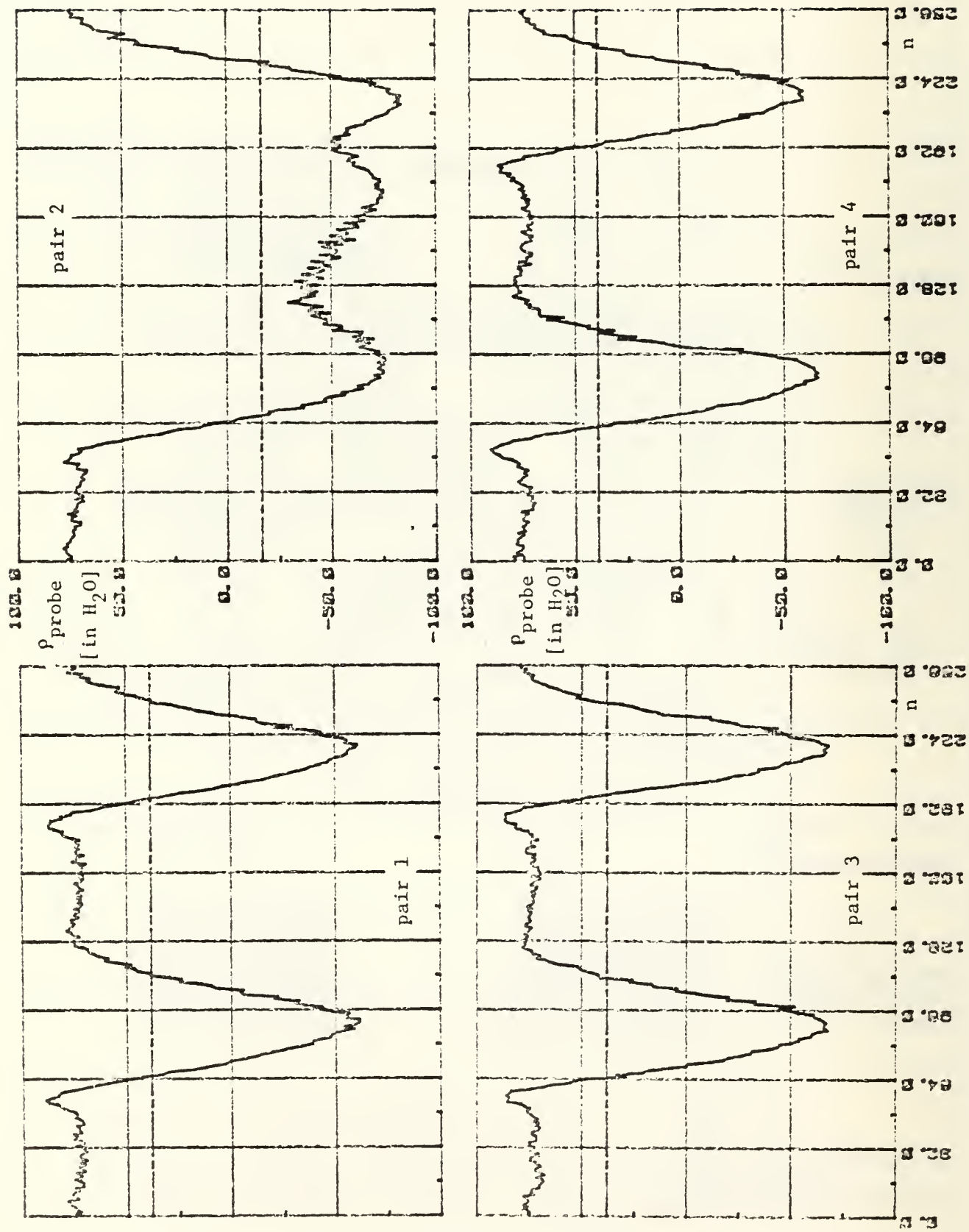

Figure 10: Results from the PFG; p_{plenum} = 15l in H_2O; p_{ref} = 80 in H_2O; f = 4.5 kHz; rep = 10

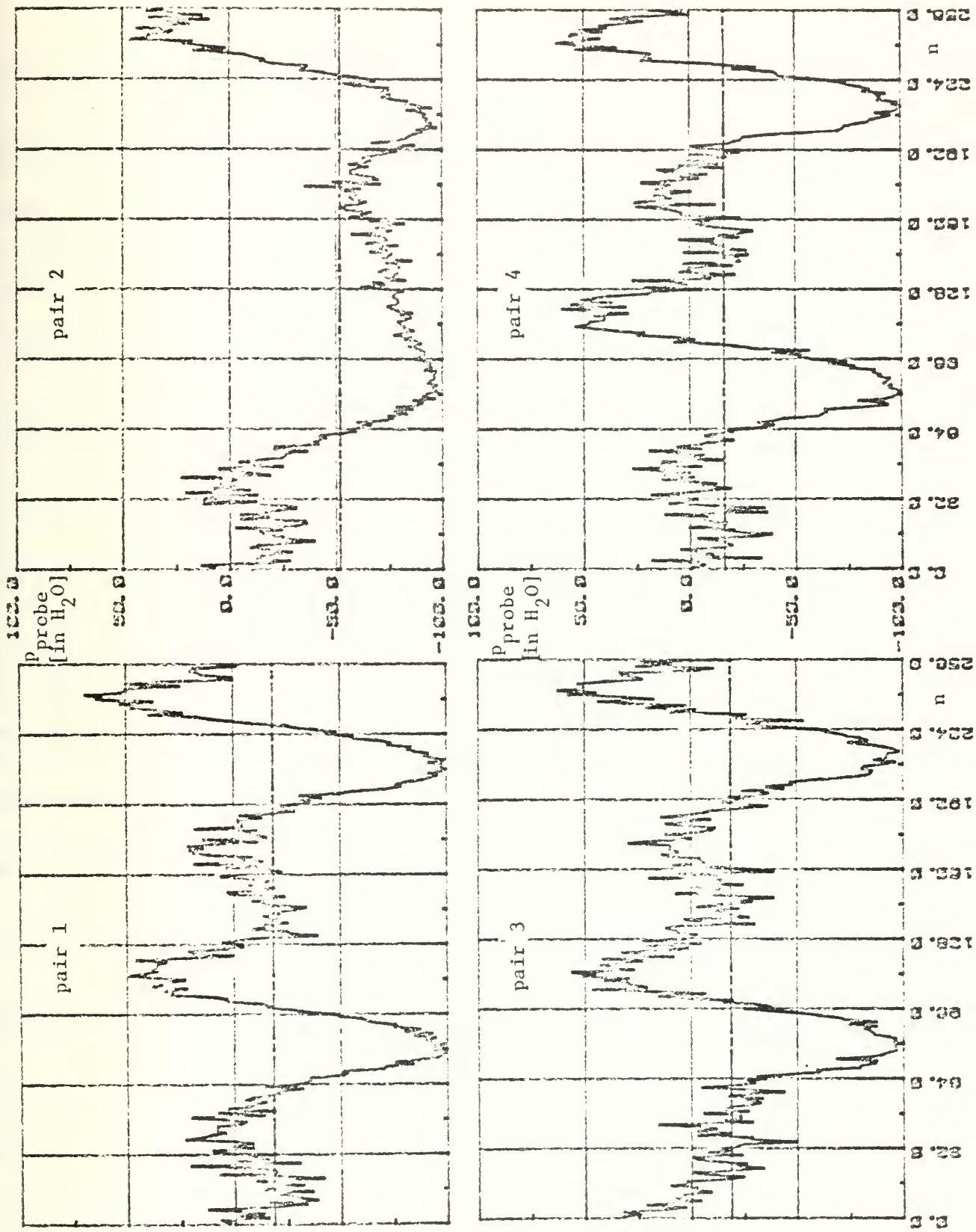

Figure 11: Results from the PFG; p_{plenum} = 146 in H_2O; p_{ref} = 80 in H_2O; f = 9.8 kHz; rep = 10

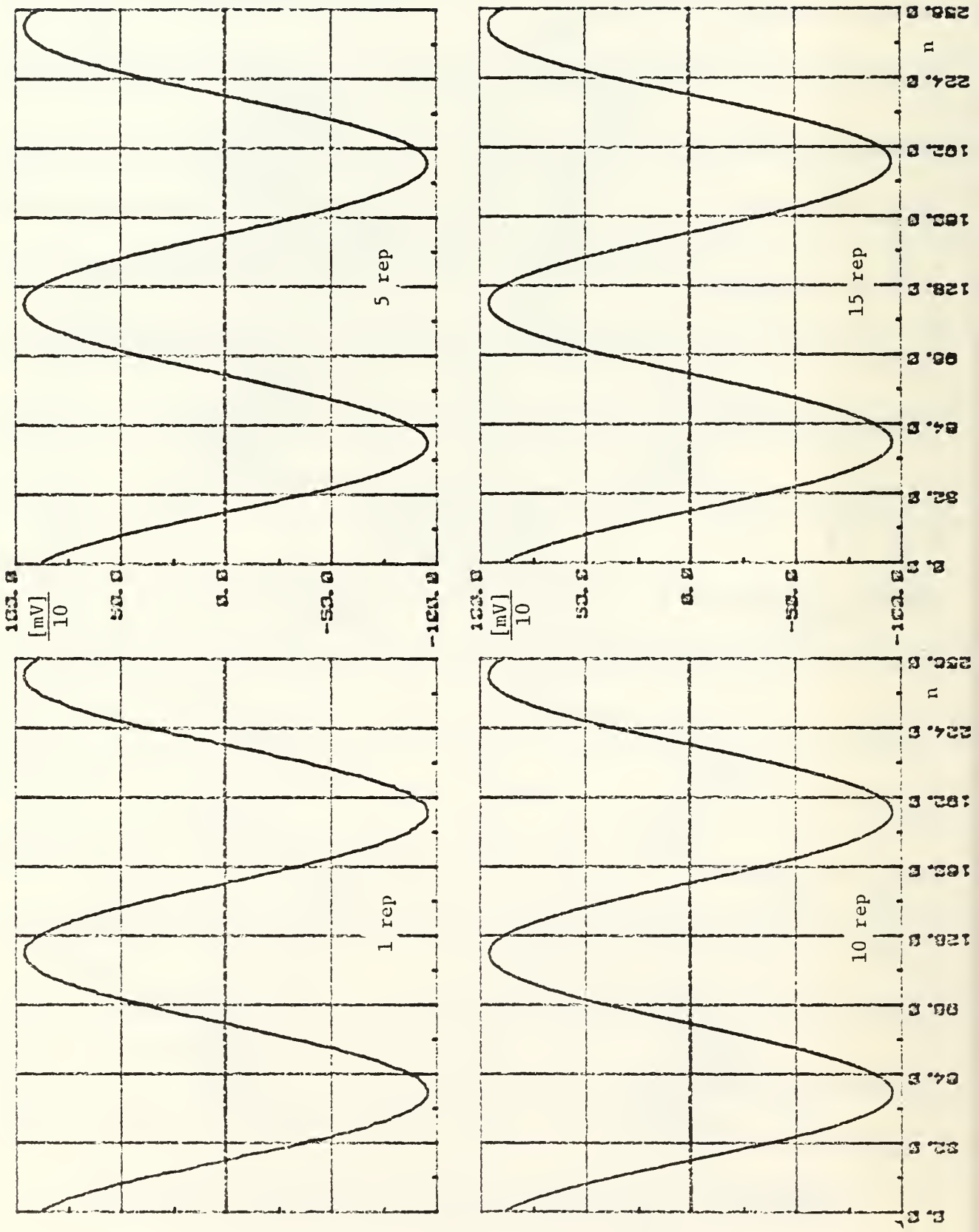

Figure 12: Frequency, generated with wave-generator; f = 10 kHz

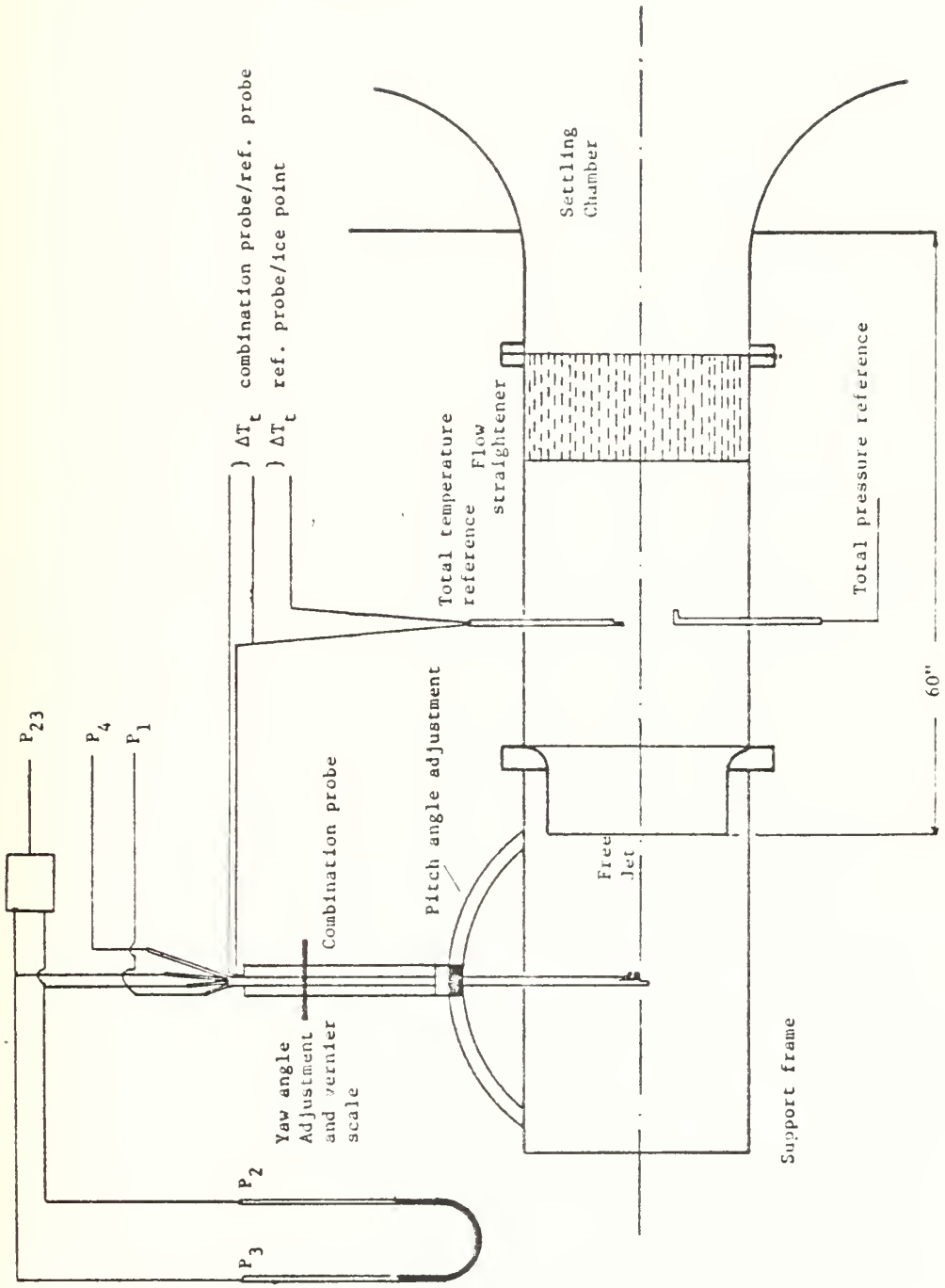

Figure 13: Calibration facility geometry (not to scale)

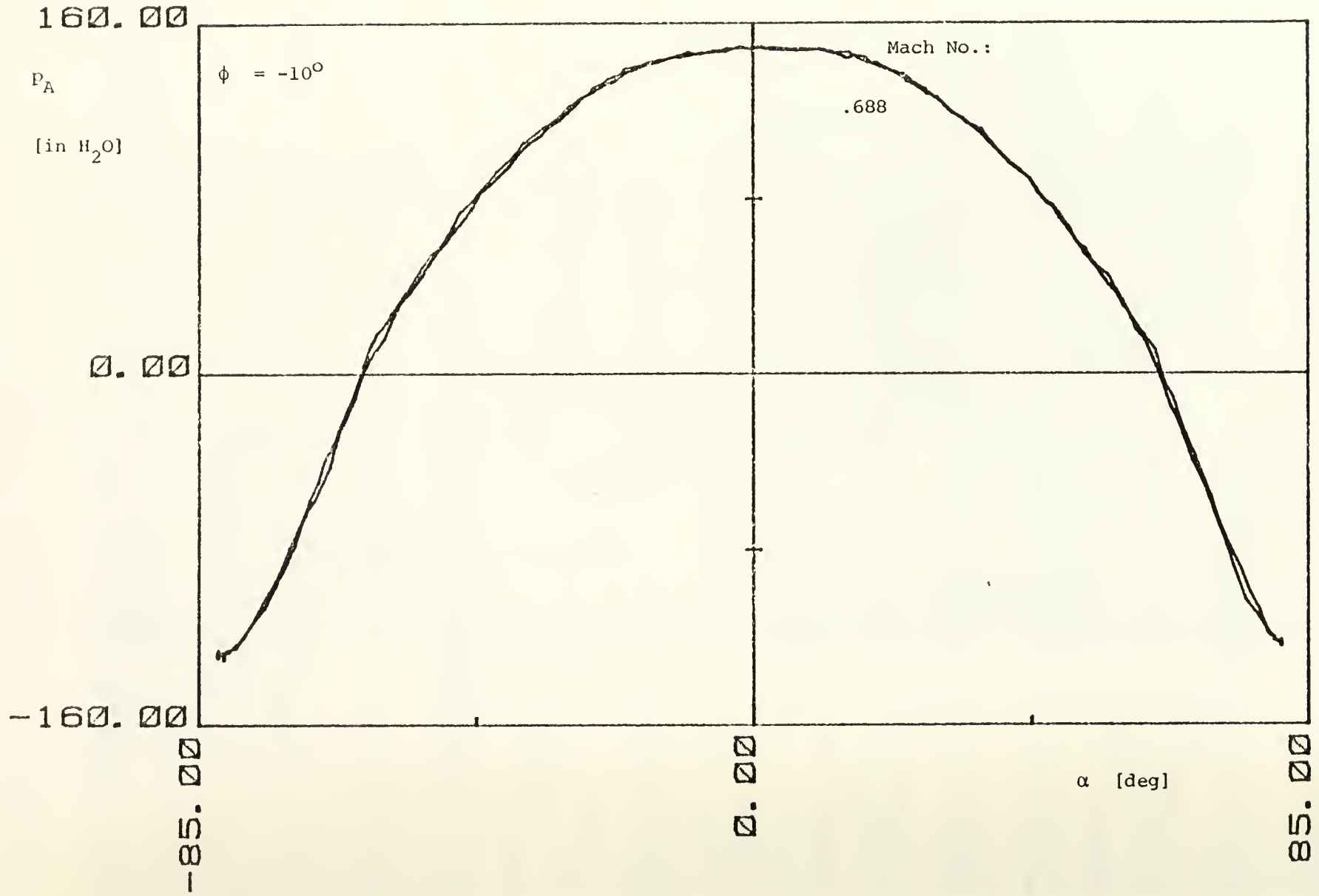

Figure 14: $p_A = f(\alpha)$

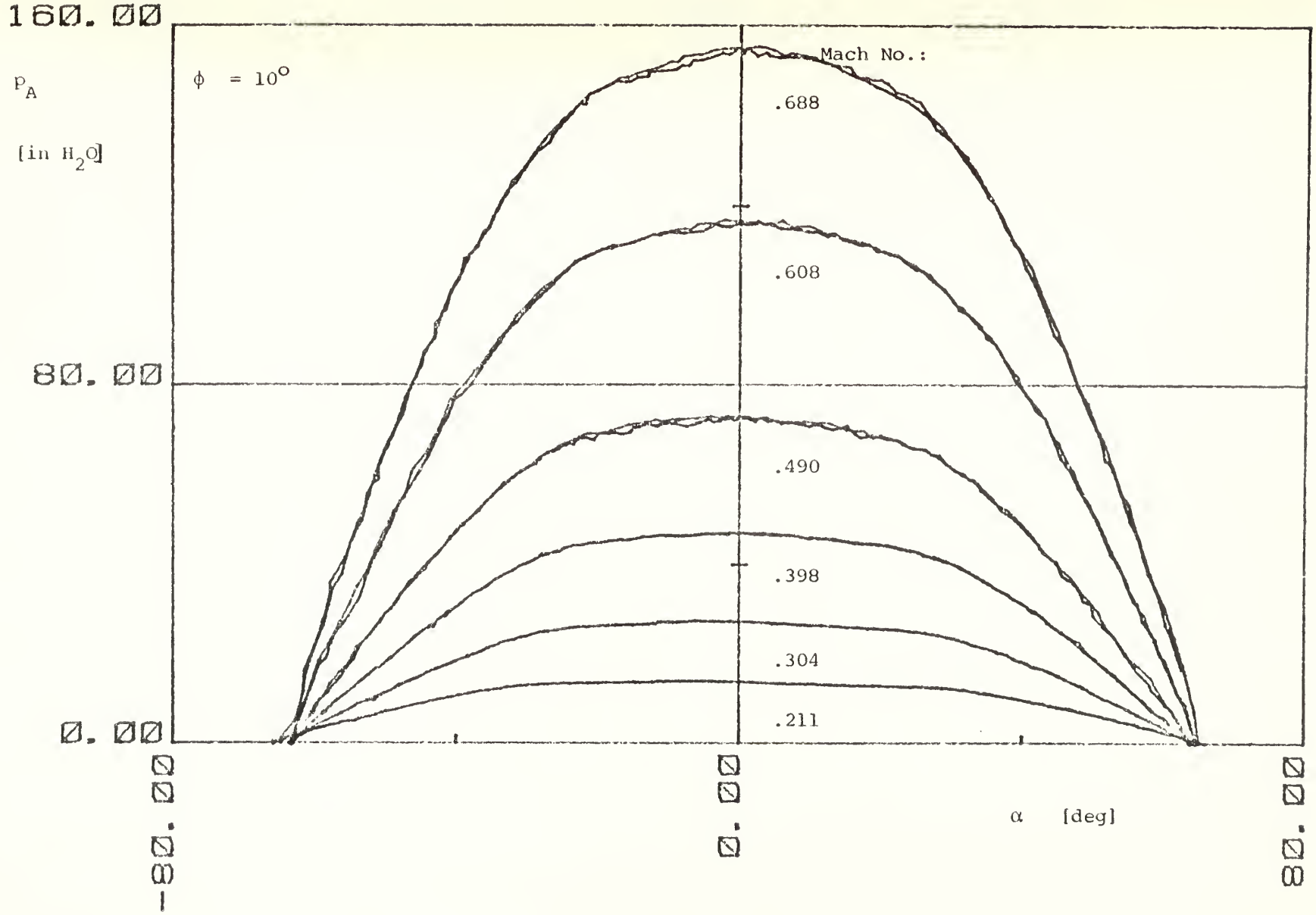

Figure 15: $p_A = f(\alpha)$

Figure 16: $p_A = f(\alpha)$

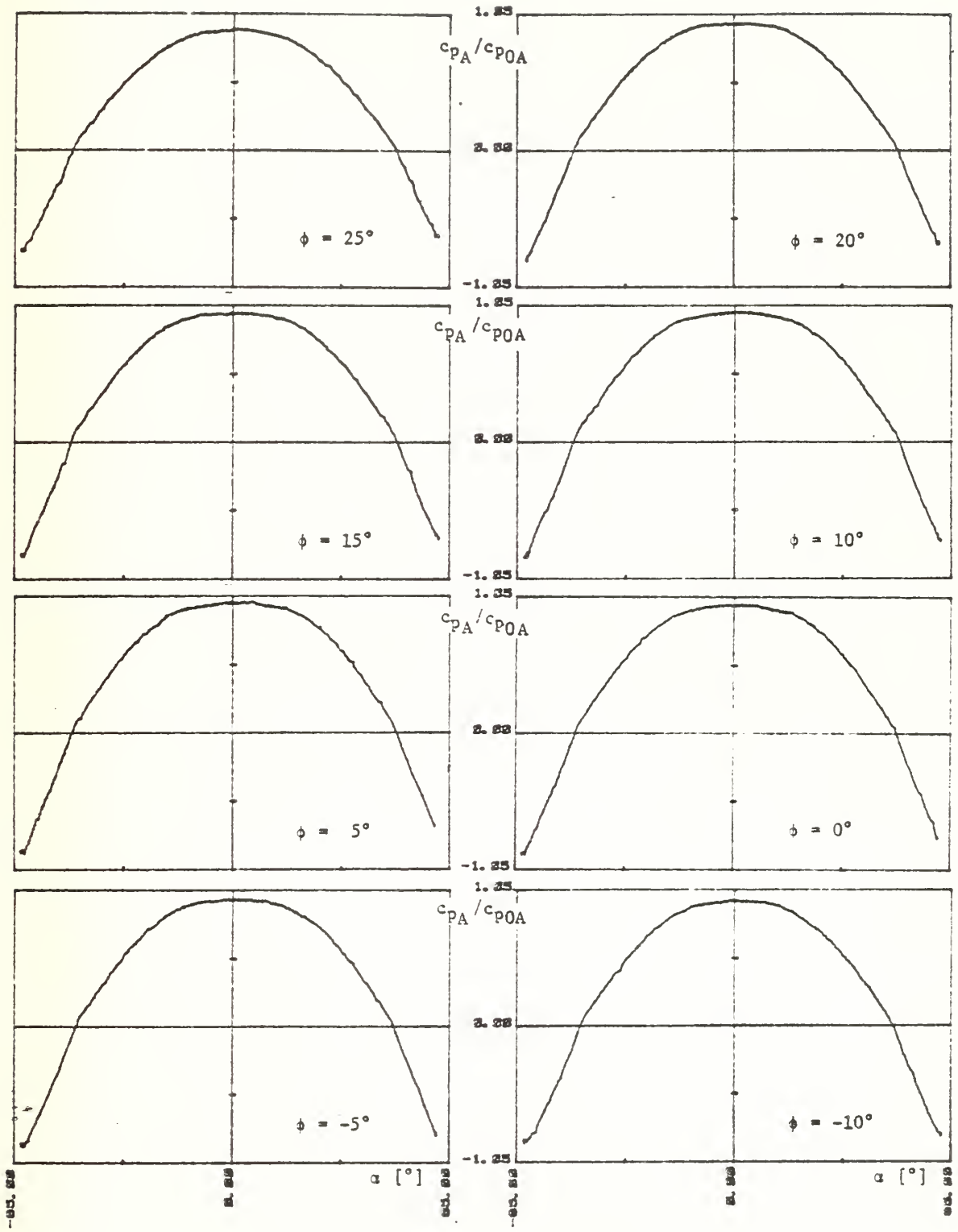

Figure 17: c_{pA}/c_{p0A} versus α; M = .6

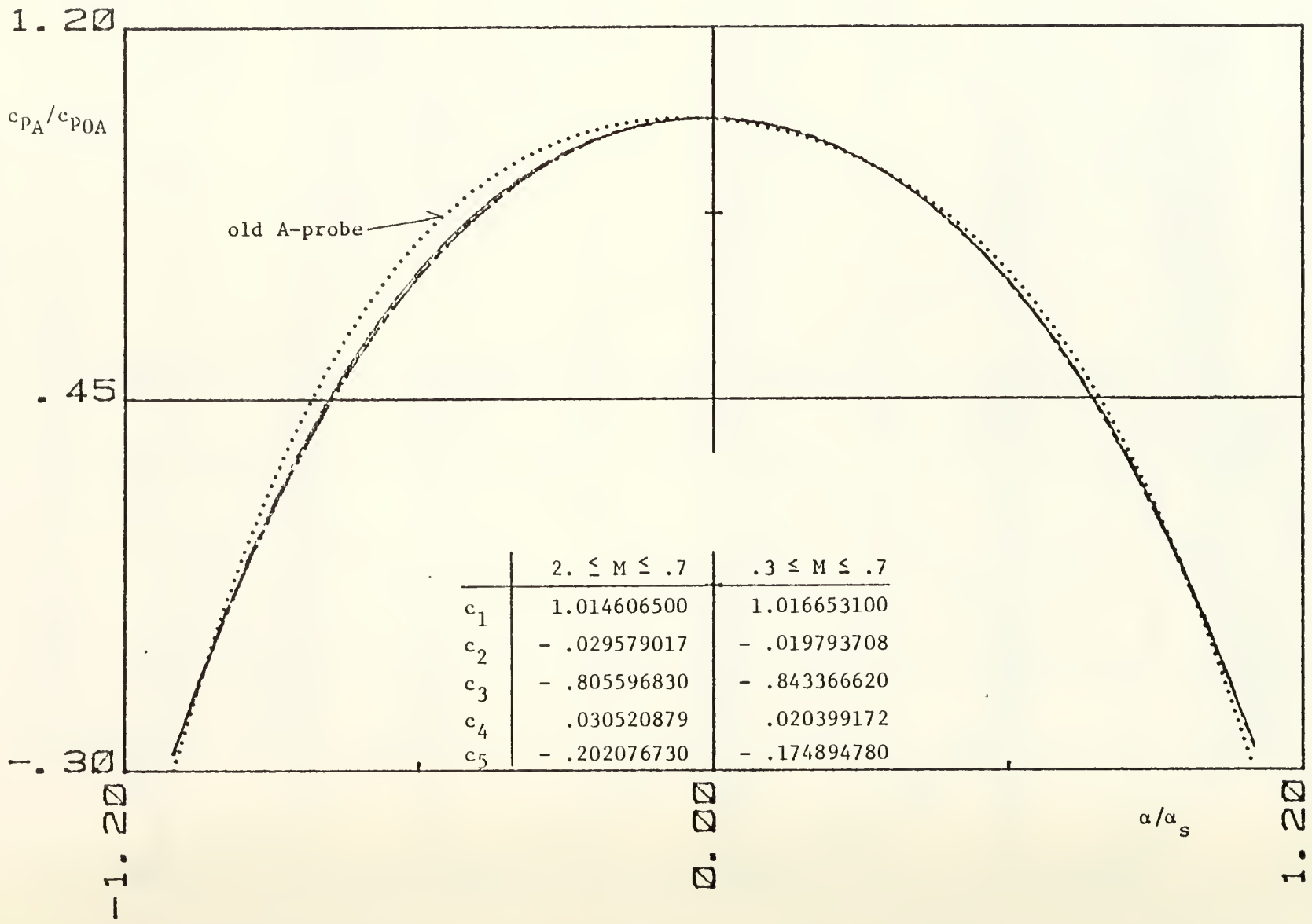

	2. ≤ M ≤ .7	.3 ≤ M ≤ .7
c_1	1.014606500	1.016653100
c_2	- .029579017	- .019793708
c_3	- .805596830	- .843366620
c_4	.030520879	.020399172
c_5	- .202076730	- .174894780

Figure 18: $c_{P_A}/c_{P0A} = f(\alpha/\alpha_s)$

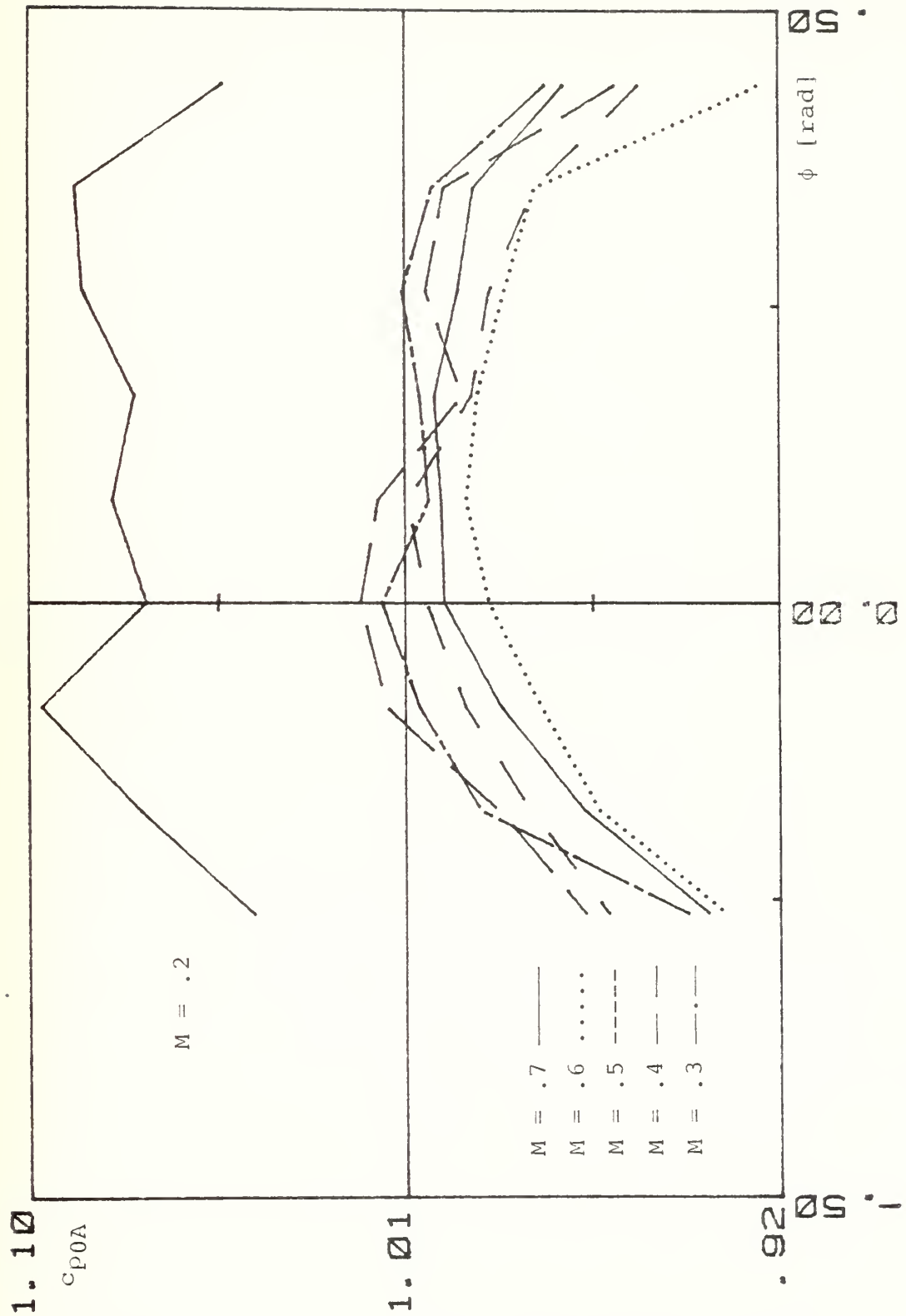

Figure 19: $c_{p_{0A}} = f(\phi)$; experimental results

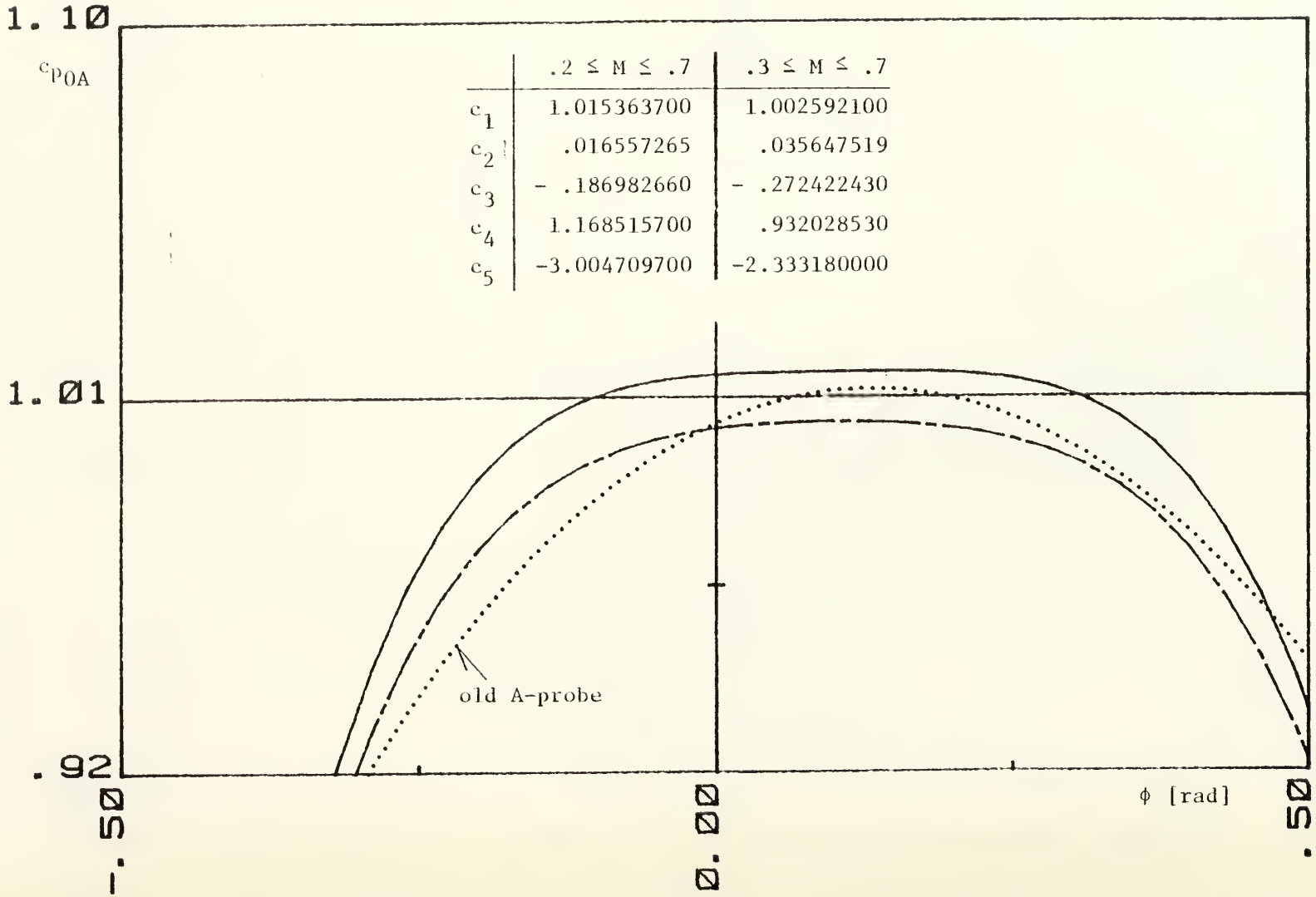

	.2 ≤ M ≤ .7	.3 ≤ M ≤ .7
c_1	1.015363700	1.002592100
c_2	.016557265	.035647519
c_3	- .186982660	- .272422430
c_4	1.168515700	.932028530
c_5	-3.004709700	-2.333180000

Figure 20: $c_{p_{0A}} = f(\phi)$; after curve-fit

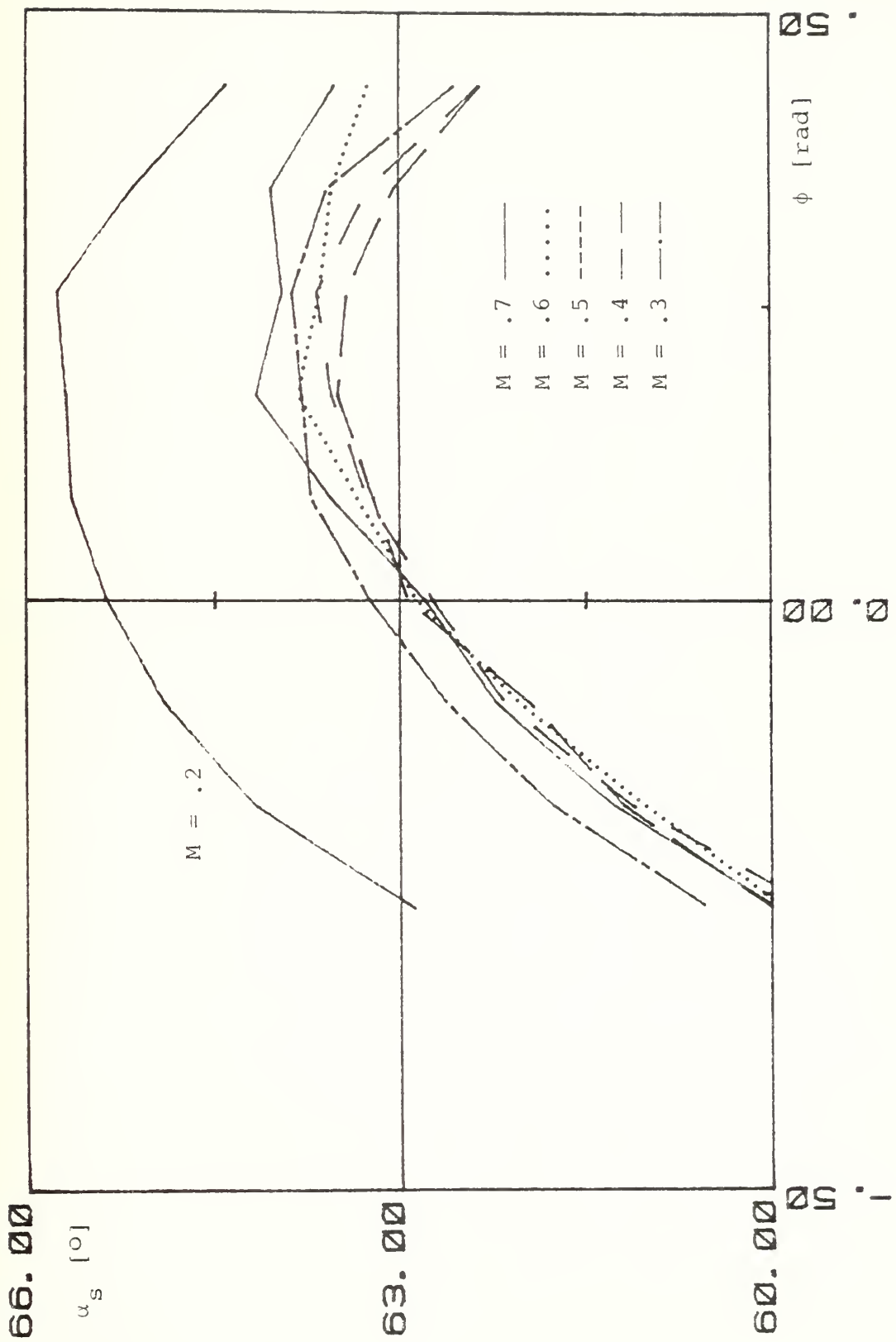

Figure 21: $\alpha_s = f(\phi)$; experimental results

Figure 22: $\alpha_s = f(\phi)$; after curve-fit

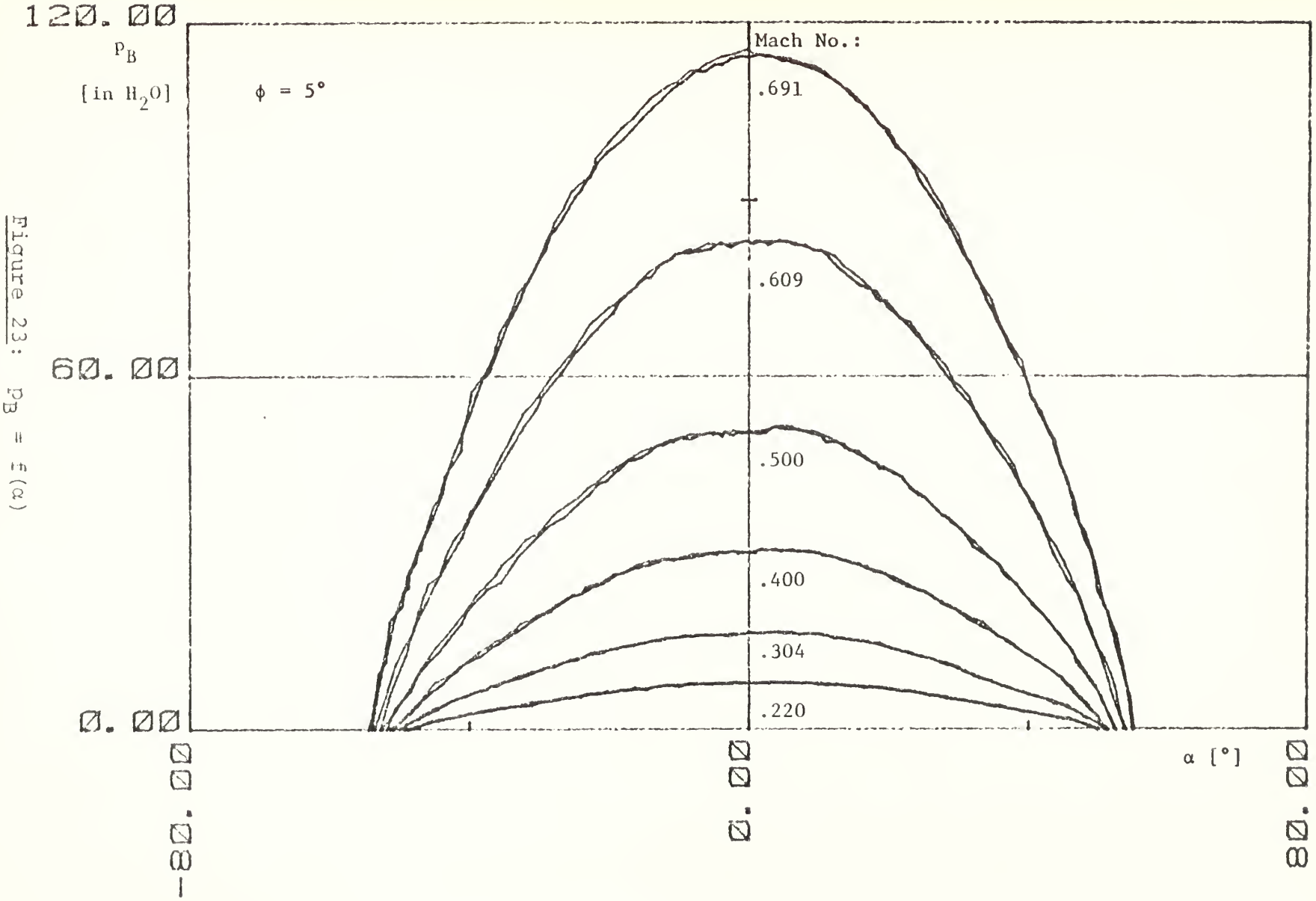

Figure 23: $p_B = f(\alpha)$

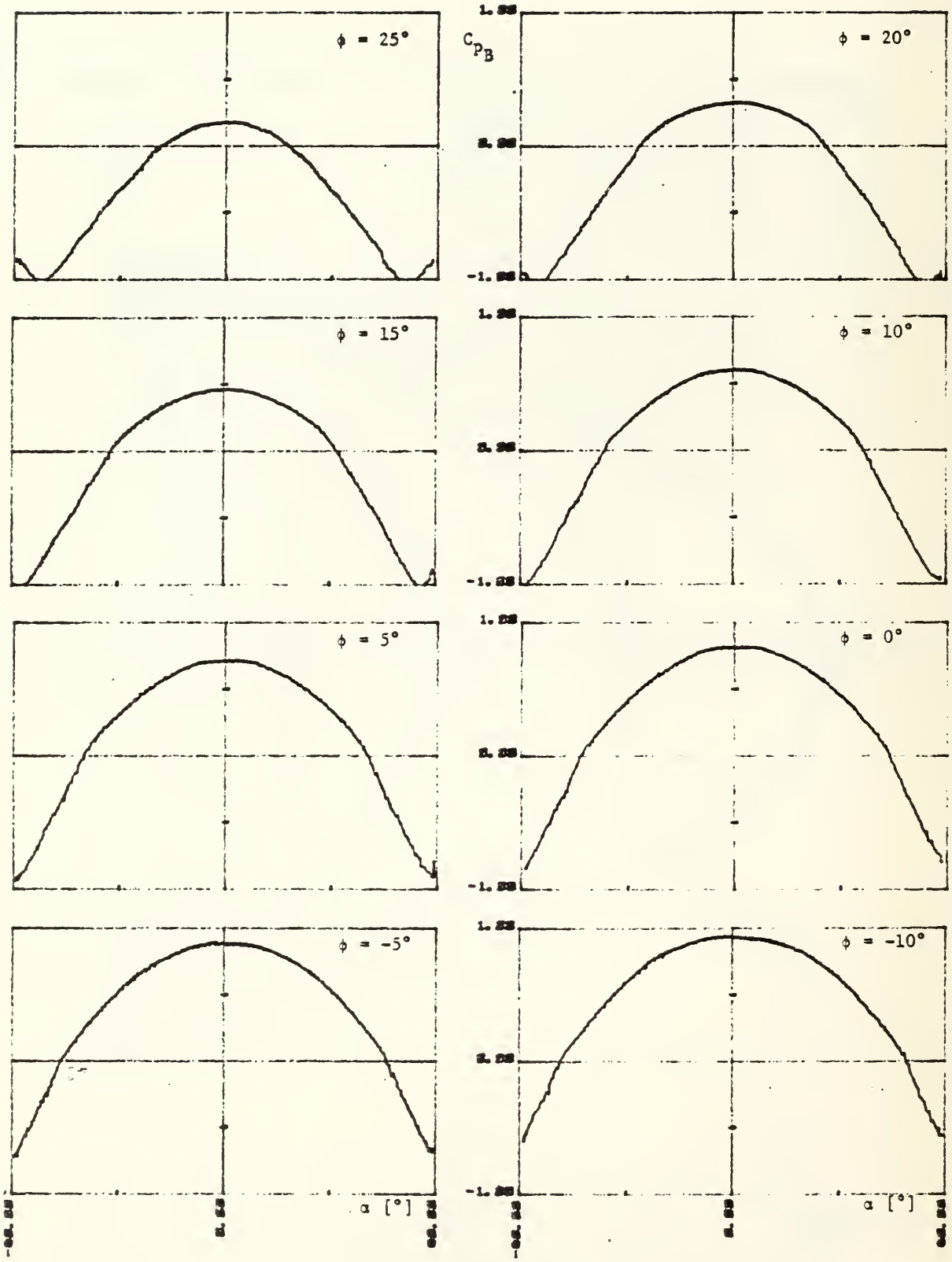

Figure 24: $C_{p_B} = f(\alpha)$; M = .6

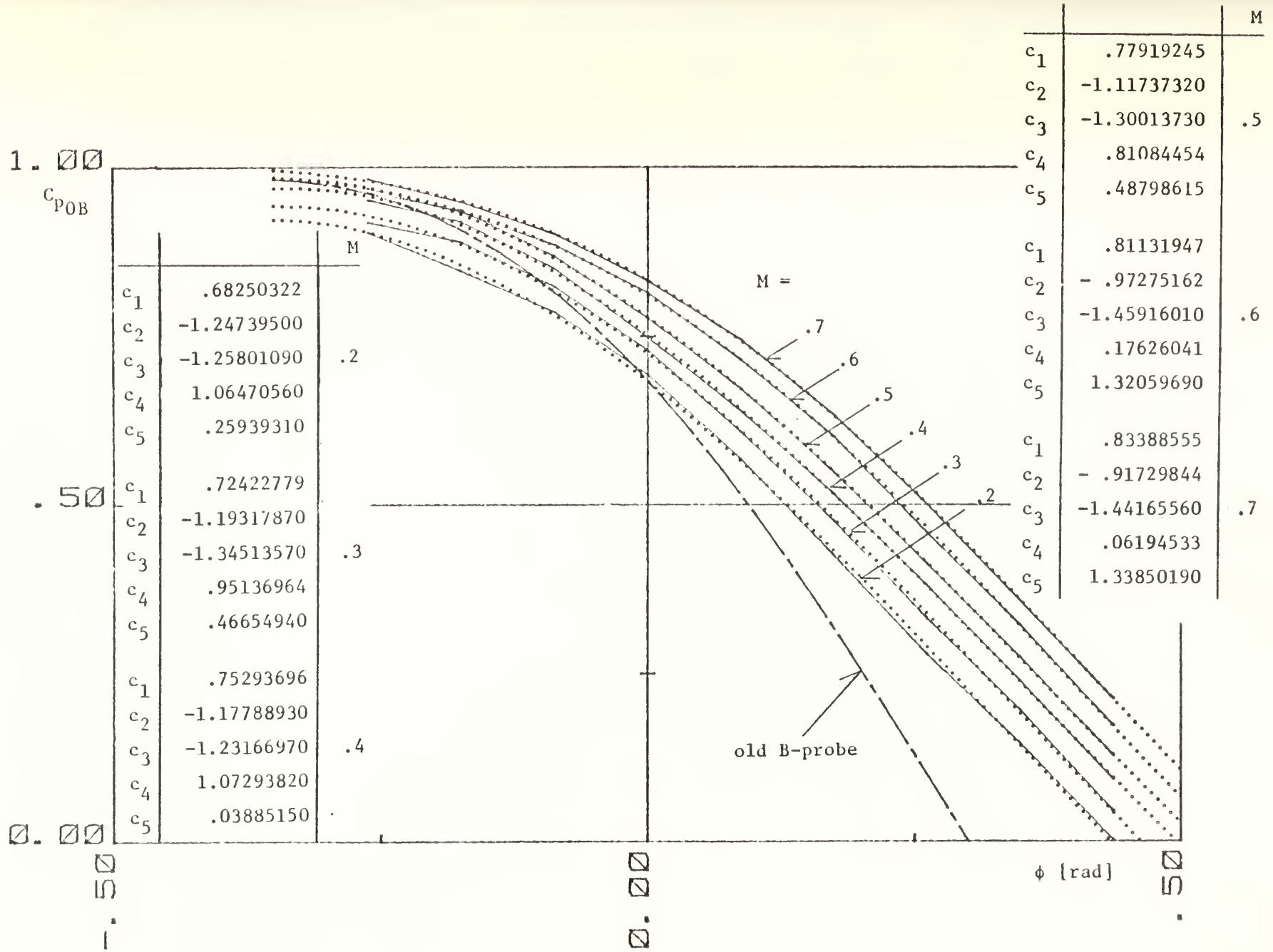

Figure 25: $c_{p_{OB}} = f(\phi)$

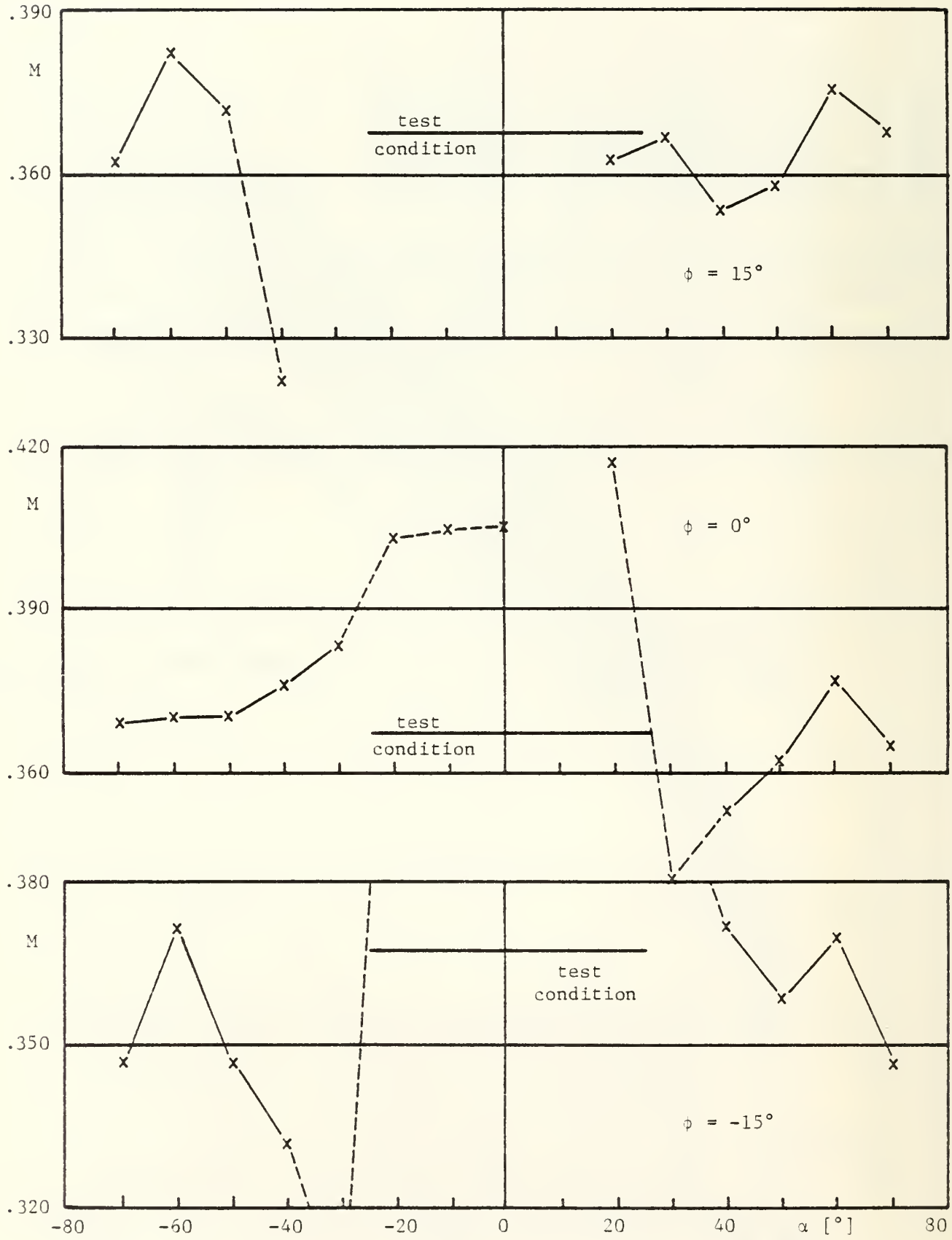

Figure 26: Results of analytical data reduction applied to calibration data (old A- and B-probes)

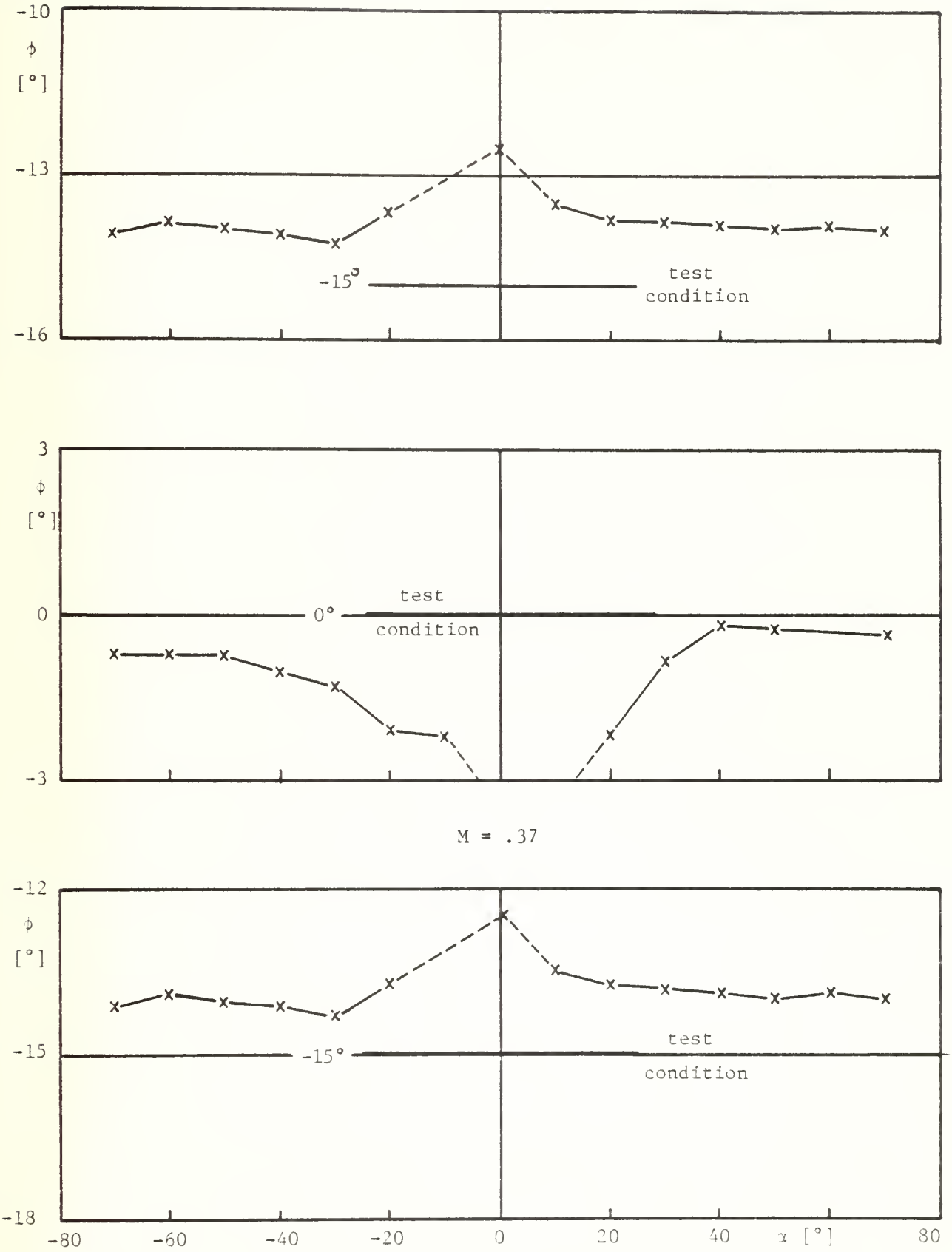

Figure 27: Results of analytical data reduction applied to calibration data (old A- and B-probes)

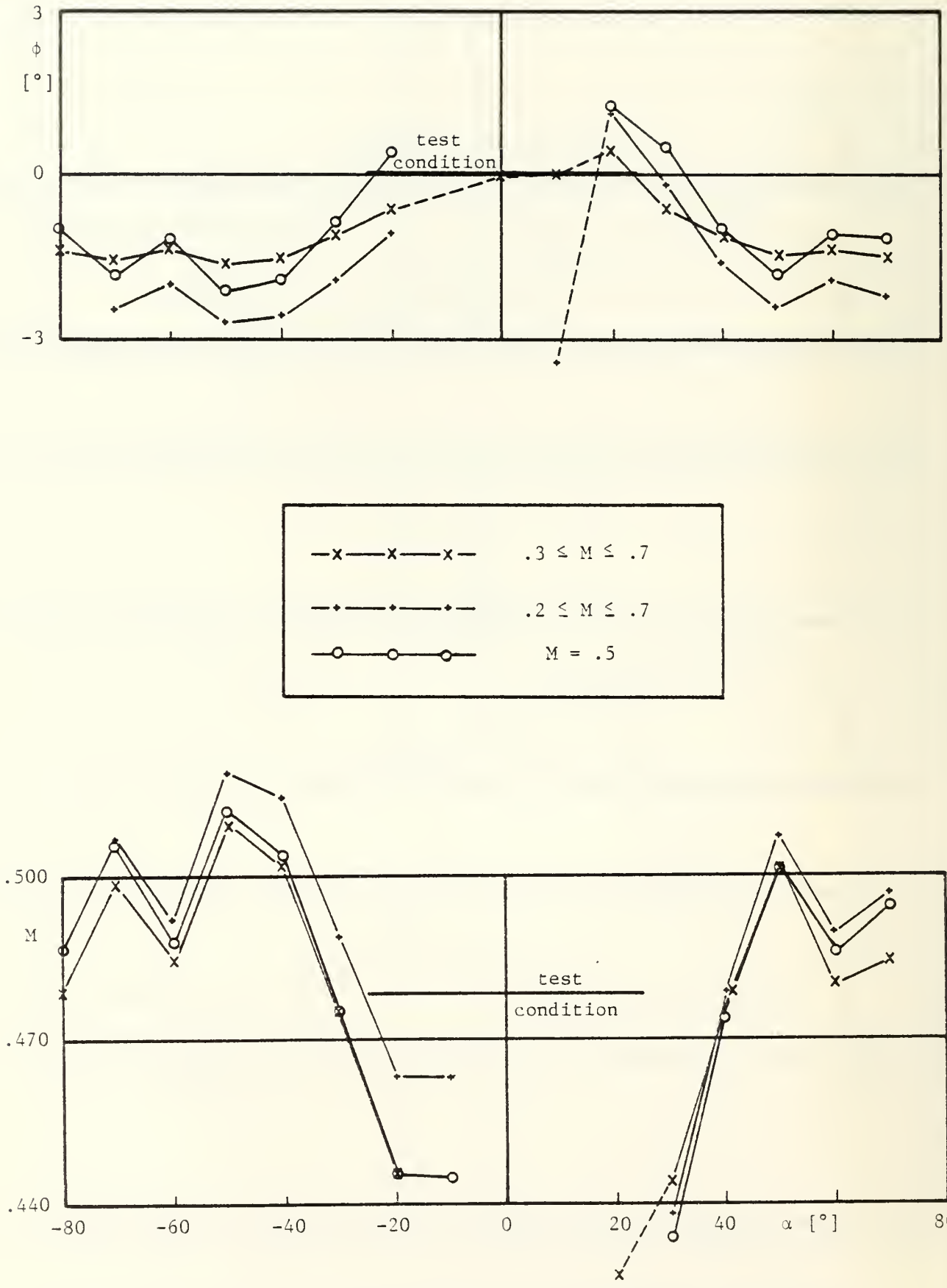

Figure 28: Results of analytical data reduction applied to calibration data (new A- and B-probes)

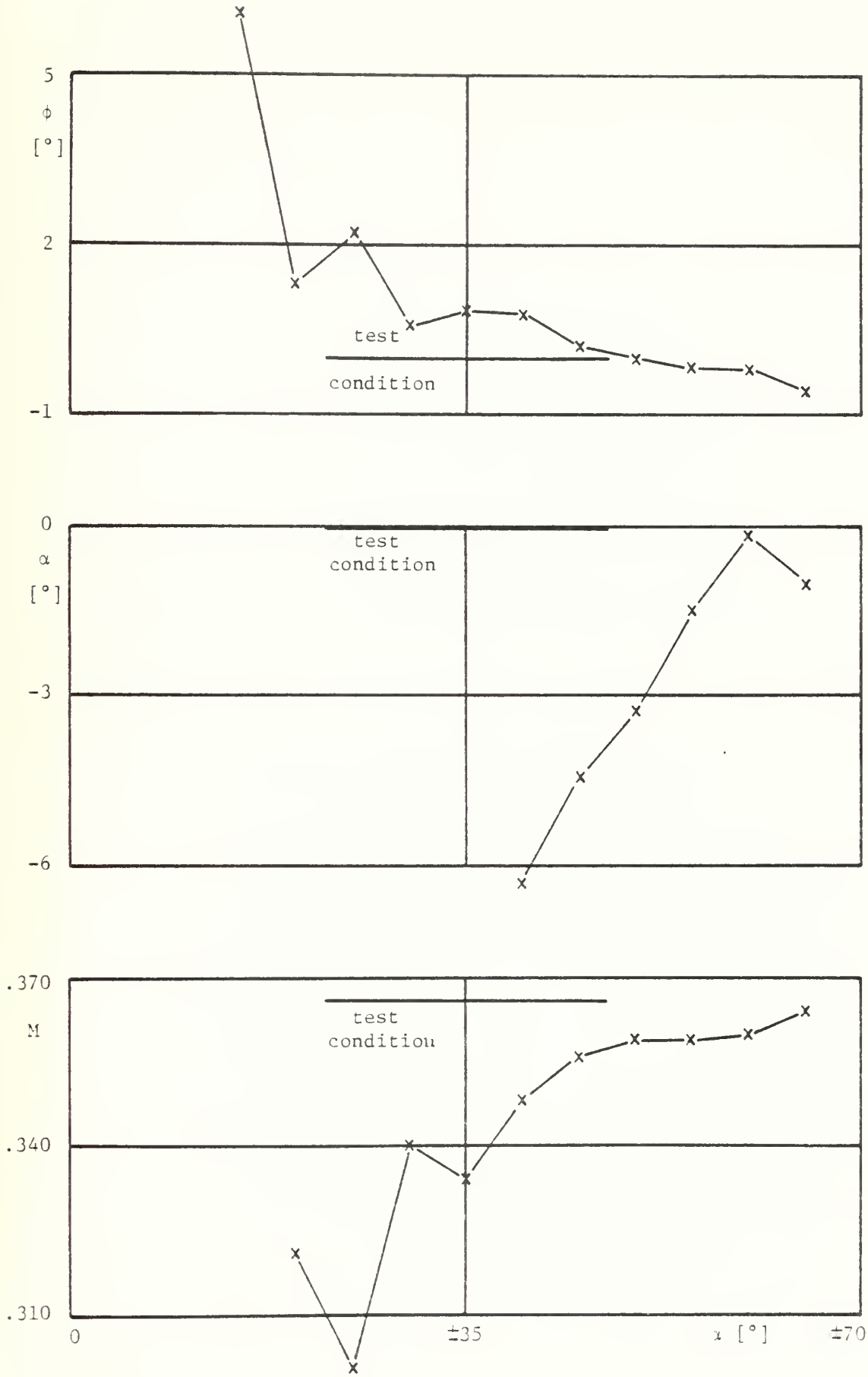

Figure 29: Results of numerical data reduction applied to calibration data

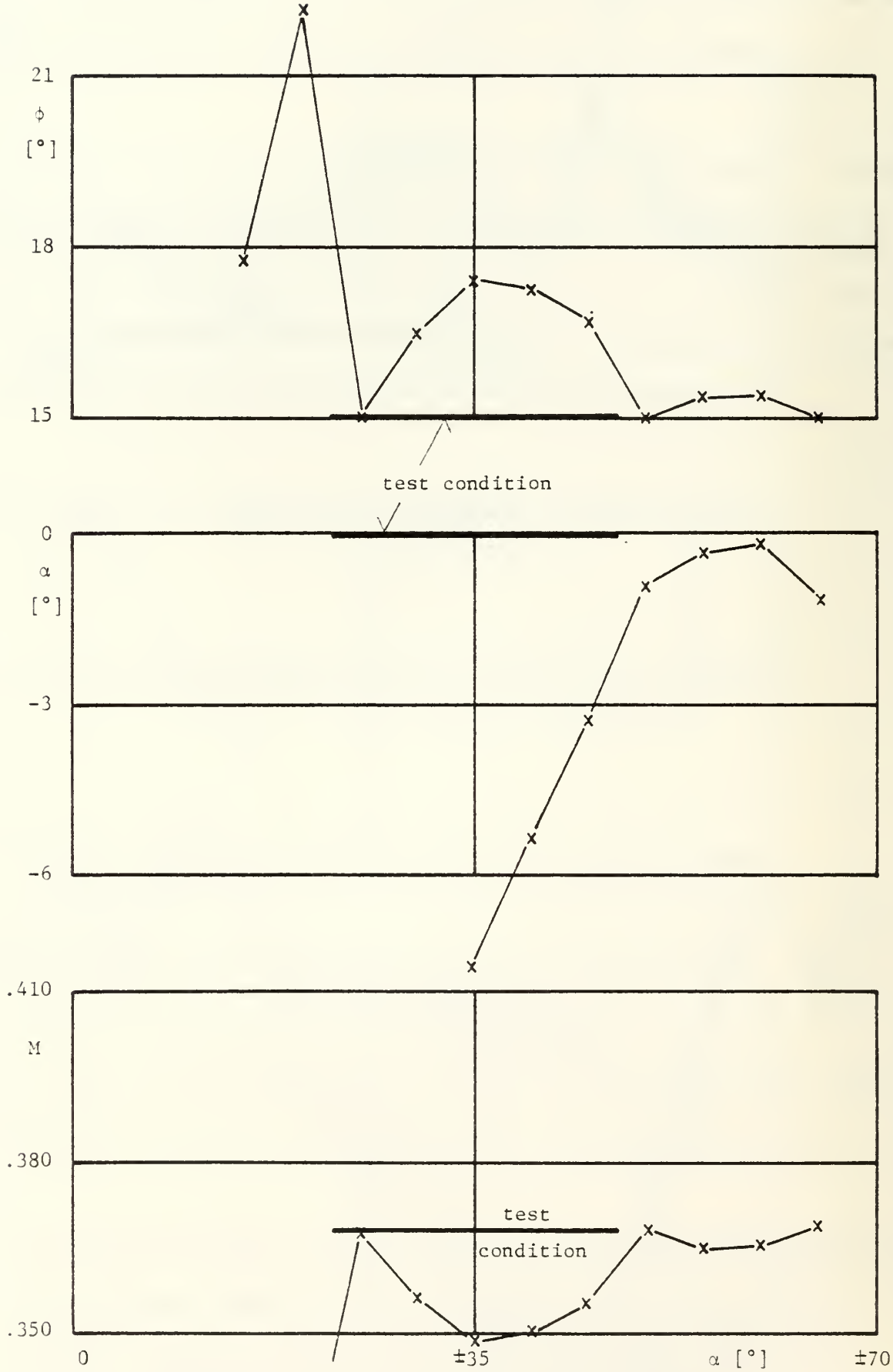

Figure 30: Results of numerical data reduction applied to calibration data

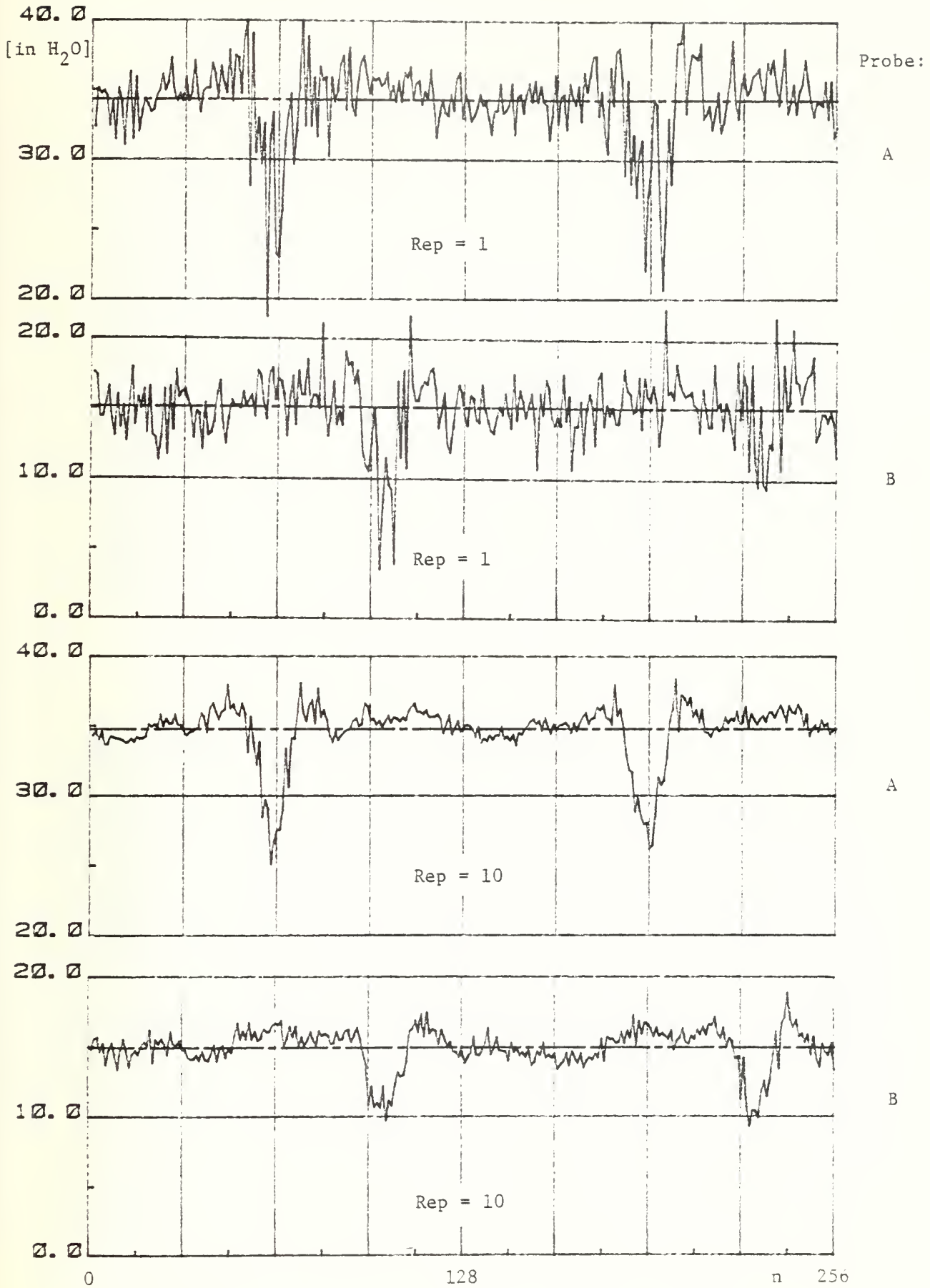

Figure 31: Results for the A- and B-probe with different repetitions

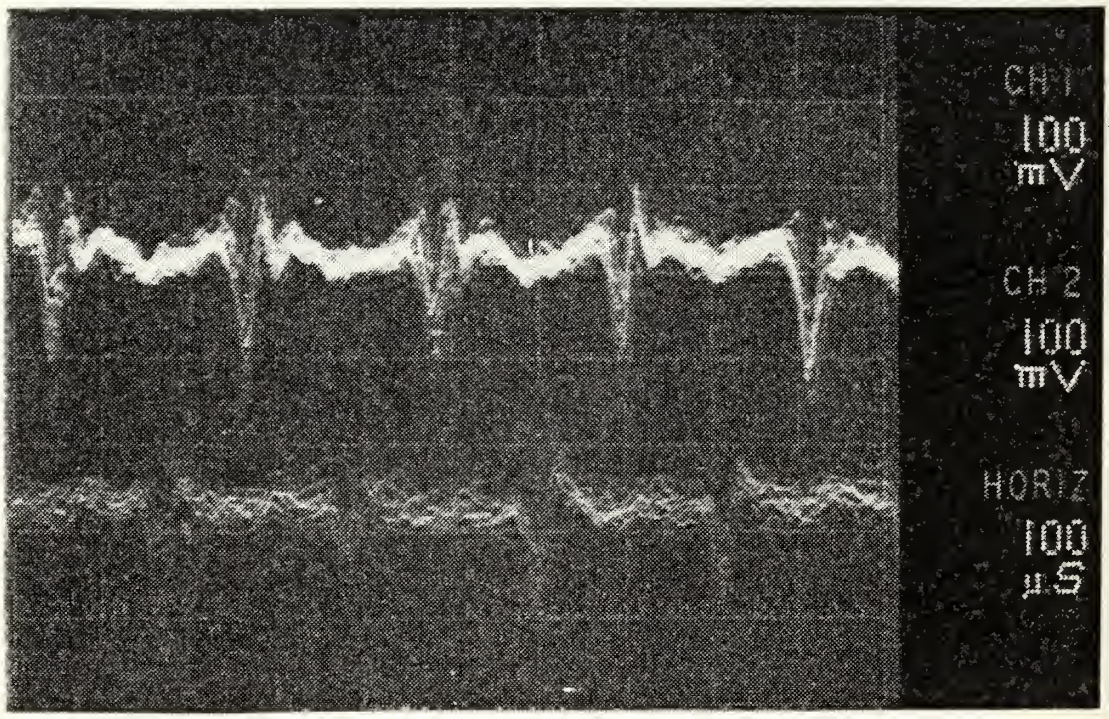

Probe

A

B

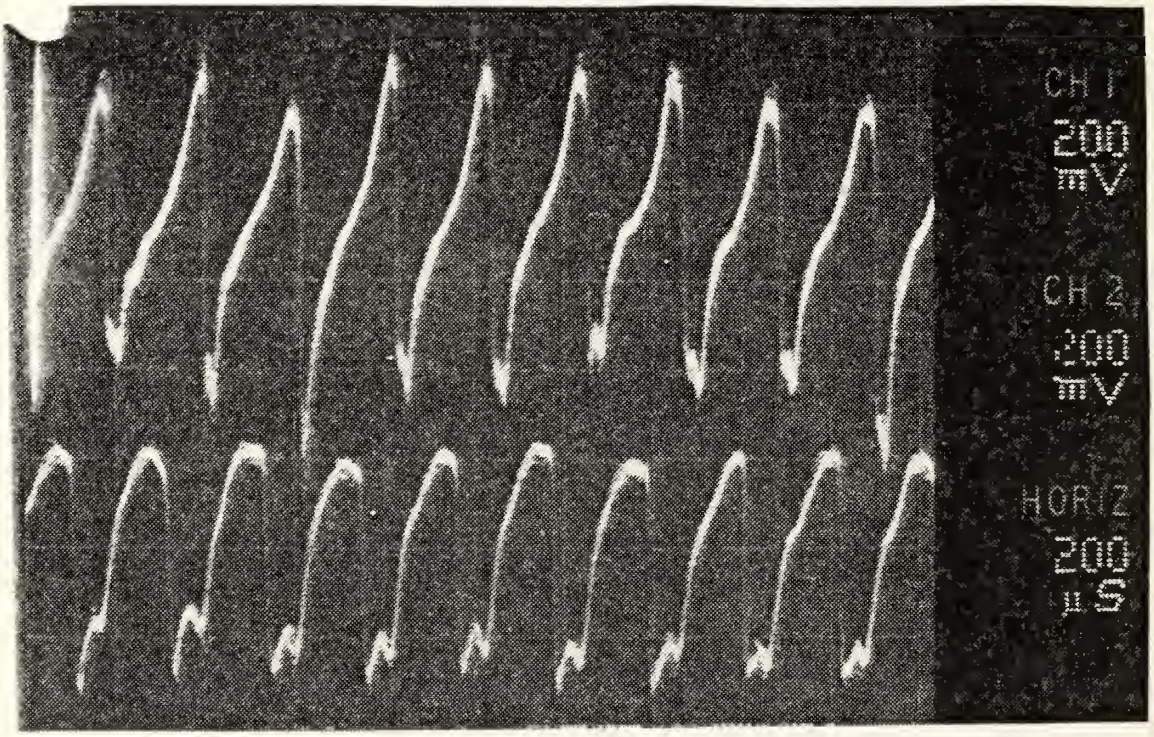

K9.5

K10

Figure 32: Probe signals taken from oscilloscope

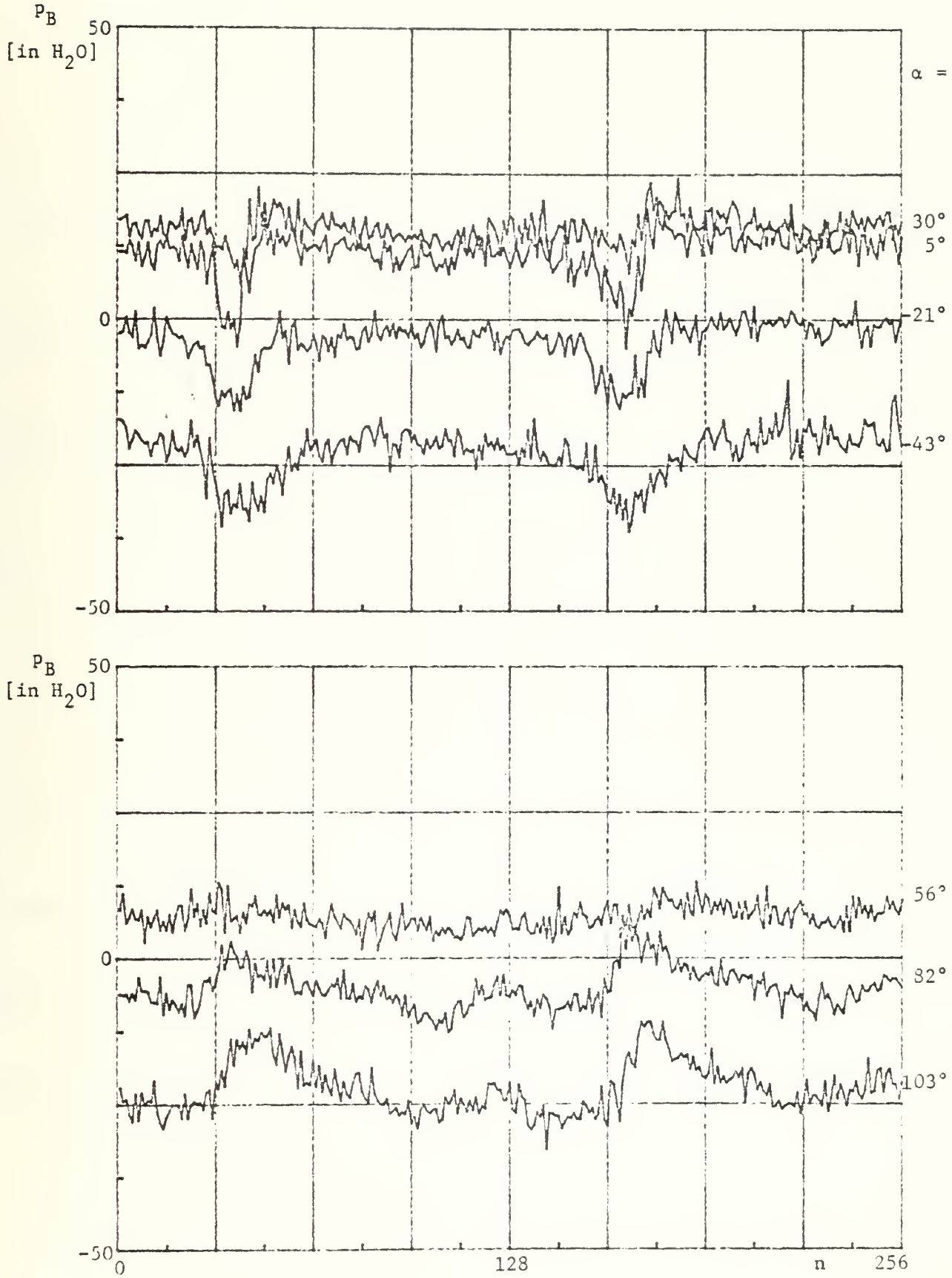

Figure 33: Results for B-probe; Rep = 1

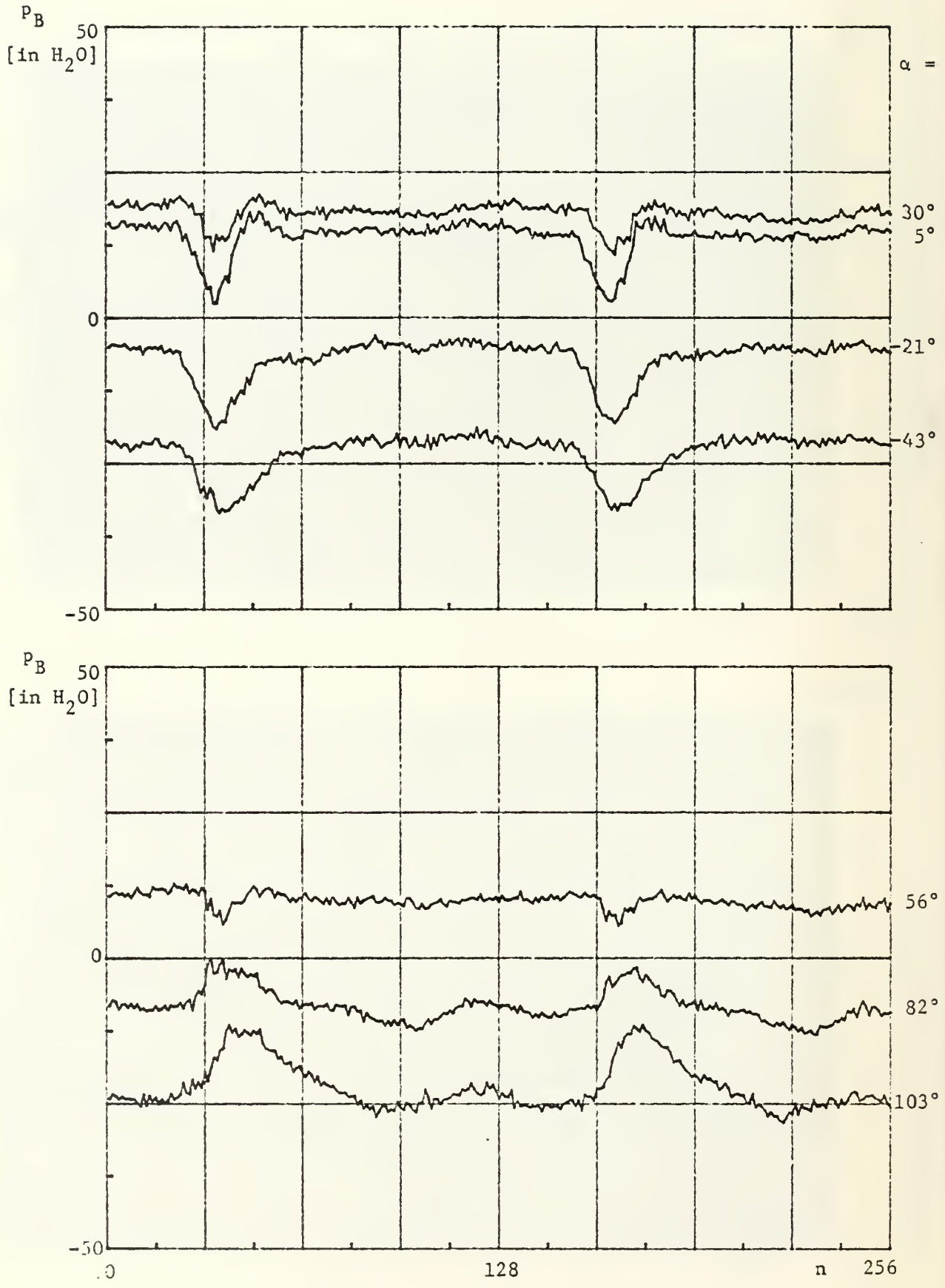

Figure 34: Results for B-probe; Rep = 10

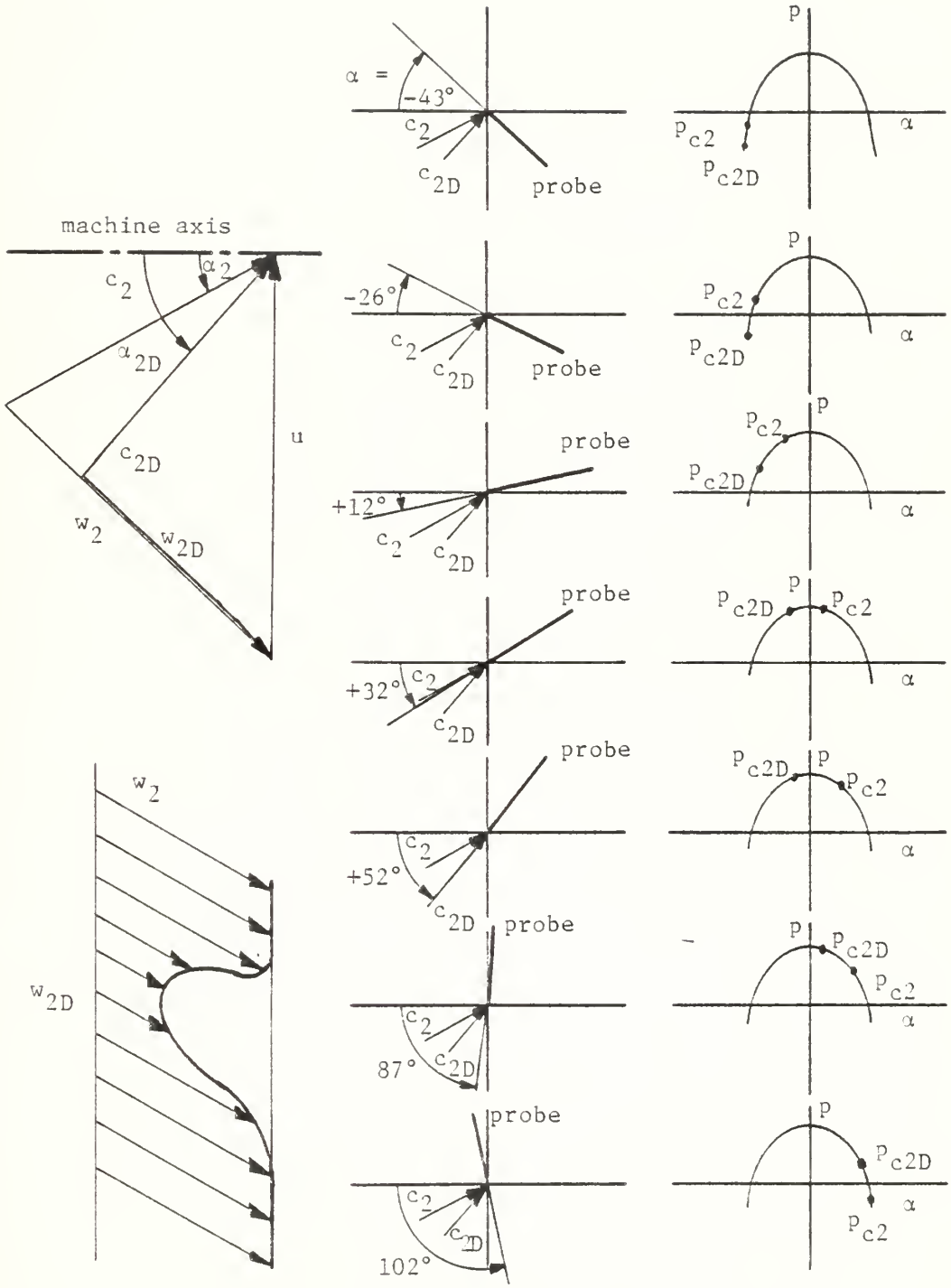

Figure 35: Qualitative explanation of wave behavior

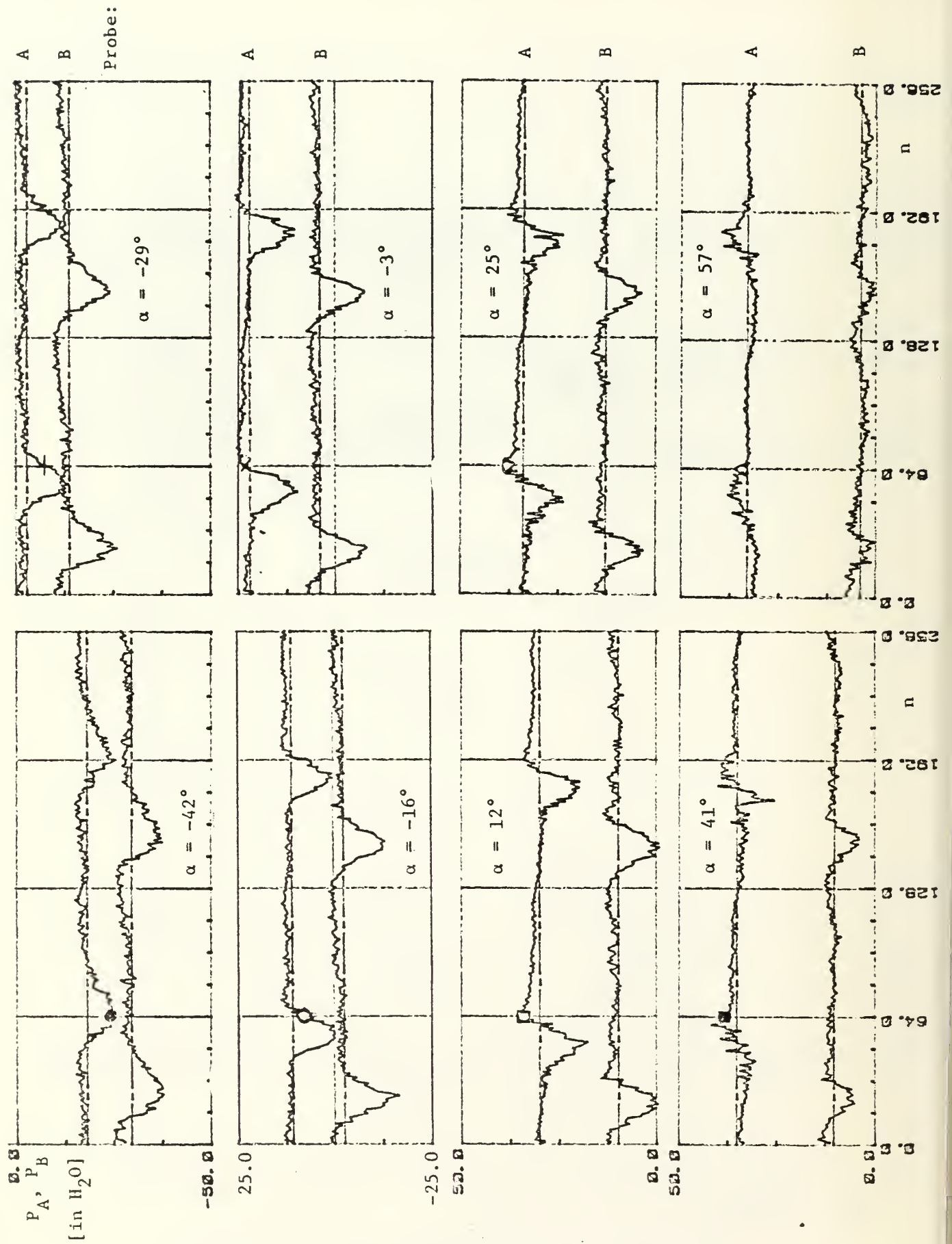

Figure 36: A and B probe signals; Rep = 10

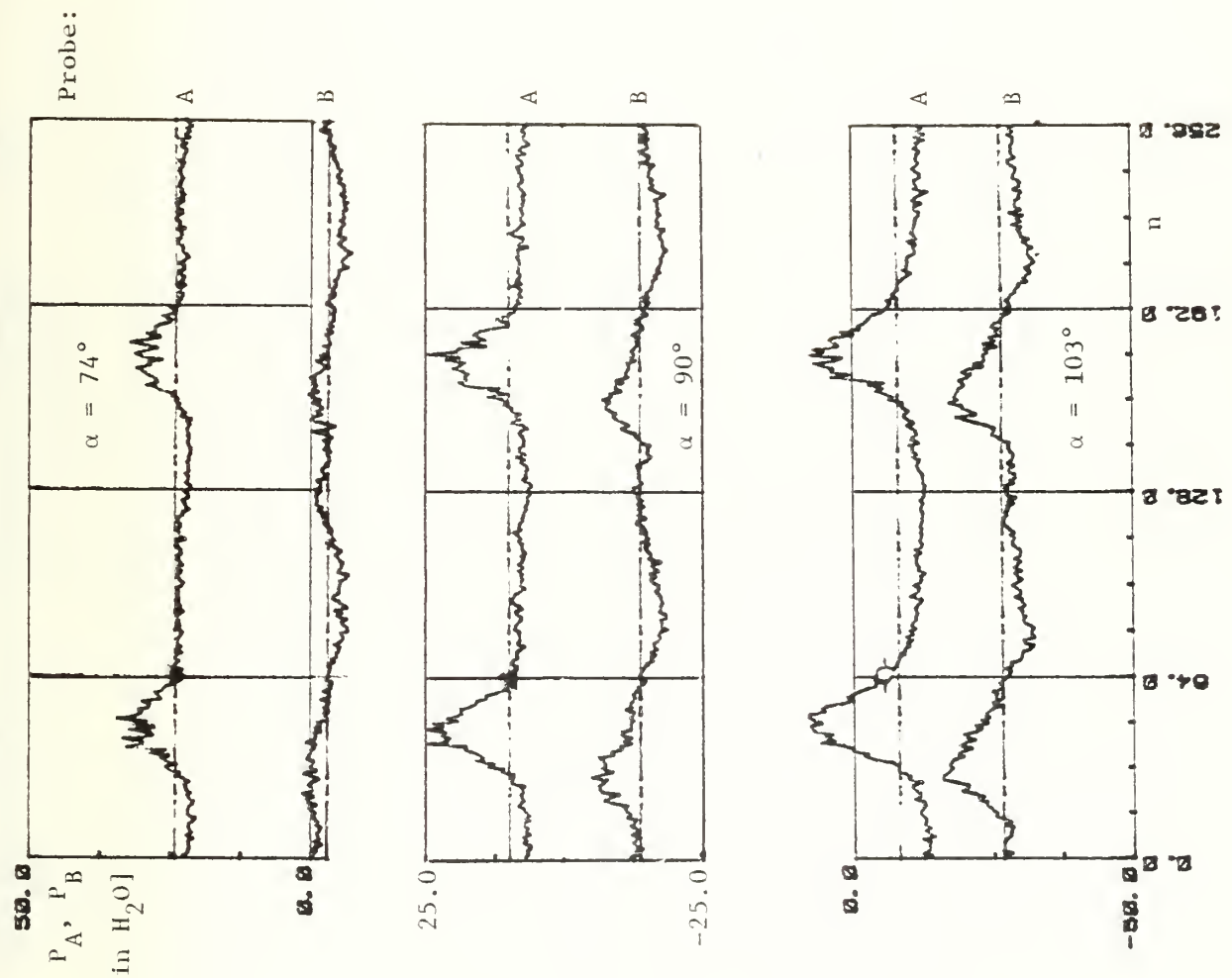

Figure 37: A and B probe signals; Rep = 10

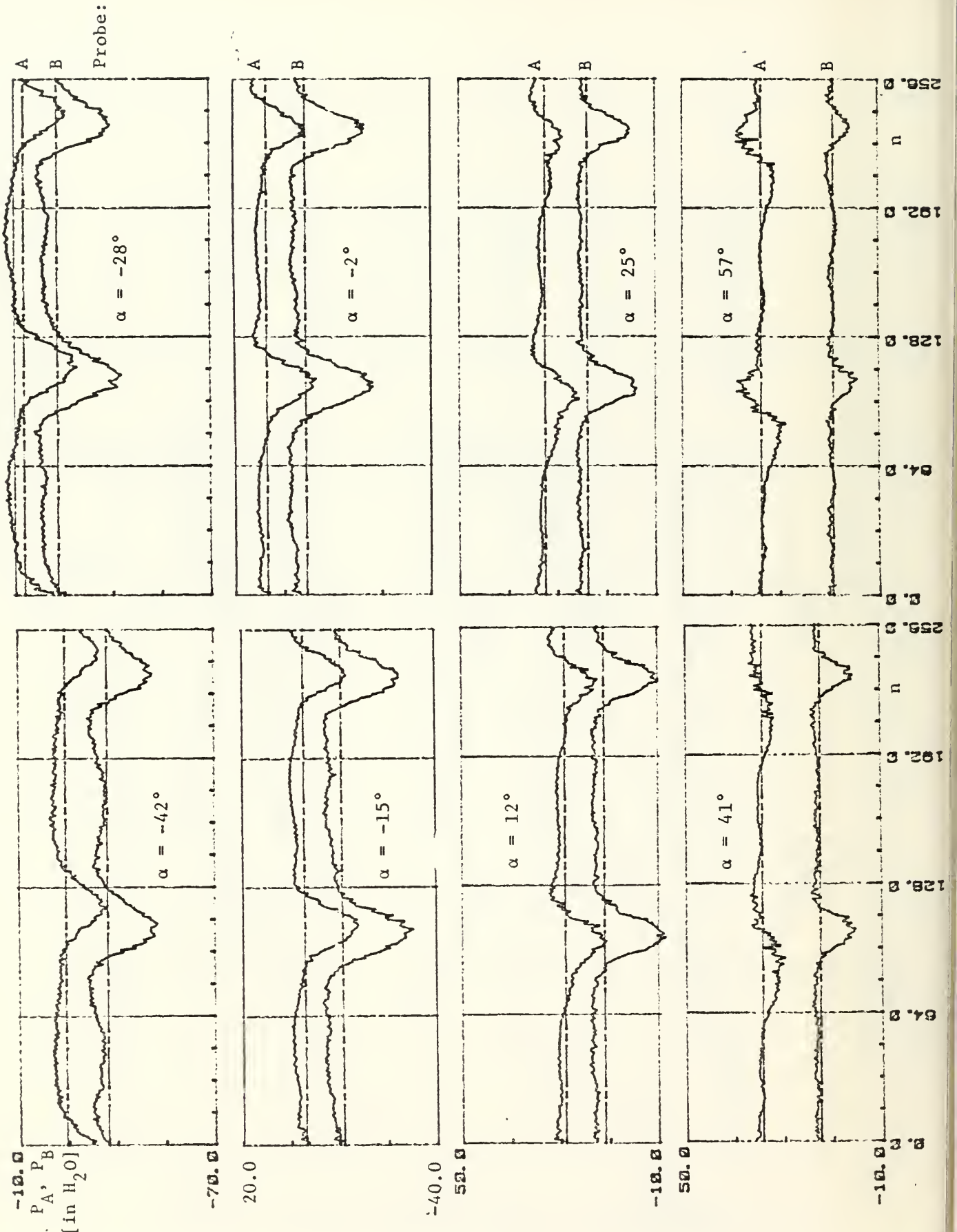

Figure 38: A and B probe signals; Rep = 40

Figure 39: A and B probe signals; Rep = 40

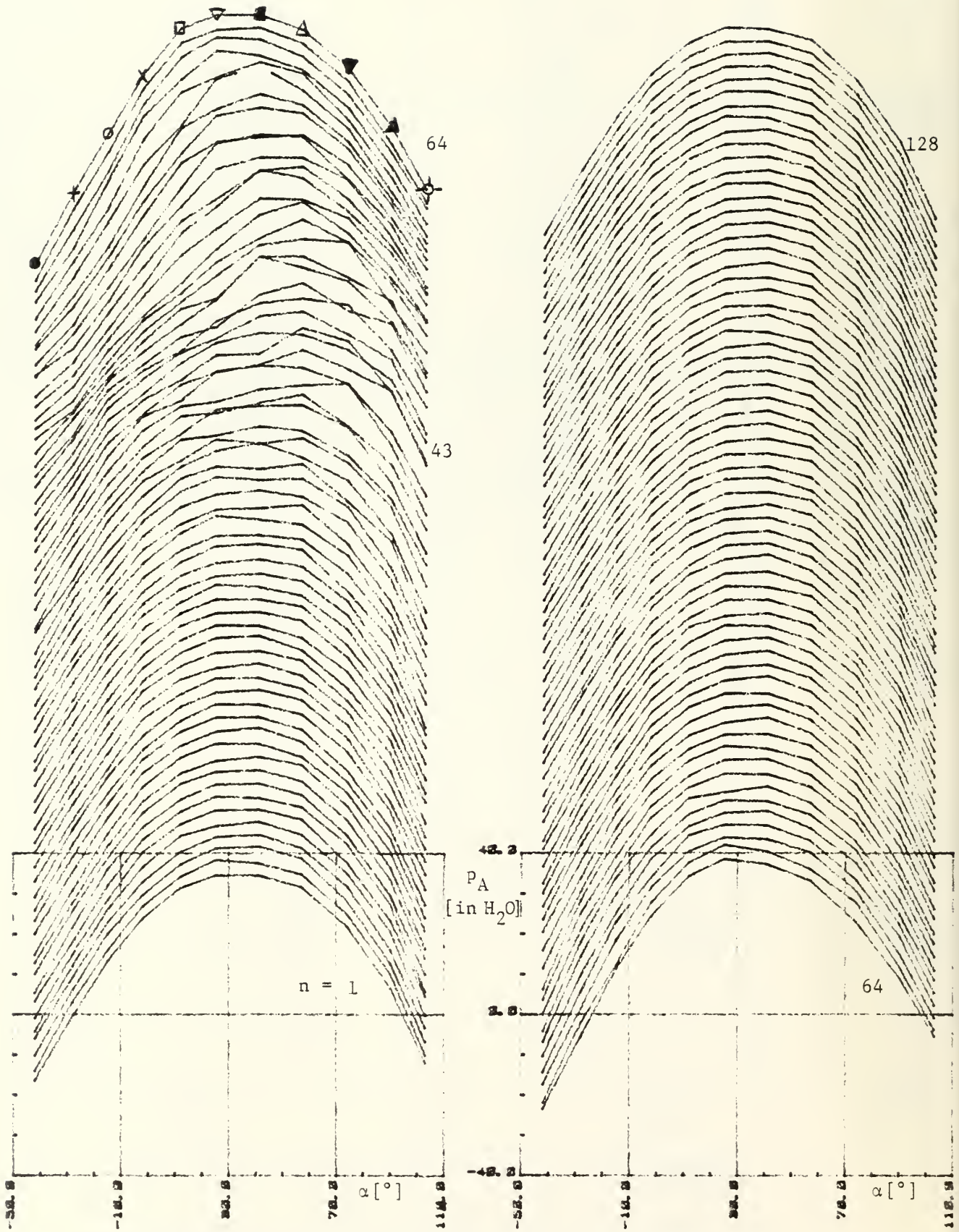

Figure 40: $p_A = f(\alpha)$ for A probe (step 1 to 128); Rep = 10

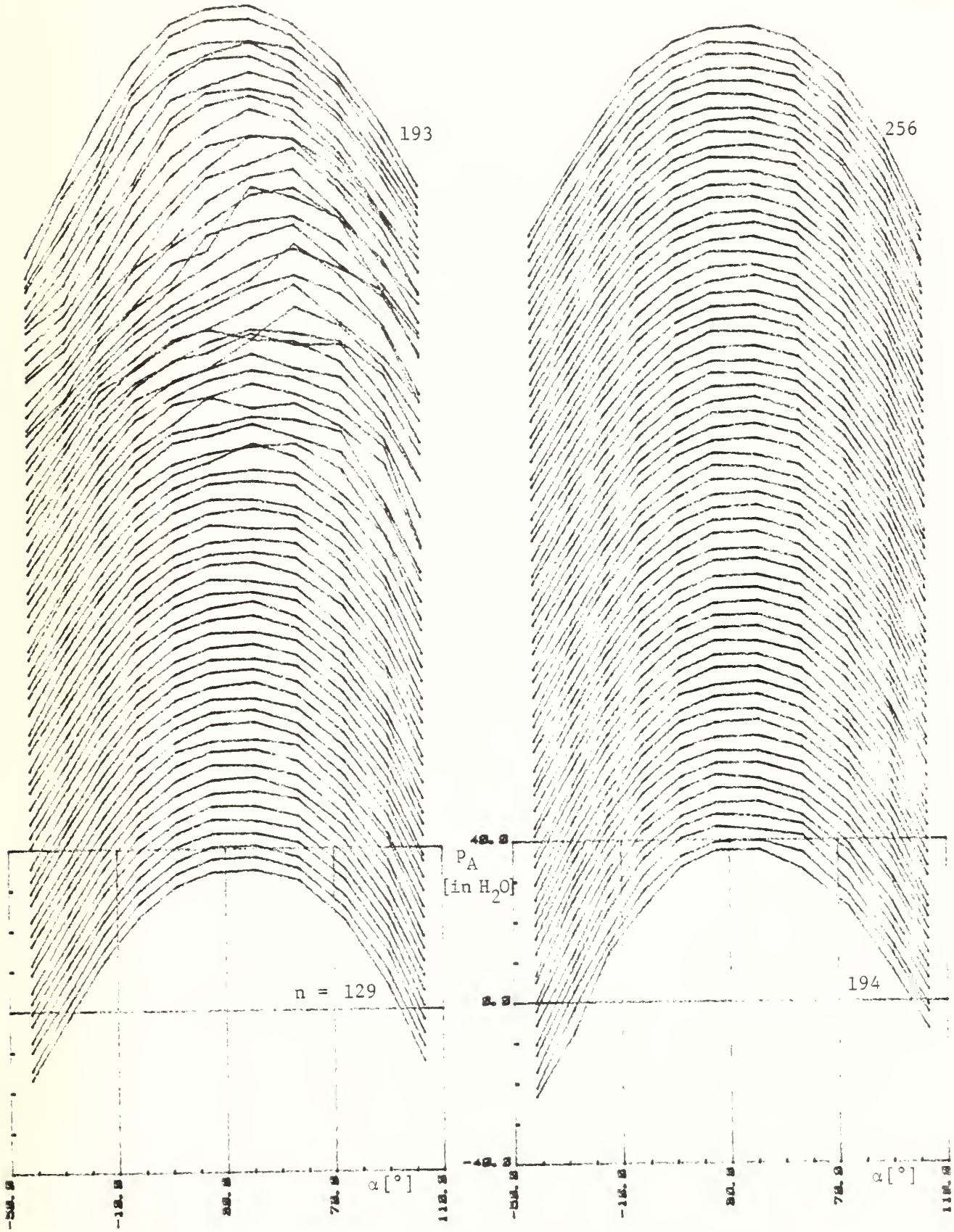

Figure 41: $P_A = f(\alpha)$ for A probe (step 129 to 256); Rep = 10

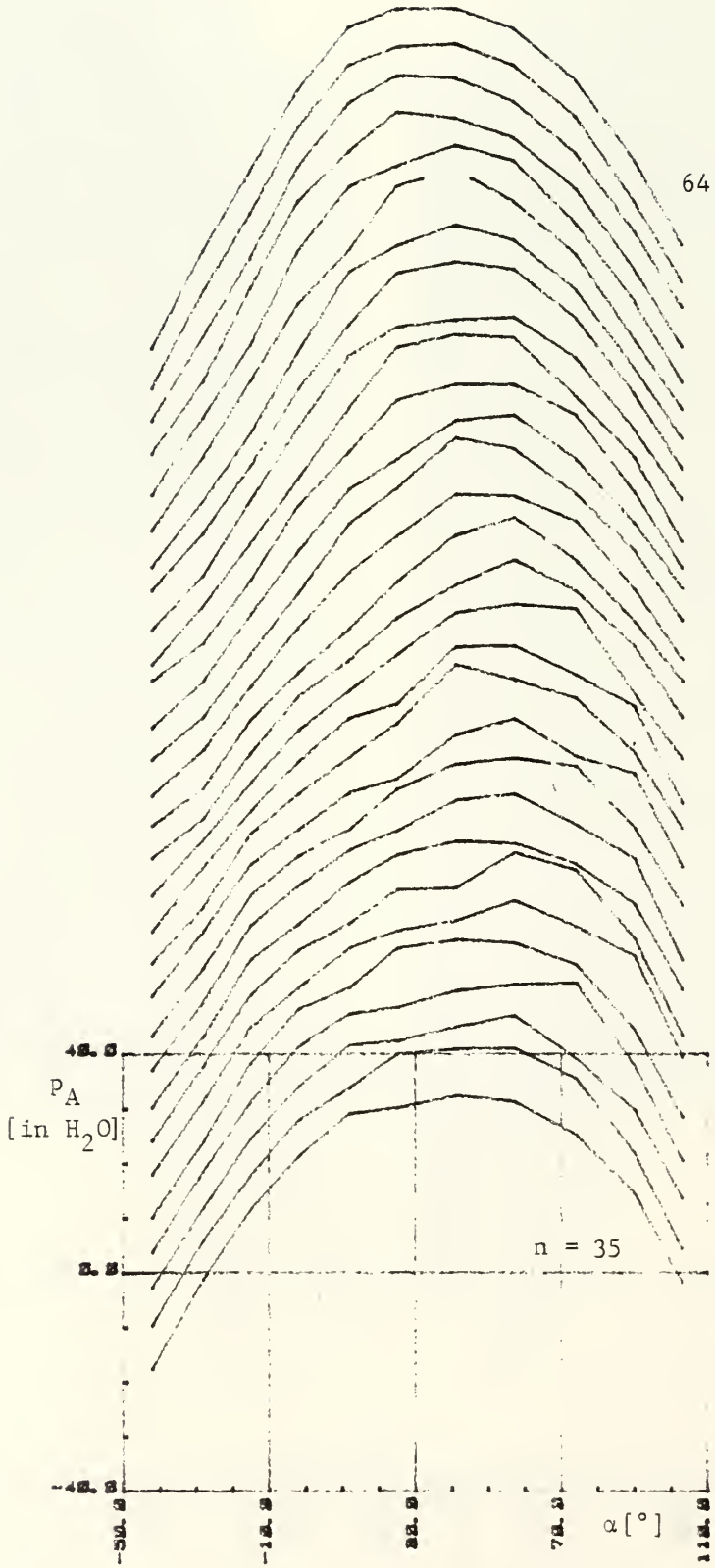

Figure 42: $p_A = f(\alpha)$ for A probe (step 35 to 64); Rep = 10

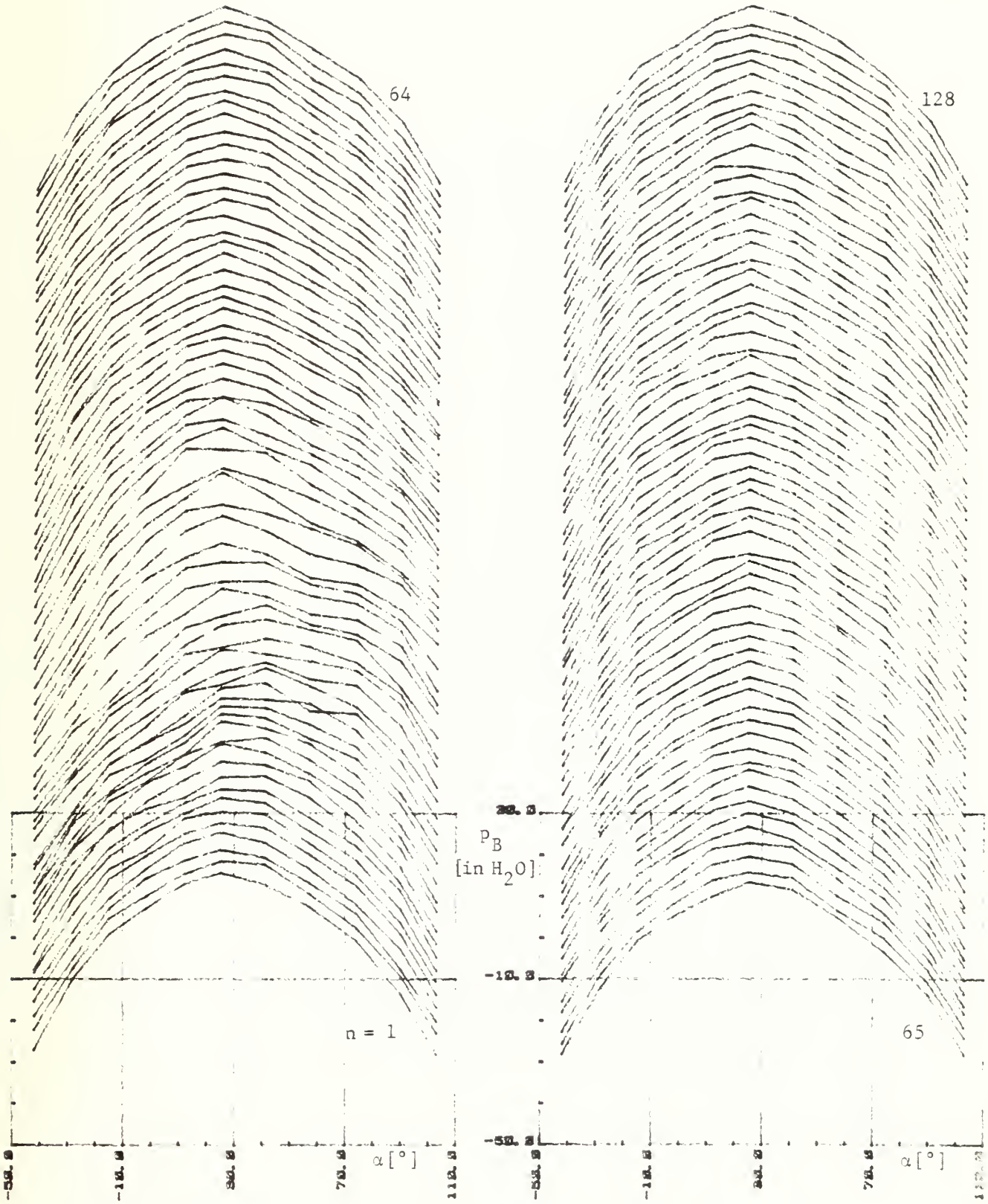

Figure 43: $p_B = f(\alpha)$ for B probe (step 1 to 128); Rep = 10

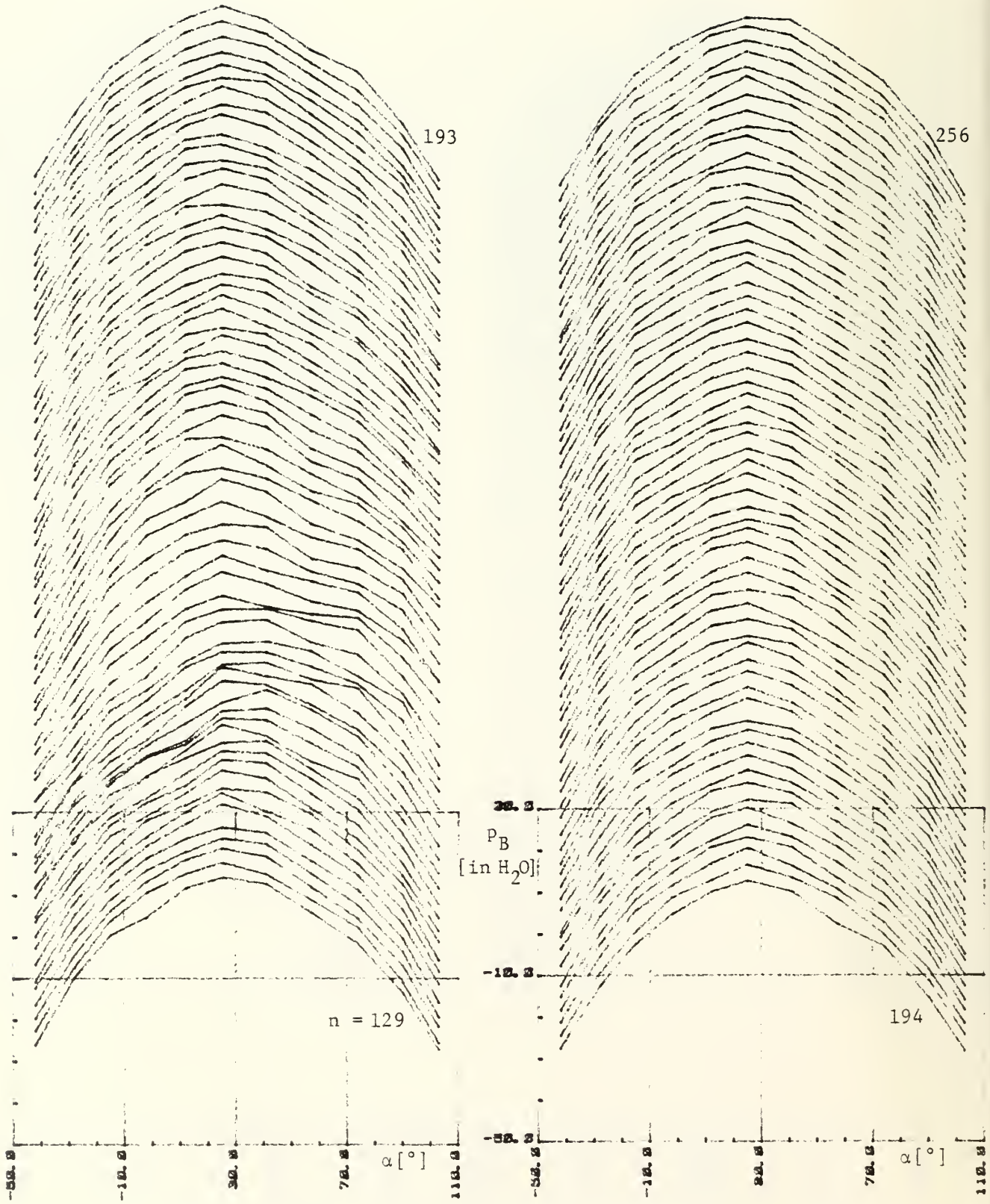

Figure 44: $P_B = f(\alpha)$ for B probe (step 129 to 256); Rep = 10

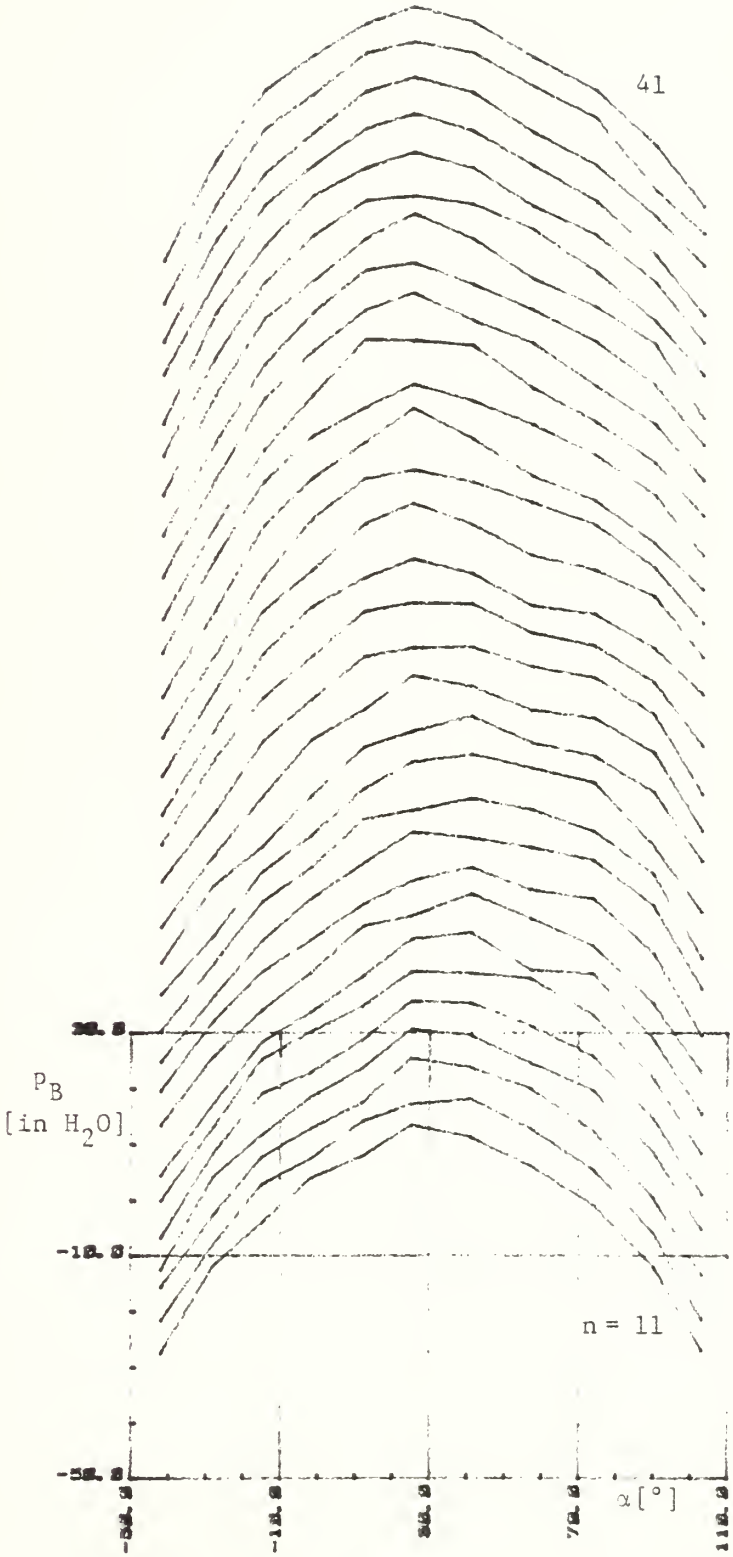

Figure 45: $p_B = f(\alpha)$ for B probe (step 11 to 41); Rep = 10

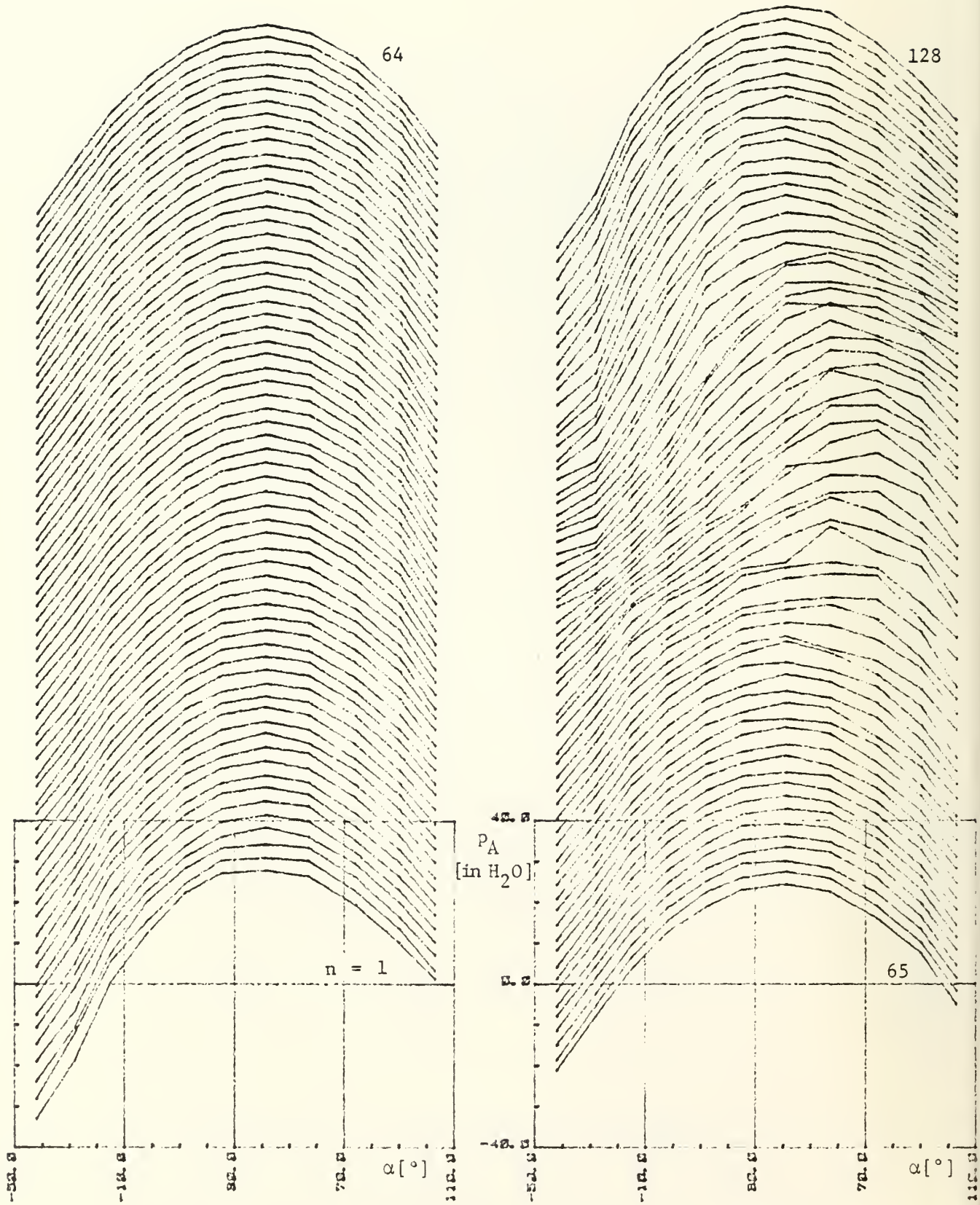

Figure 46: $P_A = f(\alpha)$ for A probe (step 1 to 128); Rep = 40

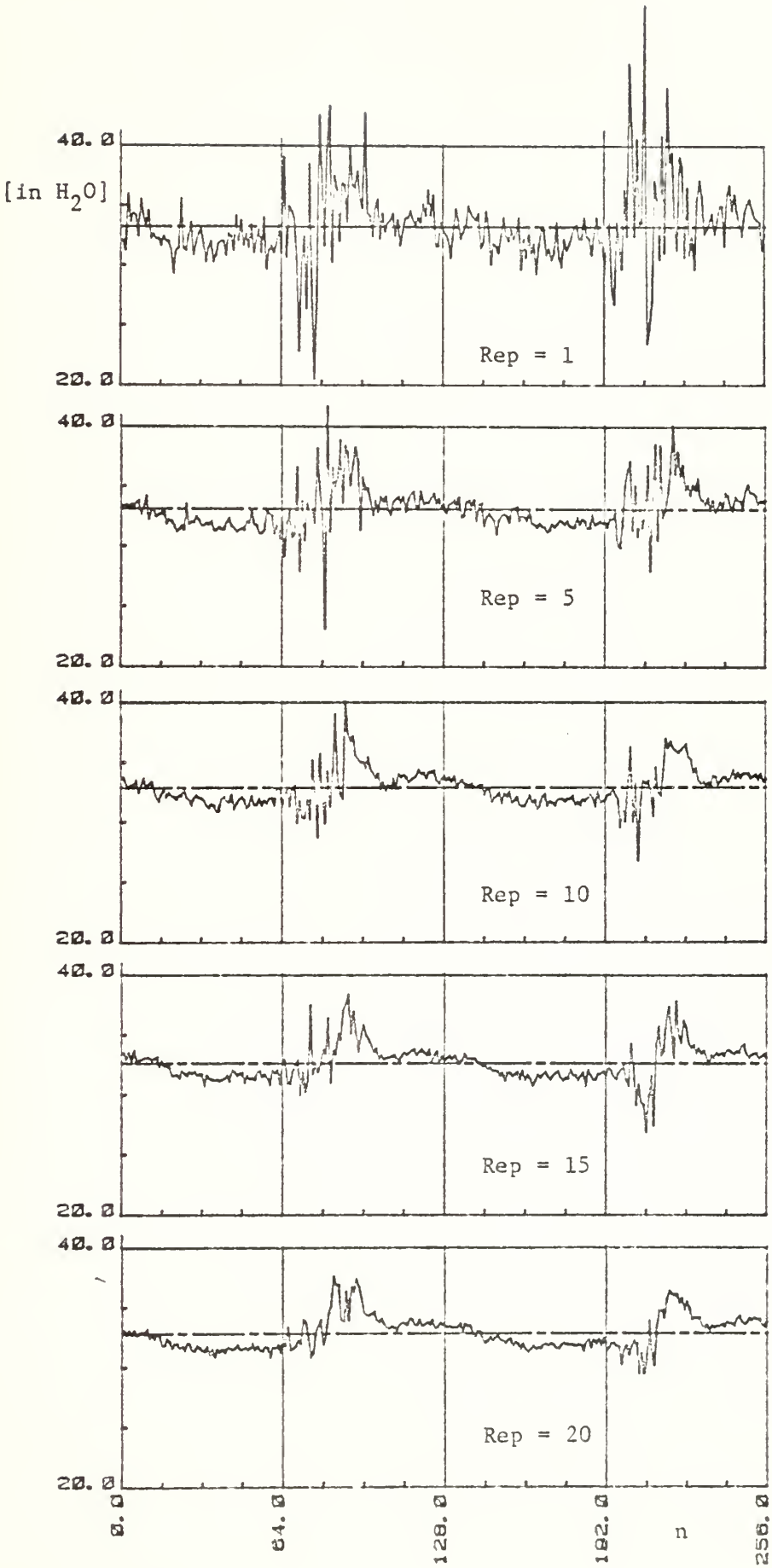

Figure 46a: Results from A probe; $\alpha = 52^{\circ}$

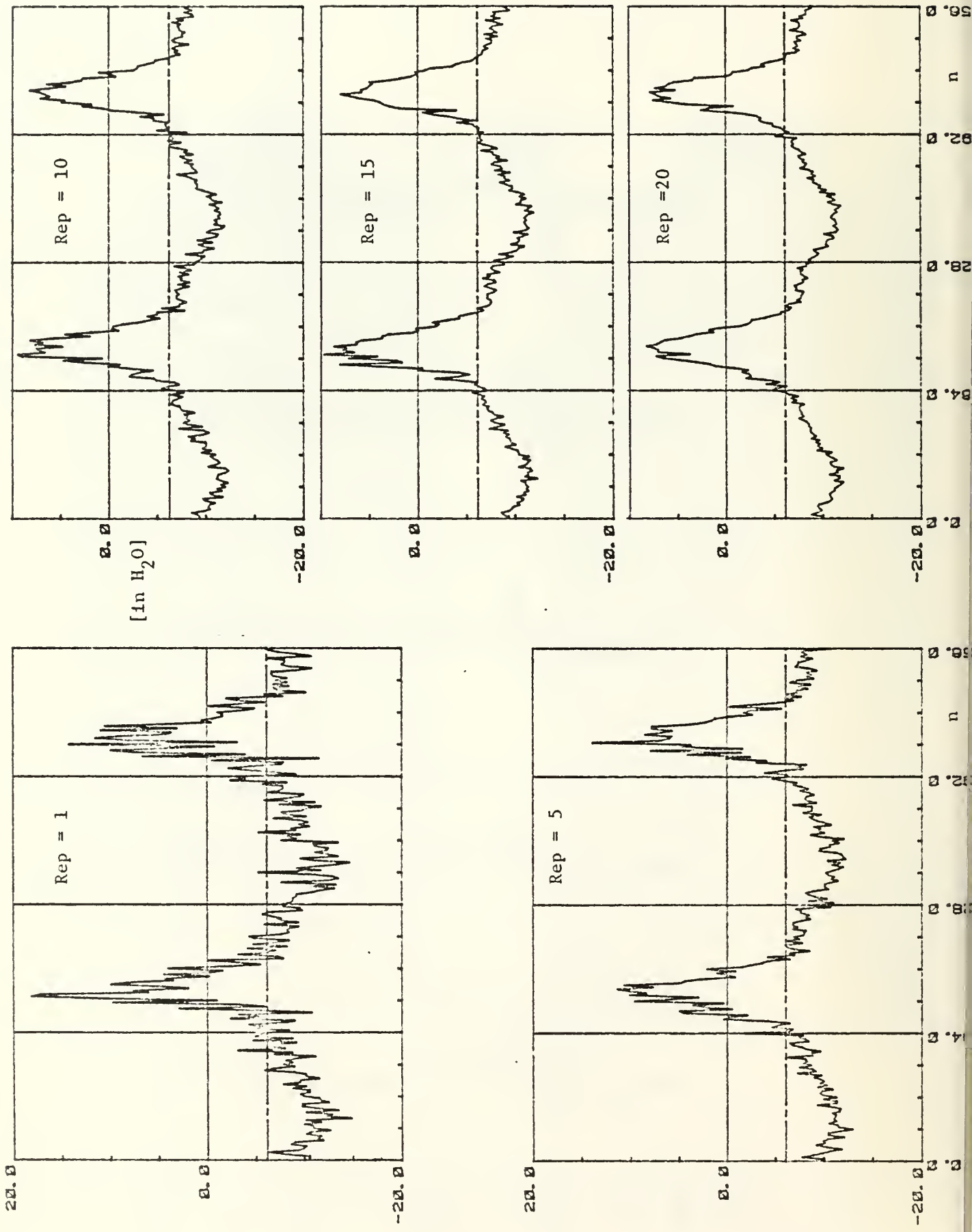

Figure 46b: Results from A probe; $\alpha = 103^{\circ}$

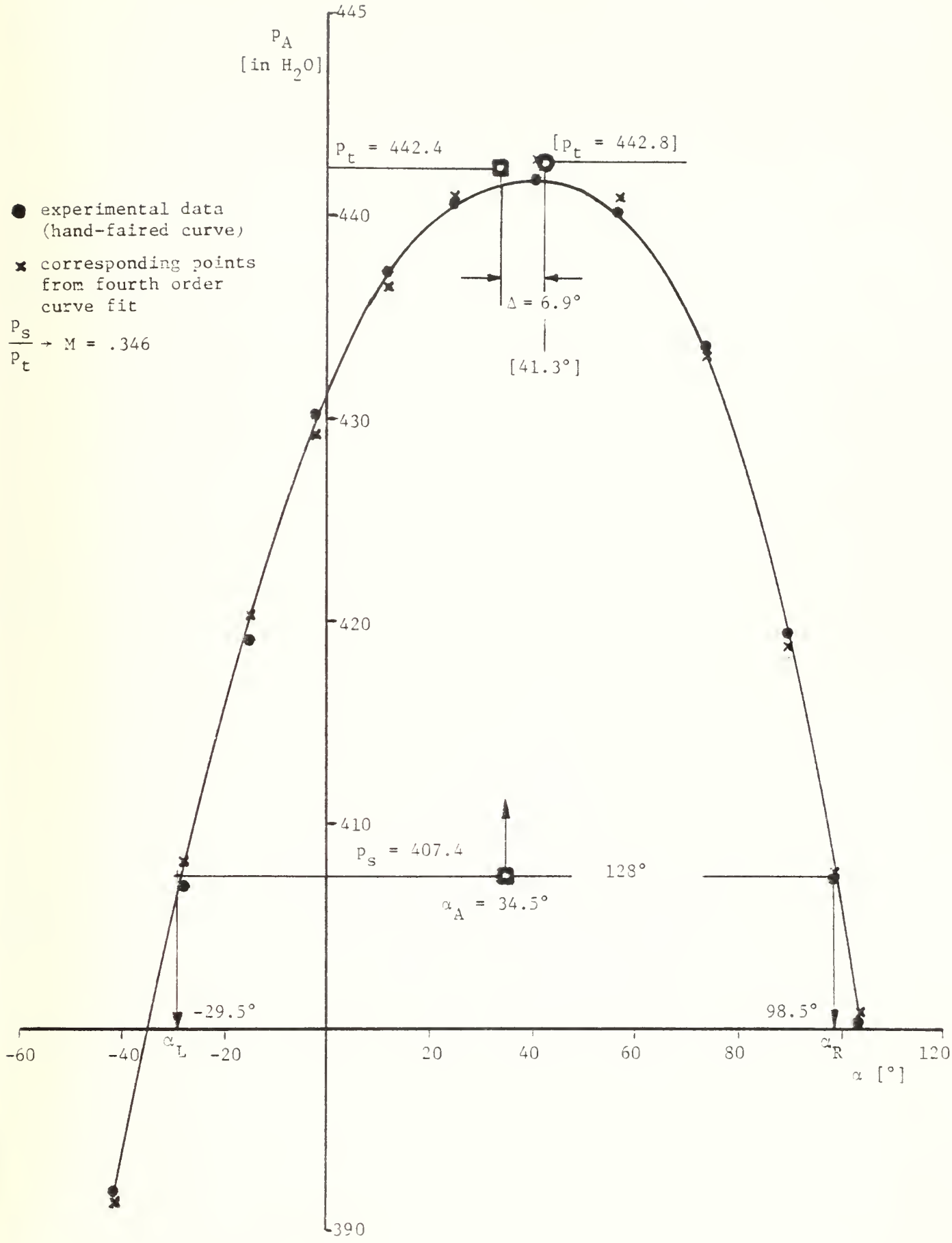

Figure 47: $p_A = f(\alpha)$ for A probe (count 31)

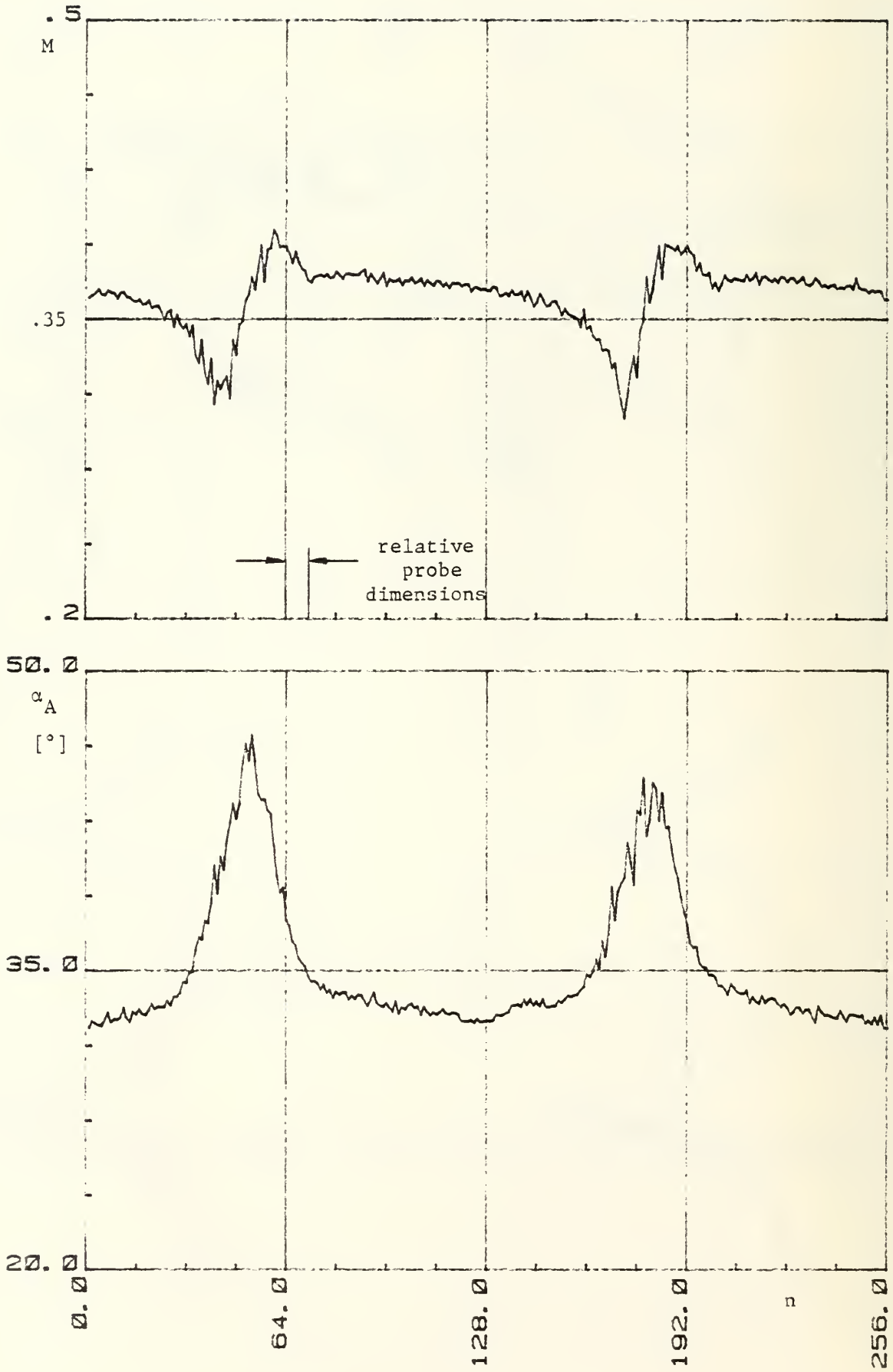

Figure 48: M-number and flow angle distribution versus peripheral position

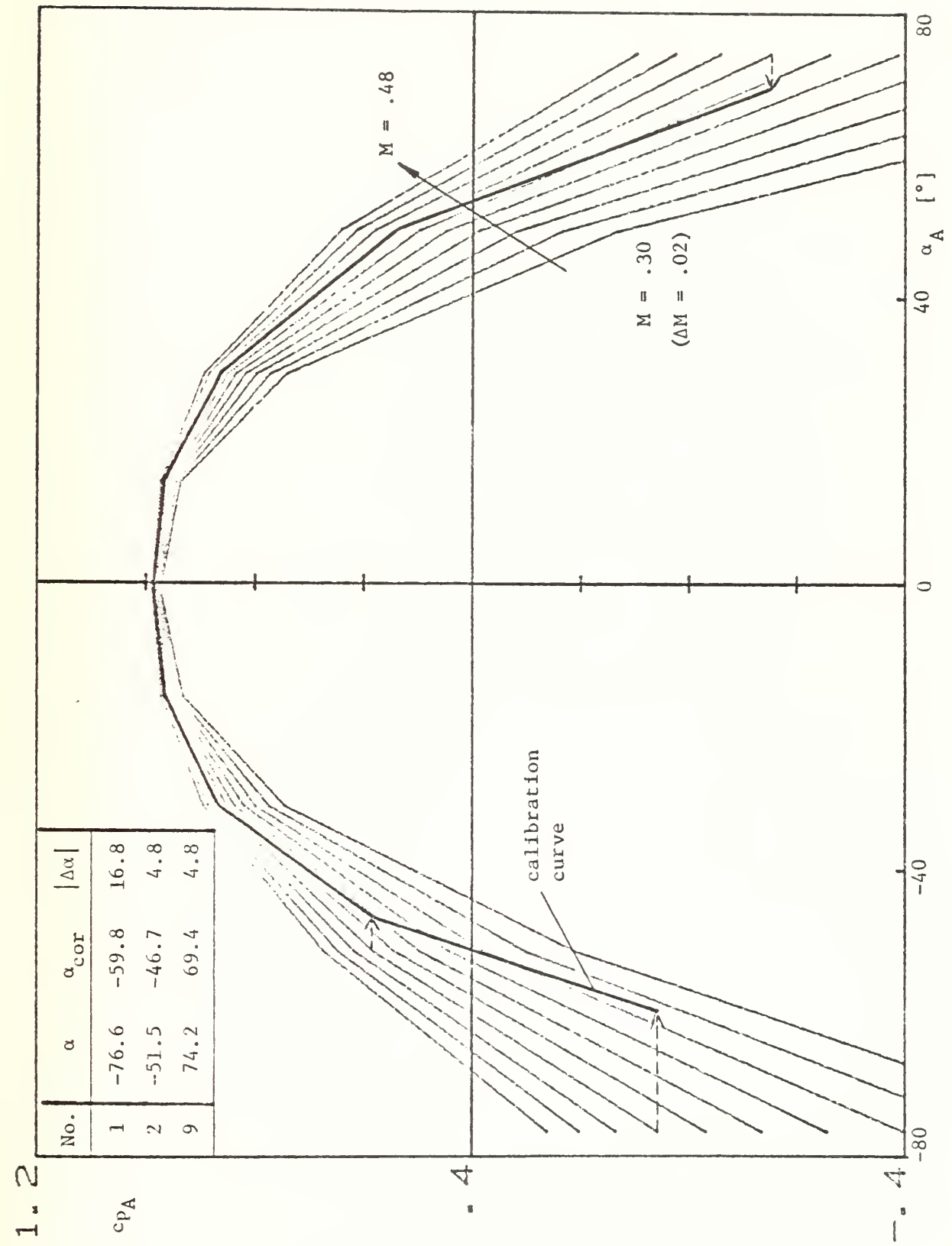

Figure 49: Correction for α_A values (position: outside wake flow)

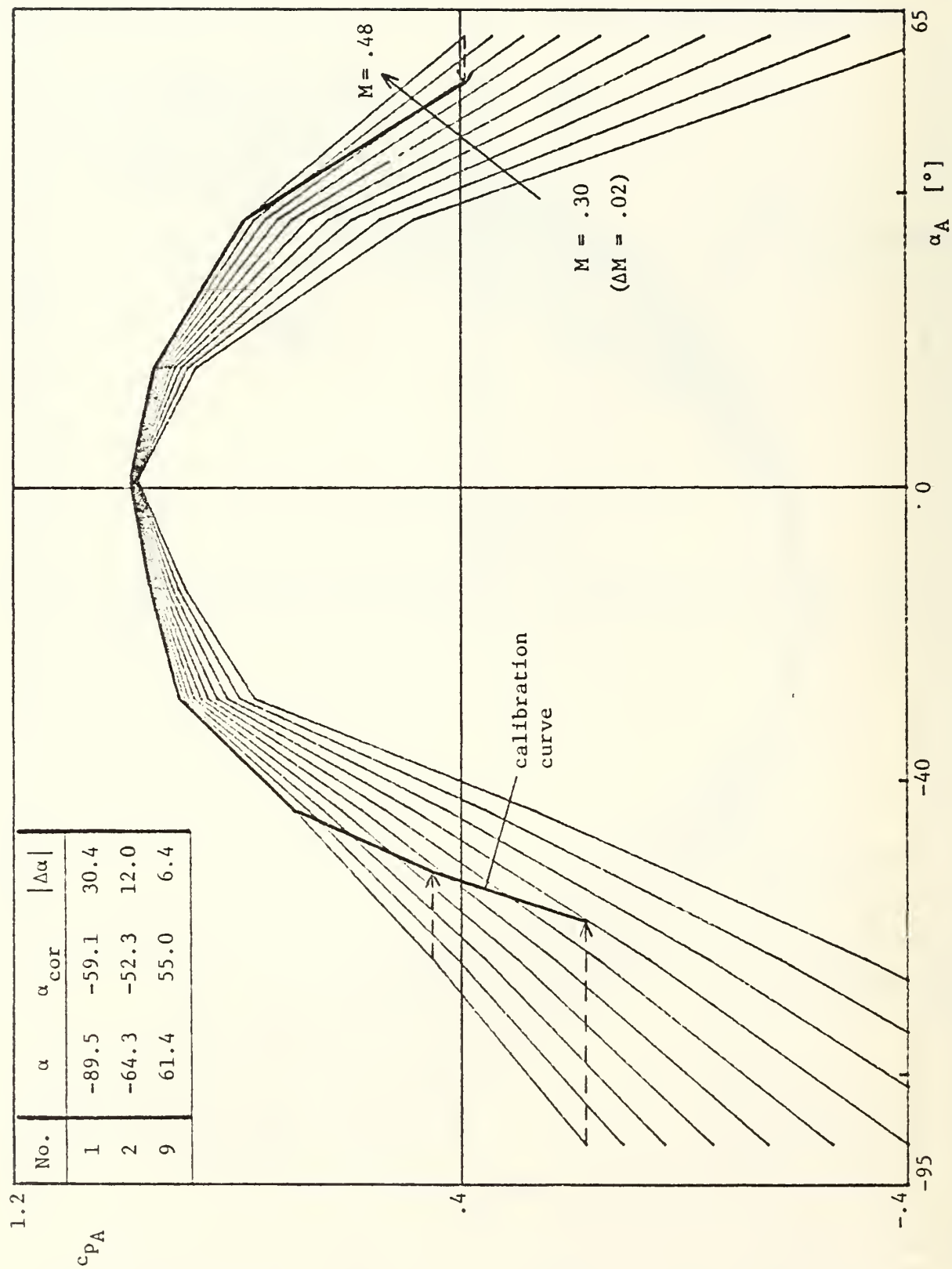

Figure 50: Correction for α_A values (position: within wake flow)

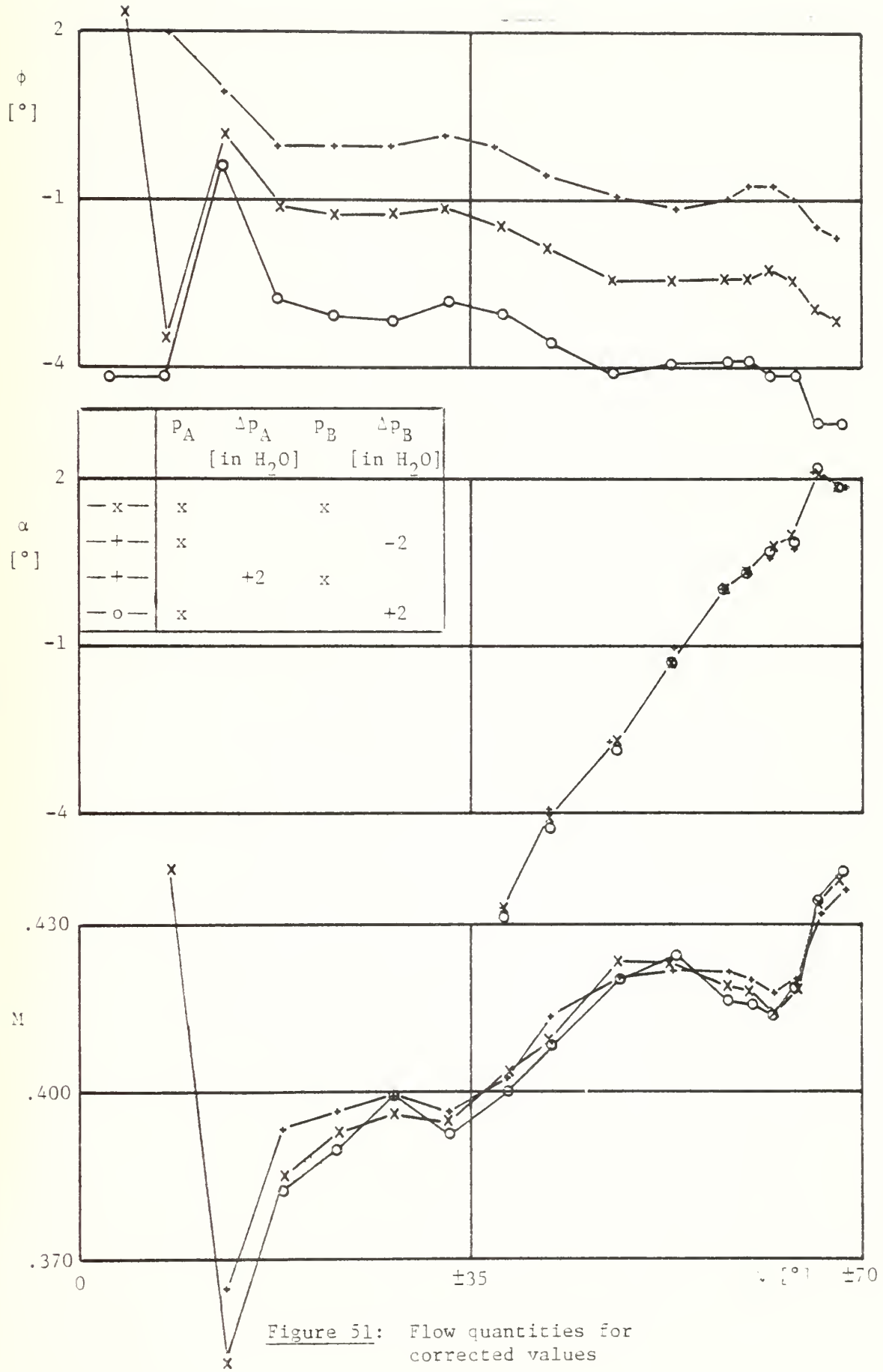

Figure 51: Flow quantities for corrected values

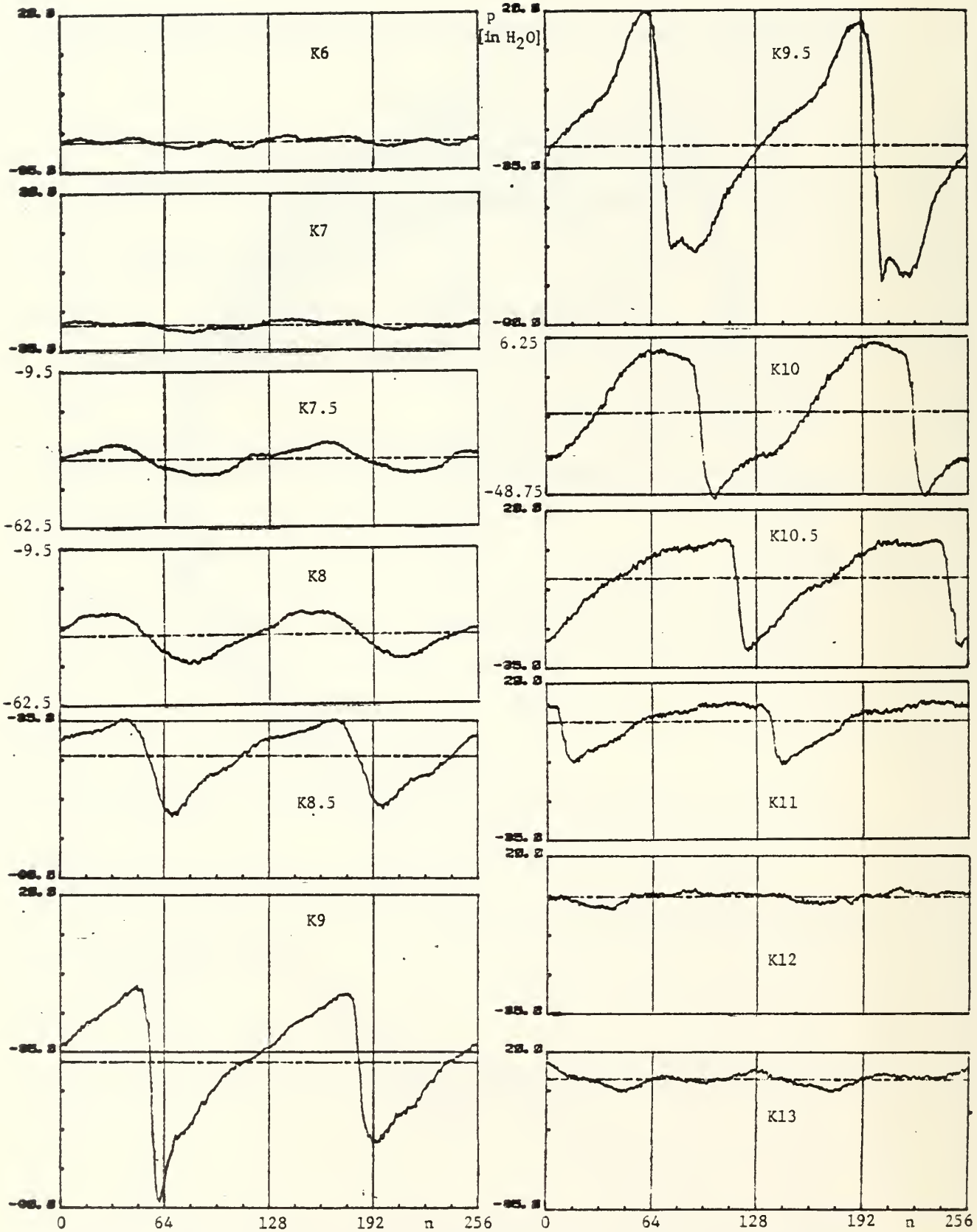

Figure 52: Case-wall results; Rep = 20

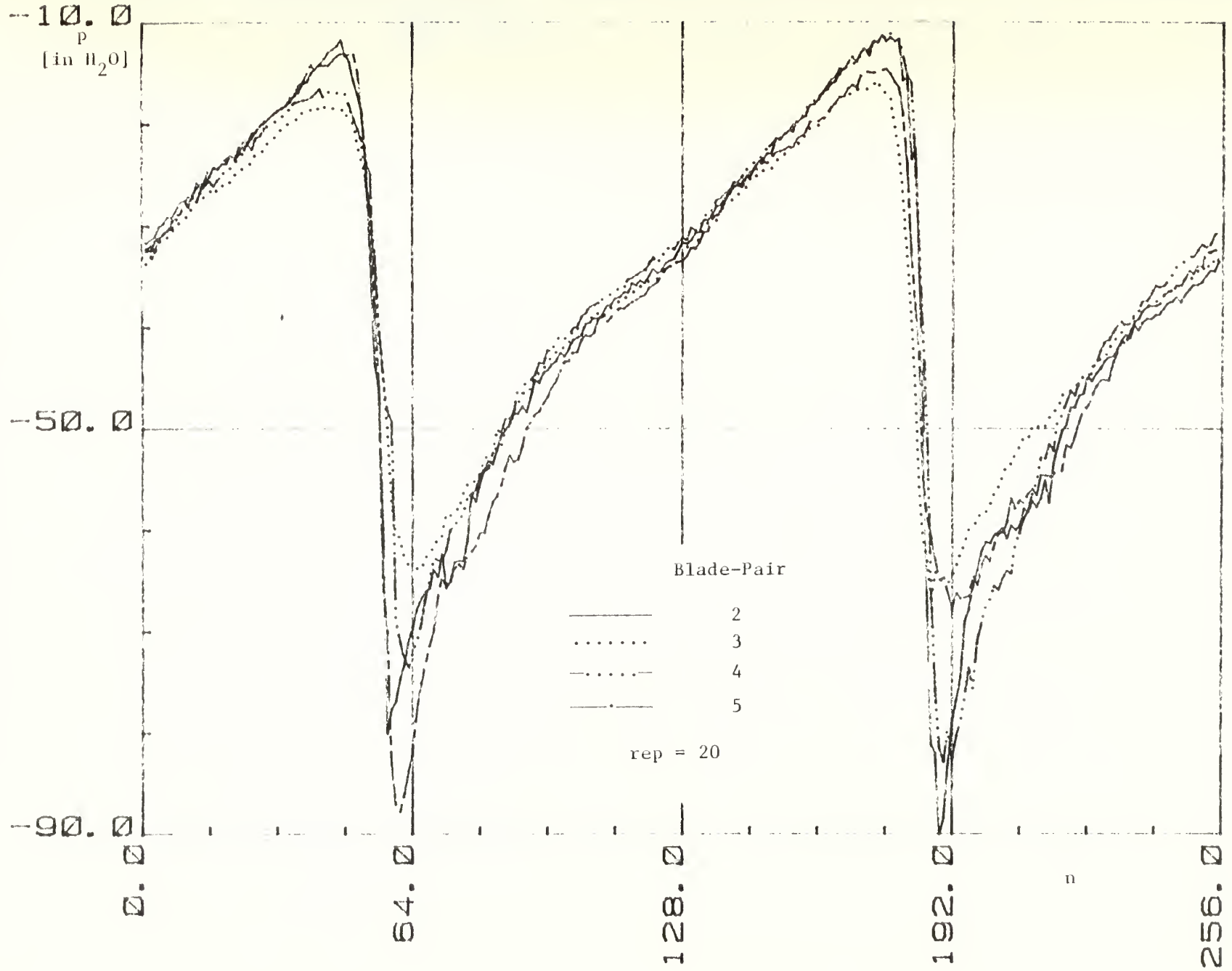

Figure 53: Signals from K9 for different blade-pairs

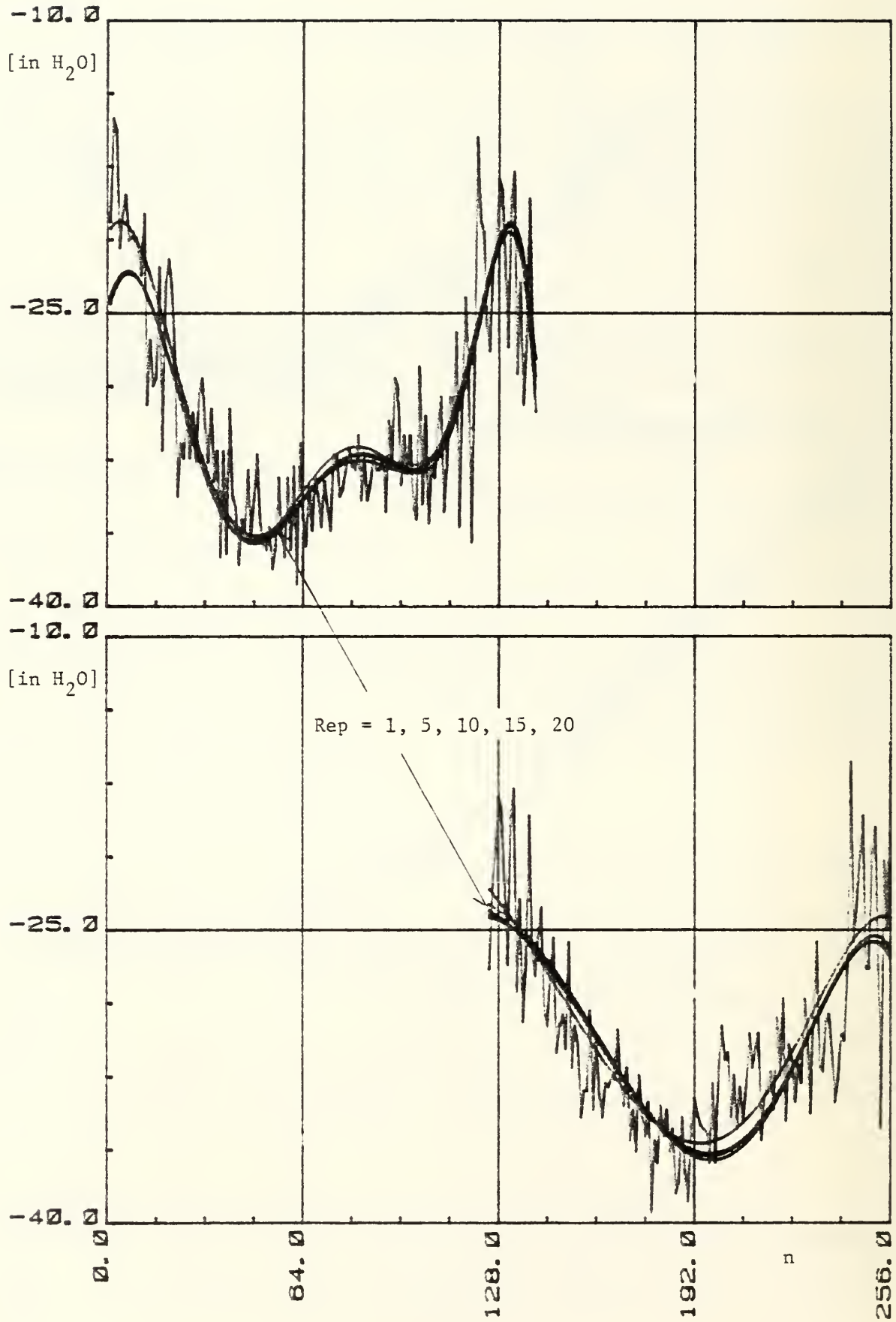

Figure 54: Curve-fit for signals from different numbers of repetitions

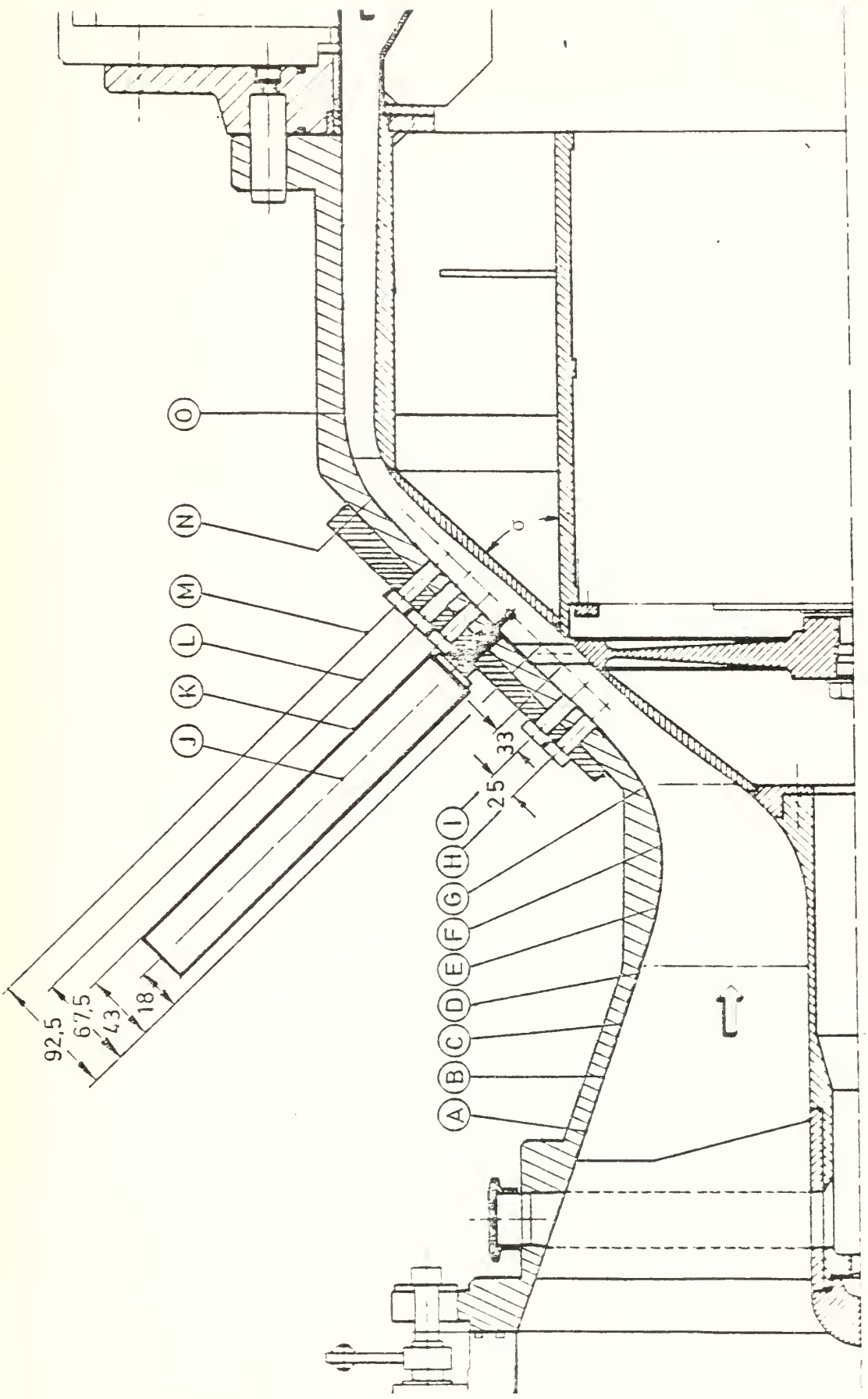

Figure 55: Test section RGG ($\sigma = 45^{\circ}$)

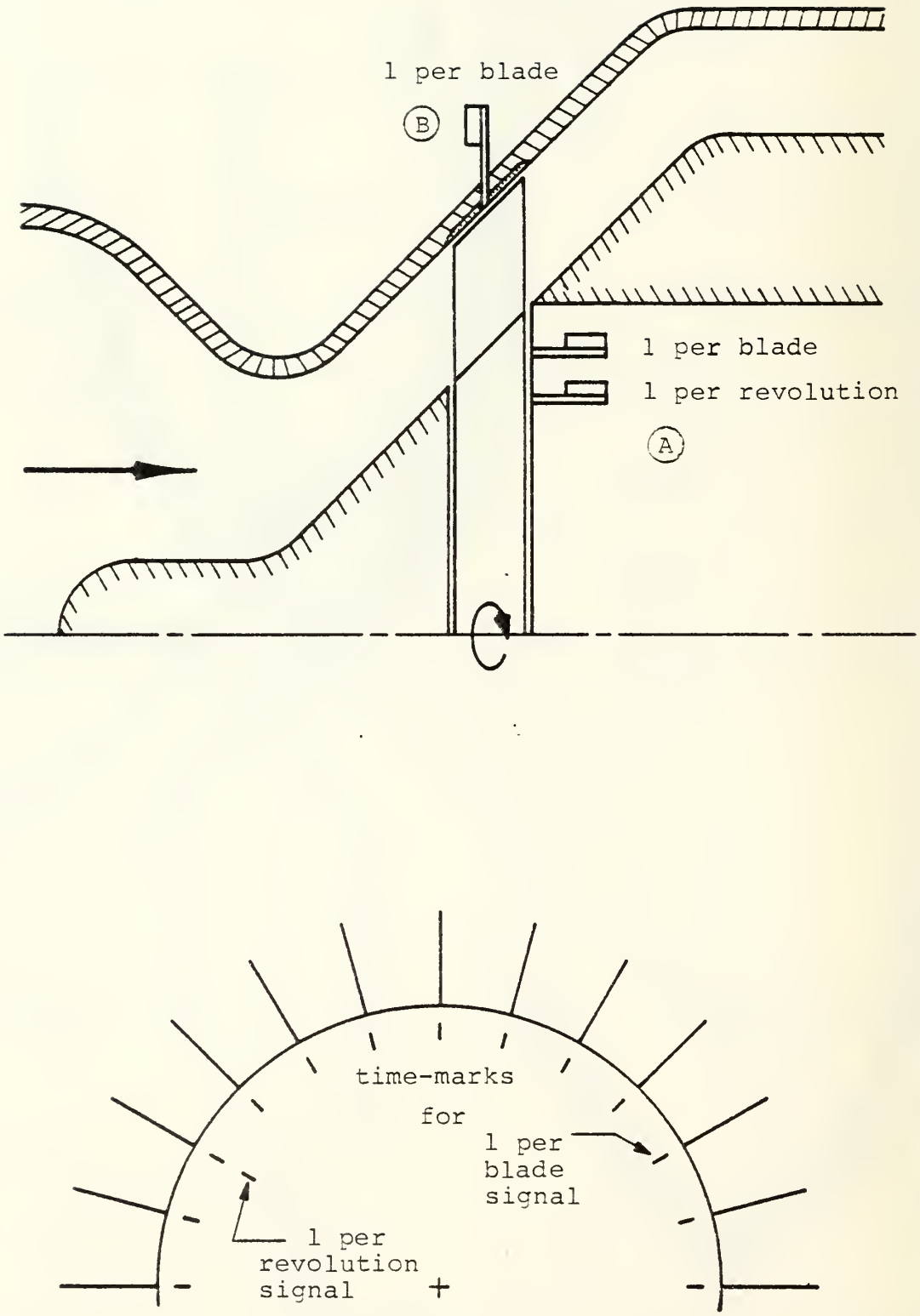

Figure 56: Proposal of trigger system for RGG

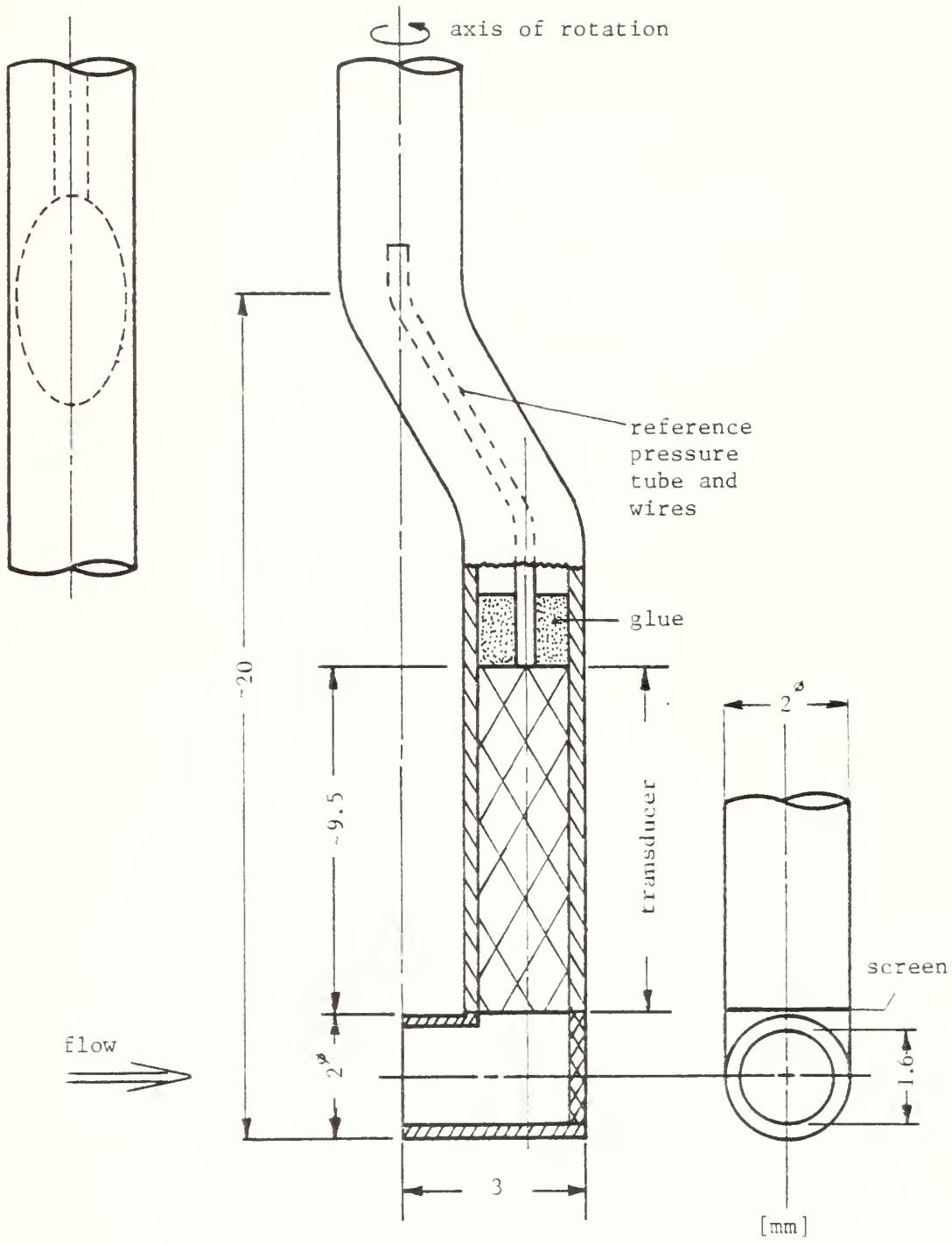

Figure 57: Sketch of total pressure probe for RGC (not to scale)

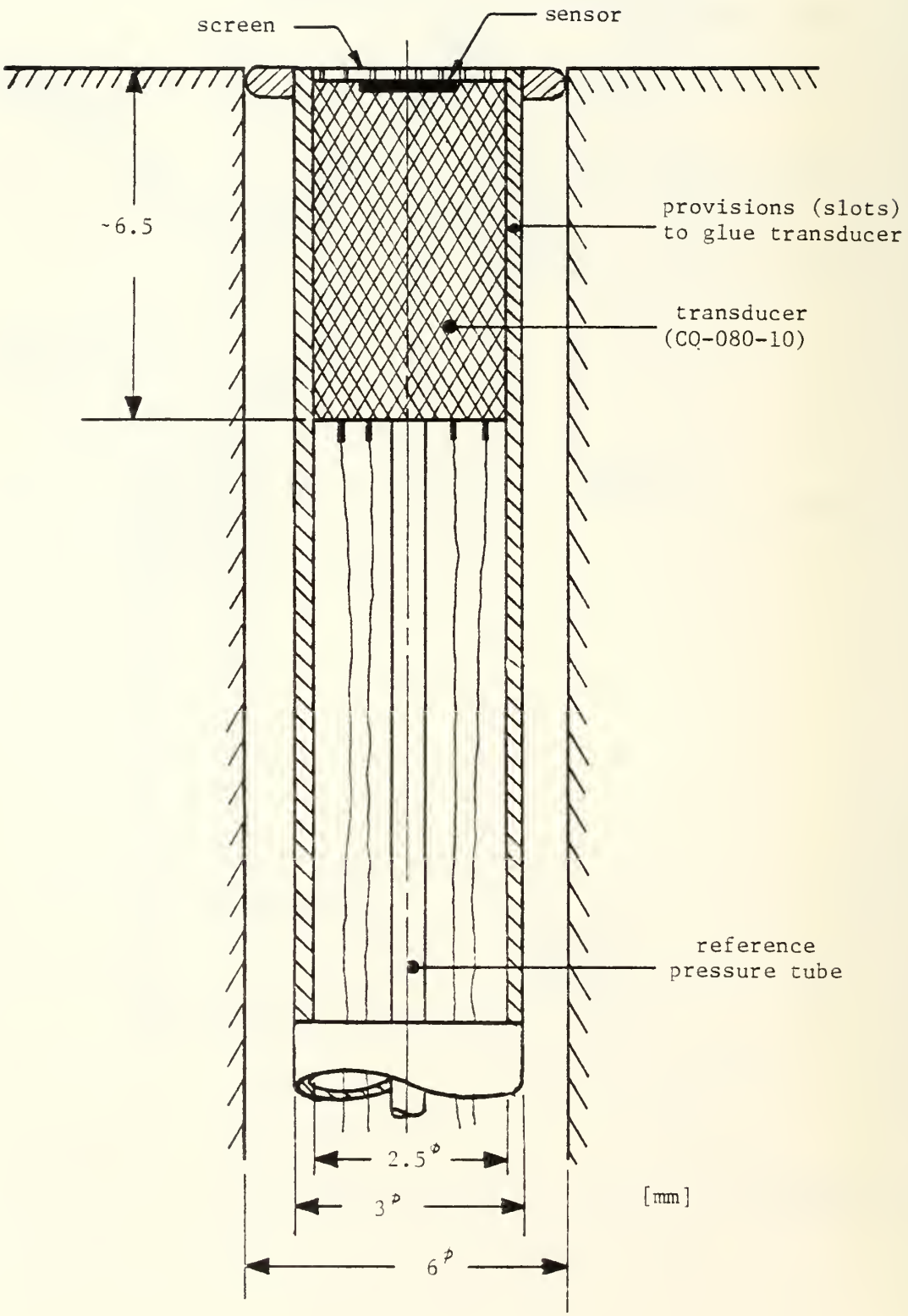

Figure 58: Sketch of static pressure probe for RGG (not to scale)

DISTRIBUTION LIST

		No. of Copies
1.	Library Code 0212 Naval Postgraduate School Monterey, California 93940	4
2.	Office of Research Administration Code 012A Naval Postgraduate School Monterey, California 93940	1
3.	Chairman, Code 67 Department of Aeronautics Naval Postgraduate School Monterey, California 93940	1
4.	Director, Turbopropulsion Laboratory Department of Aeronautics, Code 67Sf Naval Postgraduate School Monterey, California 93940	20
5.	Dr. Gerhard Heiche Naval Air Systems Command Code AIR-03D Navy Department Washington, D.C. 20360	1
6.	Mr. George Deoderian Naval Air Systems Command Code AIR-312A Navy Department Washington, D.C. 20360	1
7.	Dr. A. D. Wood Office of Naval Research 800 North Quincy Street Arlington, Virginia 22217	1
8.	Commanding Officer Naval Air Propulsion Test Center Attn: Mr. Vernon Lubosky Trenton, New Jersey 08628	1
9.	Dr. Ing. Hans-J. Heinemann DFVLR-AVA Bunsenstrasse 10 3400 Göttingen, WEST GERMANY	10